ARMY RESEARCH LABORATORY

Mechanical Tests and Failure Analysis on Selected Components of the Class 60 Armored Vehicle Launched Bridge (AVLB) During the Class 70 Modification Program

by Howard E. Horner

ARL-TR-1269 December 1996

The findings in this report are not to be construed as an official Department of the Army position unless so designated by other authorized documents.

Citation of manufacturer's or trade names does not constitute an official endorsement or approval of the use thereof.

Destroy this report when it is no longer need. Do not return it to the originator.

Army Research Laboratory
Fort Belvoir, VA 22060-5812

ARL-TR-1269 **December 1996**

Mechanical Tests and Failure Analysis on Selected Components of the Class 60 Armored Vehicle Launched Bridge (AVLB) During the Class 70 Modification Program

Howard E. Horner
Weapons and Materials Research Directorate, ARL

Abstract

The current Class 60 armored vehicle launched bridge (AVLB), with an overall length of 63 ft, is capable of carrying Class 60 (military load classification [MLC] - 60 tons) tracked and wheeled loads over a 60-ft-wide gap. The heavier, wider M1A1 main battle tank (Class 70 load) can cross the AVLB over a 50-ft-wide gap with precautions. Several modifications were proposed to upgrade a number of AVLBs from Class 60 to Class 70 for the 60-ft clear span crossings. The objective of the work was to conduct necessary mechanical tests on selected AVLB components to obtain pertinent data to verify their load carrying capability and the proposed modifications.

Various AVLB components were cut or removed from several AVLBs as samples for a variety of mechanical and special tests. Special test jigs were designed and built to test the samples of the components on the testing machine. Failure analyses were performed on the components that failed during the special tests or the fatigue tests of the modified AVLBs undergoing the simulated crossings. Two Class 60 AVLBs were converted to Class 70, with extensive modifications to the bottom chords, and then were tested. One of them was deliberately tested to failure by static overloading to observe the mode of failure. The bridge buckled in the top chords at about 190 tons. The modified bottom chords did not fail by cracking, indicating the success of the Class 70 modification program to upgrade the AVLB.

TABLE OF CONTENTS

LIST OF FIGURES

LIST OF TABLES

INTENTIONALLY LEFT BLANK.

1. INTRODUCTION

The current scissoring-type aluminum Class 60 armored vehicle launched bridge (AVLB) (Figure 1) with an overall length of 63 ft is capable of carrying Class 60 (military load classification [MLC] - 60 tons) tracked and wheeled loads over a 60-ft-wide gap (60-ft clear span). The heavier, wider M1A1 main battle tank (Class 70 load) can cross the AVLB over a 50-ft-wide gap (50-ft clear span) with precautions. Modifications were considered to upgrade a number of AVLBs from Class 60 to Class 70 for the 60-ft clear span crossings.

The AVLB is a girder bridge constructed mainly of a high-strength aluminum alloy. The structural system is composed of boxed sections with treads, transverse braces, curbings, supports, and connecting hardwares. The bridge consists of two wide treadways connected transversely by braces. Each treadway (two center and two ramp end sections) is hinged in the middle (large forged aluminum center hinges) so that the bridge can be folded in the scissor configuration and normally carried atop a heavily armored vehicle bridge launcher such as a modified M48A5 or M60A1 chassis tank. The bridge is transportable and maneuverable. It can be deployed to cross ravines, gullies, enemy-placed obstacles, creeks, small streams, and rivers. It can be hydraulically launched and/or retrieved from either end by an operator in the bridge launcher.

Welding is not used in the bridge fabrication because the aluminum alloy 2014-T6 used will lose its structural strength when heated. The major aluminum components, such as the bottom- and top-chord angles, forged center hinges and connectors, cross members, and girder plates, were riveted together rather than welded. The treads of the bridge were made of extruded aluminum deck panels that were fastened with steel bolts and nuts on top of the boxed sections to form the treadways. Aluminum alloy 7277 rivets were used throughout the bridge. They were hot-driven at elevated temperatures between 850° F and 975° F so that high shear strength could be developed.

In this work, a variety of tests and material evaluations were performed on a number of critical AVLB components, including the modified versions, to determine their properties for Class 70 loads. Modifications included use of stronger aluminum alloy 7050 to replace alloy 2014 for selected components such as the forged center hinges and bottom-chord angles. Another type of aluminum fastener (Huckbolt) was evaluated to replace the failed corroded aluminum alloy 7277 rivets in the critical areas. Failure analyses were conducted on failed bridge components after the load and fatigue tests were performed on the modified Class 70 AVLBs.

After 3 yr of investigating and testing the selected AVLB-aluminum components, over 30 interim reports and memorandums were written on the results of this work. Most information used in this report was extracted from both sources.

All work on the AVLB components was done for the Bridge Division of the Mobility Technology Center - Belvoir, U.S. Army Tank-automotive and Armaments Command, Fort Belvoir, VA, which has the technical responsibility for the AVLB.

1.1 Samples. A number of aluminum and steel samples and certain bridge components were removed from several AVLBs for metallurgical evaluations and tests. These samples and components are described in more detail in section 2 ("Results") of this report for the series of work performed.

1.2 Test Methods. In addition to the standard tests to determine the compositions and mechanical properties of several bridge components, a series of special tests were designed and conducted on certain components, such as the steel tie-down and lifting devices, in order to determine their load-carry capabilities under different loading conditions. The special tests used in this work are described in more detail in section 2 ("Results") of this report for the series of work performed.

2. RESULTS

The following results cover the series of work performed on the AVLB samples and components.

2.1 Tensile Properties of Aluminum Alloy 7050-T76511 and 2014-T6 Extruded Angle Samples. One of the modifications made on the current AVLB, when upgraded from MLC-60 tons to MLC-70 tons for the 60-ft clear span crossings, was to replace aluminum alloy 2014 extruded structural angles and forged center hinges with stronger alloy 7050 for the bottom chords of the AVLB panel assemblies. Each bottom chord was composed of two 5-in equal leg (3/8 in thick) aluminum structural angles riveted together with the 3/8-in-thick aluminum alloy 2014 girder plate between them. Two large forged aluminum center hinges were riveted together to the angles and girder plate at one end of the bottom chord, and two large forged aluminum connectors were riveted together to the angles and girder plate at the other end of the bottom chord for the center panel assembly. Two forged aluminum connectors were riveted together to the angles and girder plate at one end of the bottom chord for the end panel assembly, which in turn can be joined to the center panel assembly at the top and bottom connectors with 3-in-diameter steel pins.

The Bridge Division of the Mobility Technology Center - Belvoir had several bottom chords with the center hinges and connectors cut from the AVLB center panel assembly to serve at tensile test specimens to be pulled to failure at the National Aeronautics and Space Administration (NASA) Langley Research Center. Two of them were modified with extruded angles and forged hinges made of aluminum alloy 7050. The other bottom chord retained the original angles, hinges, and connectors made of alloy 2014. The two bottom chords with the new alloy 7050 broke at 543,000 lb (with 3/4-in-diameter aluminum rivets) and 531,000 lb (with 7/8-in-diameter aluminum rivets), whereas the other chord with the current alloy 2014 broke at 405,600 lb. The breaks occurred at the last countersunk rivet hole in the angles at the rear of the center hinge. After they were tested to failure, samples were cut from the angles of both alloys for tension tests to obtain the tensile data.

Two rectangular tension test specimens with 1/2-in-wide-reduced sections and 2-in-gauge lengths were machined from the angle samples of each alloy. A 2-in-gauge-length extensiometer was used to record the load-strain curve for each test specimen tested.

The results of the tension tests on aluminum alloy 7050 and 2014 extruded structural angle samples are shown in Table 1. Alloy 7050 samples met the tensile property limits in AMS 4340 for alloy 7050-T76511 extrusions, whereas alloy 2014 samples met the tensile property limits in ASTM B 221 for alloy 2014-T6 extrusions. Alloy 7050 extruded angles were about 23% stronger than alloy 2014 angle in terms of tensile strength.

2.2 Visual Inspection for Cracks in Three Modified AVLBs. In order to conduct fatigue-loading tests (simulated crossings) on the modified AVLBs, the Bridge Division had several center panel assemblies modified to MLC-70 tons at the Anniston Army Depot (ANAD) with stronger aluminum alloy 7050 extruded angles and forged center hinges on the bottom chords, replacing similar alloy 2014 components. Then, three modified AVLBs were reassembled with the modified center panel assemblies (alloy 7075 angles and hinges) connected to the original end panel assemblies to form the complete bridges for the fatigue and field tests.

Visual inspection and some liquid dye penetrant examination for cracks were performed on the riveted structures inside and outside the center and end panel assemblies prior to and after the fatigue tests of the modified AVLBs under the load frame at the Belvoir Bridge Hangar. A flashlight and a magnifying glass were used during the inspection of the bridge.

During visual inspection of the No. 2 Modified AVLB after the fatigue-load tests, a major crack was found in the 4-in equal leg aluminum structural angle splice riveted to the web and bottom flange of the inboard aluminum girder, where the steel section of the ramp end was spliced to the aluminum section to form the end panel assembly. This crack had extended across the horizontal leg and about 4/5th of the way up the vertical leg of the splice angle inside the male end panel assembly. Another major crack was found in a similar 4-in-angle splice in another male end assembly in the other treadway at the other end of the bridge. This crack also extended across the horizontal leg, but about 3/4-in up the vertical leg of the splice angle.

In both 4-in-angle splices with the crack, a 1/2-in-wide section of the horizontal leg was already cut (probably by milling) from the leg edge in order to match the width of the steel beam girder bottom flange. This had left an angular cut (notch) at the end of the cut section, thus creating a stress concentration in that notched area where the major crack had initiated (see Figure 2 for an example). Both male end panel assemblies in the No. 2 Modified AVLB, with the cracked splice angle, were deadlined and removed.

Another visual inspection was performed on the No. 2 Modified AVLB after the two previously mentioned male end panel assemblies with the cracked splice angle were replaced with similar substitute assemblies for further fatigue tests. In this case, visible liquid penetrant examination was also performed on the angular notch area of the interior splices (four) on the bottom flange of the inboard and outboard girders of both end assemblies. The paint was stripped from around the notch cut in the splice angle, and the penetrant process was applied to the notch area. A small crack was found on the inboard splice angle inside one of the end assemblies. A strong dye indication revealed a 1/4-in-long crack, which was already visible. There was a faint indication of the same crack extending another 3/8 in for a total of 5/8 in. Two marks adjacent to this crack were scribed on the surface of the splice as the reference points to monitor the propagation of the crack during the field tests of this modified bridge at Aberdeen Proving Ground (APG). Again, the crack had initiated at the angular notch cut where a 1/2-in-wide strip was machined from the edge of the angle horizontal leg as had happened in similar angle splices in the replaced assemblies. Later, one of the substitute end assemblies on the No. 2 Modified AVLB undergoing the field tests at APG had cracked in the inner and outer angles of the spliced joint, leading to the failure analysis of the cracked splice angle in a deadlined end assembly at Belvoir, which is reported later in this report.

Visual inspection and visible liquid penetrant examination for cracks were performed on the No. 3 Modified AVLB which was assembled together and fatigue-load tested under the load frame at the Bridge Hangar. Again, a small crack was found in the inner angle splice on the inboard girder of one male end

panel assembly. It also had initiated in the sharp angular notch cut at the angle horizontal leg edge, which may have propagated when this bridge was sent later to APG for the field tests.

In addition, a crack about 5 in long was found in the sharp inside corner of a vertical 3-in × 2 1/2-in aluminum angle which was part of the cross member inside another male end assembly of the No. 3 Modified AVLB. The cracked angle was riveted to the web of the inboard girder. It was a nonstandard structural shape with a sharp inside corner (very little radius), not the standard structural shape with a generous inside corner radius that was observed in other bridge panel assemblies inspected, depending on the contracts at the time they were fabricated. The sharp inside corner acted as the stress concentration (notch), leading to crack initiation in the inside corner of the angle. Cracks also were found in several vertical standard angles, but they initiated from the bottom rivet hole of the narrow angle leg and not in the inside corner with the generous radius.

Later, ANAD made a modification to the bottom joint splices in the end panel assemblies, based on the findings observed during the bridge inspections done at Belvoir. Stronger alloy 7050 angles with no machining made on the horizontal leg edge, as was done on the original splice angles resulting in a sharp notch, were used. The modified end assemblies were reassembled on the No. 2 Modified AVLB, and the bridge was field tested at APG before it was sent back to Belvoir for additional fatigue tests. Visual inspection and liquid penetrant examination were performed on this bridge to establish the baseline on the cracks found, if any, prior to the fatigue tests under the load frame at the Bridge Hangar. Two major cracks (one 7 in long and the other 12 in long) were found in two vertical aluminum nonstandard structural angles riveted to the inboard girders of the male and female center panel assemblies connected together end to end in one treadway of the bridge. They were already labeled as 1 and 2 when the bridge was inspected earlier at APG before it came to Belvoir. Each crack had occurred in the sharp inside corner at the upper end of the angle. The end tip of each crack was marked on the angle in order to check on the crack propagation after the fatigue tests. Vertical aluminum nonstandard aluminum angles with sharp inside corners should be replaced with standard structural angles with generous inside radius during AVLB refurbishment or modification to eliminate potential stress concentration.

2.3 Failure Analysis of a Cracked Aluminum Splice Angle From an AVLB Male End Panel Assembly. A failure analysis was conducted on a cracked 4-in × 4-in × 1/4-in aluminum inner splice structural angle that was riveted to the inboard girder of the male end panel assembly (NSN 5420-00-542-3117, Contract DAAE07-84-C-A177, S/N 148), which was one of the major structures of the AVLB. The

angle splice, which was 30 1/2 in long, was riveted to the aluminum bottom chord angle, aluminum bottom reinforcement plate, steel beam bottom flange, and web and bottom flange of aluminum girder, where the steel section of the ramp end was spliced to the aluminum section to form the end panel assembly. The aforementioned assembly was the same one on the original No. 2 Modified AVLB that was inspected earlier when a major crack was found in the angle splices.

The cracked inner splice angle, uncracked outer splice angle, and bottom reinforcement plate were removed from the same joint in the deadlined male end panel assembly for material evaluation and failure analysis. Samples were cut from the bottom plate and both angles for chemical analysis, and a single rectangular tension test specimen was cut from each angle to determine its mechanical properties.

Figures 2 and 3 show the major crack in the damaged splice angle. The crack had initiated at a sharp angular notch at the edge of the horizontal leg, extended across this leg, and then 4/5th of the way up the vertical leg. A 1/2-in-wide section of the horizontal leg edge was already machined from the angle in order to match the width of the steel beam bottom flange, resulting in an angular notch cut with a sharp corner as seen in Figures 4 and 5. When the splice components were removed from the assembly bottom flanges, the exposed bottom chord inner and outer aluminum angles were examined visually for cracks. A crack about 7/16 in long was found in the corner radius where the horizontal leg and a portion of the vertical leg were cut out in order to accommodate the thicker bottom flange of the inboard steel beam girder so that the end of the bottom chord aluminum angle could extend several feet beyond the joint (see Figure 6). This crack apparently had occurred after the inner splice angle had cracked considerably. If given time, the same crack could propagate across the vertical leg of the bottom chord angle.

The results of the chemical analysis on the samples from the bottom reinforcement plate and both splice angles are given in Table 2. Their composition was within the chemical limits for aluminum alloy 2014 as specified. The results of the tension tests on both angles are given in Table 3. They met the minimum mechanical properties for alloy 2014 in T6 temper condition as specified.

The primary cause of the failure in the cracked splice angle was due to the presence of the sharp inside corner in the machined angular notch at the edge of the horizontal leg, which served as a stress concentration. This was a poor design. A crack had initiated at this sharp corner and propagated by fatigue and then by brittle fracture almost across the angle. A visible liquid penetrant examination was performed on the similar machined angular notch of the outer splice angle and on both sides of the bottom

reinforcement plate in the area of the joint for cracks. No indication of the cracks was observed on both parts.

2.4 Failure Analysis of a Broken AVLB Forged Aluminum Male Bottom Connector. The No. 2 Modified AVLB, which was mentioned earlier in this report, was undergoing a series of fatigue tests under the load frame at the Bridge Hangar when a male bottom connector on a female center panel assembly broke suddenly. The connector, with a 3-in-diameter eyehole, was composed of two large forged aluminum alloy 2014 parts (inboard and outboard) riveted together to the end of the bottom chord aluminum angles on the inboard girder of the panel assembly. It was connected with a 3-in-diameter steel pin in the eyeholes to the female bottom connector of the female end panel assembly (ramp) to form a portion of the bridge treadway. The test, when the failure occurred, involved an eccentric loading at the midspan of one treadway of the bridge where the connector broke near its eyehole.

The broken eyehole piece of the failed connector (see Figure 7) was removed as a sample for failure analysis. Meanwhile, the panel assembly (NSN 5420-60-542-3115, Contract DAAK07-84-C-A177, S/N 028) with the remaining broken connector was sent back to APG for additional vehicle crossings. It was assembled to another modified AVLB and tested to determine if the bridge with a broken bottom connector can still function during the vehicle crossings. It was reported later that this bridge was still functional after a number of crossings were made on it.

Visual examination of the fractured surfaces (see Figure 8) of the broken connector sample revealed that the failure initiated at a short vertical machined notch (sharp fillet) on the side at a short distance behind the eyehole of the inboard forged connector part. The feature of the brittle fracture pointed toward the crack initiation site at the machined notch (see Figure 9). The crack initiation site exhibited a light-discolored semi-circular area which indicated a fatigue crack (see Figure 10). The small fatigue crack (see Figure 11) was initiated at the machined notch which was observed on the broken part of the connector still on the panel assembly sent back to APG. Apparently, the fatigue crack grew to the critical size during the fatigue tests at the Bridge Hangar to the point that the brittle fracture occurred in the inboard forged connector part first. The crack continued across the cross section through a small rivet hole and to the eyehole. The final break on the same part then occurred through the cross section on the other side of the eyehole in a more ductile manner. No necking in the base metal was observed at the crack initiation site. The presence of a sharp notch intentionally or unintentionally machined in the critical parts, such as the connectors and hinges, can act as stress raisers, resulting in premature failure of the bridge under cyclic loadings from heavy vehicle crossings.

The incidence of the connector failure led to visual examination of similar male bottom connectors on other AVLB panel assemblies located at the Bridge Hangar. Variations in the amount of machining done on the side of the forged connector eyehole section that resulted in a sharp vertical notch (fillet) were observed in the same area where the crack had initiated in the broken connector examined in this work. There were other similar bottom connectors that had no machining done in the same areas. Apparently, the dimensions varied from piece to piece during the forging operation of the connector parts, which may or may not require necessary machining in order to meet the drawing requirement. Machined sharp notches also were observed elsewhere on the forged connectors, for example, the bottom surface of the connector part which was fastened to the horizontal leg of the bottom chord aluminum angle by aluminum rivets. The presence of sharp notches from machining can act as stress raisers where potential premature failures of the Class 70 Modified AVLBs can occur.

Incidently, a new crack about 12 in long was found in the sharp corner of the inboard vertical aluminum angle inside the same failed assembly. The crack emerged from the bottom of the angle, which already had a 7-in-long crack at the top prior to the bridge failure. This was reported earlier in this report. The new crack in the bottom of the angle may have occurred before or after the connector broke during the fatigue test.

In general, the primary cause for brittle failure of the forged male bottom aluminum connector was due to the small fatigue crack that had initiated at the vertical machined sharp notch (fillet) on the side at a short distance behind the eyehole. This crack grew to a critical size during cyclic loadings, resulting in the initial brittle fracture of the inboard connector part first and then in ductile fracture of the outboard connector part by overloading. Because machined sharp notches can act as stress raisers, the modification of AVLBs to Class 70 should include removal of the machined notches from the forged bottom connectors, if possible, by blending or machining a generous radius to eliminate sharp fillet in the notch.

2.5 Failure Analysis of Three Broken AVLB Forged Aluminum Bottom Connectors. Failure analysis was performed on three broken forged aluminum bottom connectors from the No. 2 Modified AVLB that failed the second time during the fatigue tests under the load frame at the Bridge Hangar. The failure analysis of a broken bottom connector from the first bridge failure was reported earlier. In the case of the second bridge failure, one outboard female bottom connector on the male center panel assembly and two male bottom connectors (inboard and outboard) on the male end panel assembly (ramp) broke through the 3-in-diameter eyehole section (see Figures 12 and 13 for an example). Both male center and female end panel assemblies were connected end to end to form a section of the bridge treadway. The fatigue test at the time of the bridge failure involved an eccentric loading at the bridge midspan of this treadway.

After the female center panel assembly that broke during the first bridge failure was replaced, the No. 2 Modified AVLB was inspected again, and the fatigue tests were continued until the second failure had occurred elsewhere on the bridge.

Initial visual examination of the fractured surfaces of three broken bottom connector samples revealed that the origin of the AVLB's second failure appeared to be in a fatigue crack initiated at the bottom edge of the eyehole of the outboard forged part of the outboard female bottom connector (see Figure 14). Characteristic features of the fatigue crack were observed only in this broken part, not in other broken connector parts. In addition, when the fatigue crack was examined visually at a higher magnification, a small discolored area that may indicate corrosion was observed at the edge of the eyehole where the crack had initiated (see Figure 15). The internal surface of the eyehole of the broken part was observed to be slightly worn and corroded (white corrosion products), with most of the paint gone.

Based on the possibility that corrosion had taken place in the worn, bare area of the broken eyehole connector section (see Figures 12 and 13), a metallographic specimen for microstructural examination was sectioned through the fatigue crack that contained the discolored area. Figures 16–19 show that intergranular corrosion had occurred in the area the fatigue crack had initiated and in several small corrosion pits on the exposed internal surface of the eyehole. If not properly heat-treated, alloy 2014-T6 that was specified for the forged parts of the bottom connectors for the AVLBs could be susceptible to intergranular corrosion and possibly to stress corrosion cracking (SCC). Because of intergranular corrosion, a fatigue crack had apparently initiated at a small intergranular corrosion pit. The crack eventually grew to the critical size during the bridge fatigue tests, in addition to previous field tests at APG, to cause brittle fracture of the forged connector through the eyehole section. As a result of this initial fracture, overloading then occurred to cause two other bottom connectors in the same bridge treadway to break also.

Based on these findings, the origin of the second failure in the No. 2 Modified AVLB was located in a fatigue crack at the bottom edge of the eyehole of the broken outboard forged part of the outboard female bottom connector on the male center panel assembly. The fatigue crack had initiated at a small intergranular corrosion pit, which grew to the critical size during cyclic loadings, resulting in the brittle failure of the connector eyehole. Small corrosion pits occurred in the bare internal surface of the eyehole where the paint was rubbed off by the steel pin and when the moisture or water entered the gap between the pin and eyehole for the corrosion to take place.

2.6 Visual Inspection of the AVLB Bottom Chord 5-in-Aluminum Angles of the Failed Male End Panel Assembly. After the No. 2 Modified AVLB broke for the second time during the fatigue tests under the load frame at the Bridge Hangar, the modified male end panel assembly with both broken forged bottom aluminum connectors was removed from the bridge for further investigation, particularly at the bottom splice joints where the steel section (ramp end) was spliced to the aluminum section with aluminum plates, angles, spacers, and rivets to form the end panel assembly. Previously, the failed assembly—prior to the fatigue tests—was modified with stronger aluminum alloy 7050 structural angles, replacing the lower strength alloy 2014 angles for the 4-in-splice angles. The bottom chords were still the original alloy 2014 5-in-equal leg angles. As noted earlier in this report, the horizontal leg and a portion of the vertical leg were cut out at one end of the bottom chord 5-in-aluminum angle in order to accommodate the thicker bottom flange of the steel beam girder of the steel ramp section of the end panel assembly and extend a short distance beyond the splice joint. Also noted earlier, a small crack was found in the 90° corner of the angle cutout (see Figure 6), hence the reason for the inspection of the corner area for cracks in the bottom chord angles once the 4-in-splice angles were removed from the splice joint to expose the cutout section at the end of the 5-in angles.

Visual inspection for cracks was performed on the exposed bottom chord 5-in angles after the 4-in-splice angles were removed. A crack was found in the 90° internal corner of the cutout at the end of each chord angle. The length of each crack was measured and recorded as follows:

Outboard bottom chord	-	inside angle: 2 3/4 in
		outside angle: 1 1/4 in
Inboard bottom chord	-	inside angle: 1 3/16 in
		outside angle: 9/16 in

Permanent deformation (necking) was observed along each crack, which may indicate ductile fracture by overloading. According to the information provided about the modifications made on the end assembly, no cracks were observed in the corner of the cutout in the bottom chord 5-in angles at the time of the assembly modification at ANAD. Therefore, the cracks may have occurred during the second failure of the modified AVLB during the fatigue tests at the Bridge Hangar and possibly during the field tests at APG.

The 90° internal corner of the cutout at the end of the bottom chord angle can act as a stress raiser where a crack can initiate. Modification to the splice joint should include machining more generous radius in the 90° corner cut to reduce the stress concentration.

2.7 Failure Analysis of a Broken Bottom Chord Angle on the No. 2 Modified AVLB. After the field and fatigue tests on the No. 2 Modified AVLB, the bridge was undergoing the static overload test under the load frame at the Bridge Hangar to 133 tons when one of the bottom chord aluminum angles broke suddenly at 74 tons in a female center panel assembly. The failed 5-in-equal leg angle, which was the outside angle of the chord riveted to the outboard girder aluminum plate of the assembly, broke across the last countersunk rivet hole in its horizontal leg underneath the bottom leg of the center hinge.

Previously, modifications were made to the AVLB from Class 60 to Class 70 by changing the aluminum material from alloy 2014 to stronger alloy 7050 for the large forged center hinges and bottom chord angles on the center panel assembly. The horizontal leg at one end of the angle was fastened underneath to the bottom leg of the hinge with large countersunk head aluminum rivets. A series of countersunk rivet holes were made in the angle horizontal leg in line with the rivet holes in the bottom leg of the hinge. The vertical legs of both the angles and hinges were, in turn, fastened to both sides of the girder plates of the assembly with large buttonhead aluminum rivets. The rivets were hot-driven.

Figure 20 shows the broken section of the failed bottom chord angle that was cut from the damaged center panel assembly of the No. 2 Modified AVLB for the material evaluation. The crack went across the last rivet hole in the horizontal leg and then up the vertical leg of the angle. Visual examination of the fractured surfaces revealed that the origin sites of the crack were in the small discolored areas at the corner of the fractured rivet hole on the top surface of the angle leg in contact with the bottom surface of the forged center hinge (see Figures 21–23). Characteristic fatigue beach marks were observed below the discolored areas in the fractured surfaces.

The small broken piece (A), adjacent to the fractured hole in Figure 20, contained a portion of the rivet hole edge. Both fractured surfaces of the piece also contained a small discolored area and beach marks at the hole edge. Visual examination of the hole edge at higher magnifications revealed a small crack between the fractures (see Figures 24 and 25). A small metallographic specimen containing the crack was cut from the piece for microstructural examination. The crack is seen in Figures 26 and 27. It was transgranular with some branching (see Figure 28). The specimen was deliberately broken apart to expose the surfaces of the crack. Small discolored areas and beach marks were observed in the fractured surfaces.

Additional small cracks also were found in the other countersunk rivet hole next to the fractured hole. Two specimens containing the cracks at C and D in Figure 20 were cut from that rivet hole. The cracks widened after the specimens were cut. Apparently, some residual stress was still present in the angle as

the results of hole drilling, hot riveting, extrusion process, or permanent deformation of the hole from loading of the bridge. One of the specimens with a small crack also was deliberately broken apart to expose the fractured surfaces. Similar features of discolored area and beach marks, as seen on the fractured surfaces of the fractured hole, also were observed in the fractured surfaces of the broken specimen. The other specimen with a small crack was used as metallographic specimen for microstructural examination. The crack also was transgranular, as was observed in the previous metallographic specimen of the small broken angle piece.

Furthermore, blackened areas were observed around the countersunk rivet holes and along the inside corner of the broken angle where the contact was made between the top surface of the angle and the bottom surface of the forged center hinge when both parts were riveted together. They appeared to be black corrosion products. Even the impression of the machined marks on the bottom of the hinge was observed on the top surface of the angle (see Figure 20). Visual examination of the blackened areas revealed surface pitting, apparently as the result of exfoliation from the crevice corrosion because of the moisture or water trapped in the gap between both parts riveted together. A metallographic specimen was cut through a blackened area (surface pits) for microstructural examination. The microstructures of a surface pit are seen in Figures 29 and 30. Dark corrosion products were still embedded in the bottom of the pit.

Slight permanent deformation was observed in one half of the circumference of the countersunk rivet holes in the angle. This would indicate that the center hinge moved on the bottom chord angle, forcing the shank of the rivets against the edge of the holes in the angle, causing permanent deformation to the edge. Visual examination was made on several countersunk rivets that were removed from the broken angle section. The shank on the rivet also was deformed slightly in the area in contact with the edge of the holes.

Based on these findings, it was speculated that the probable cause of the brittle failure in the broken bottom chord angle on the No. 2 Modified AVLB during the static overload test was due to the small fatigue cracks 180° apart in the corner edge of the last countersunk rivet hole in the horizontal leg underneath the forged center hinge. They were perpendicular to the principal stress in the longitudinal axis of the angle. They had grown to the critical size by fatigue during the field tests at APG and fatigue tests at Belvoir, resulting in the brittle failure of the angle through the rivet hole. Similar small cracks also were found 180° apart in similar locations in the next-to-last rivet hole of the angle.

The small areas of discoloration observed in the cracked surfaces of the rivet holes were due to corrosion from the moisture or water trapped between the center hinge and angle riveted together, seen as black-colored areas. Crevice corrosion had occurred in the blackened areas on the top surface of the angle horizontal leg in contact with the bottom surface of the hinge, resulting in surface pitting by exfoliation. Movements between the hinge and angle had resulted in rubbing or fretting on the top surface of the angle horizontal leg. Slight permanent deformation had occurred on the edge of the countersunk rivet holes in the angle by the shank of the rivets acting against the hole edge during the hinge movements on the angle.

2.8 Pull Tests of the AVLB Steel Tie-Down Device Samples. A number of modifications were proposed to convert Class 60 AVLB to Class 70 based on the preliminary findings of the previous works performed for the Bridge Division at Belvoir. One of them was to do away with the large forged bottom aluminum connectors on the AVLB end and center panel assemblies. Continuous bottom chords made of larger and stronger aluminum alloy 7050 angles, in lieu of smaller and lower strength alloy 2014 angles now used on individual panel assemblies, will be used to join permanently both end and center assemblies end to end to form a sectional unit as one of four structural sections of the Class 70 Modified AVLB.

Each panel assembly (eight per Class 60 AVLB) has a steel tie-down device near each corner. The devices are to be used as tie-downs for transportation purposes only, not for lifting the bridge. During inspection of several AVLBs, a number of the devices were found bent, cracked, or broken off because they were used to lift the bridges in the field.

In order to obtain necessary information on the amount of tension load required to cause the device failures and information on the mode of the failures, several pull tests were conducted on several original AVLB steel tie-down devices positioned at different orientations to simulate different load-lifting conditions. Each device sample was tested as a lifting device in a specially designed test jig.

The tie-down device used on the Class 60 AVLB was composed of a 3/4-in-diameter steel bar formed into a U-shape with both ends welded to a 7 3/4-in × 4 5/8-in × 3/8-in steel plate (see Figures 31 and 32). It, in turn, was fastened to the 3/8-in-thick aluminum girder plate of the panel assembly with four 3/4-in-diameter hot-driven buttonhead aluminum rivets. A similar size steel back was fastened on the opposite side of the girder plate as a reinforcement to the tie-down device (see Figure 33). The steel components of the device were made of ASTM A36 structural steel, according to the AVLB drawing.

Several large sections of the aluminum girder plate containing a tie-down device (see Figure 31 for an example) were cut from several AVLB panel assemblies to serve as the test specimens for the pull tests. A special test jig to hold a specimen in the testing machine during the test was designed to simulate the lifting of the bridge under different loading conditions (orientations). The jig was fabricated of 3-in × 3-in x 3/8-in steel angles and welded together in the Belvoir Center Machine Shop (see Figures 32 and 34).

A test plate with the tie-down device was bolted to the back of the test jig which, in turn, was placed in position underneath the fixed crosshead of the testing machine (see Figures 34–36). A large chain with a clevis hook or wire rope was used to pull on the U-shaped steel bar of the device to failure. A deflectometer was placed between the bottom of the test jig and the table of the testing machine to record the movement of the crosshead in order to determine when the device will start to deform and fail (see Figure 37).

A series of pull tests were conducted on the tie-down devices depending on the orientation of the U-shaped bar with respect to the tension load as follows:

- The U-shaped bar in vertical position with the hook underneath the upper leg of the tie-down device to simulate the lifting action (see Figure 35). A tension load was applied on the bar, and the test was stopped at 36,600 lb when the load-deflection curve indicated that a permanent yielding was occurring during the test. The load was released, and the device was examined for damage. The bar was found to be deformed slightly under the hook. The tension load was applied again until the device broke at 37,200 lb. Visual examination of the failed device revealed that the end of the bar under the hook broke by shearing in the fillet weld, as seen in Figure 38. The size of the fillet weld was about 1/4 in, meeting the weld requirement of the 1/8-in-minimum-size single bevel-fillet weld joint specified in the AVLB drawing for the device.

- The U-shaped bar in horizontal position on the girder test plate (see Figure 39). Instead of using the chain and hook as before, a 1/2-in-diameter steel wire rope was looped five times around the bar to pull on it to simulate a lifting action in another direction (see Figures 40 and 41). The bar bent upward as the load increased until one welded end of it cracked at 12,050 lb. With the load still being applied, the bar continued to bend until the other welded end broke at 20,000 lb, and the test was terminated at this point. Figures 42–44 are the views of the failed device at the welds after the pull test. The ends of the bar cracked at the upper toe of both bevel-fillet welds. The size of the fillet weld was about 5/16 in. According to the load-deflections curve, the bar started to bend permanently at about 7,000 lb.

• At a much later date, three more original AVLB steel tie-down devices were subjected to more pull tests whereby the U-shaped bar of each device was being pulled straight out to simulate a lifting action in yet another direction. The devices themselves were removed from a Class 70 Modified AVLB that still has the original tie-downs. Each device sample for the pull test was refastened in the same holes to the aluminum girder test plate on the test jig with four 3/4-in-diameter Society of Automotive Engineers (SAE) grade 8 high-strength steel bolts and nuts. The bar was hooked at its apex for the straight pull-out test (see Figures 45 and 46). The tests were stopped at 40,000 lb, because of the load limitation on the chain and hook used to pull the bar, without a catastrophic failure to the first two device samples tested. However, a small crack was formed in the toe of both welds in both devices. The third device sample failed at 32,250 lb when one welded end of the bar broke loose from the base plate (see Figures 47 and 48). Visual examination of the weld failure revealed cold fusion of the weld metal to the plate (i.e., practically no weld penetration into the plate as seen in Figures 49 and 50).

The weight of the entire AVLB is about 30,000 lb. The quality of the welds at the ends of the U-shaped bar can have significant effect on the lifting capability of the original tie-down devices. Poor weld condition could mean failure of the devices at lower load. Because of this potential problem with the current devices, new lifting devices for lifting the Class 70 Modified AVLB were proposed with thicker and larger plates and larger diameter steel bars, both components made of stronger, heat-treated alloy 4130 steel. The new devices will be fastened with steel bolts to the girder plates in the same holes of the old devices which would already be removed during the modification.

2.9 Pull Tests on the Lifting Devices (Lifting Steel Bars) in the Roadway Decks of the Class 60 AVLB. Based on the findings of the pull tests conducted on the AVLB tie-down devices, another series of pull tests were conducted on the steel lifting bars in the extruded aluminum panel deck and aluminum ramp plate deck of the Class 60 AVLB in order to obtain more information on the lifting loads and failures and determine if they would be adequate to lift the entire Class 70 Modified AVLB. Each AVLB panel assembly has two lifting bars (positioned near each end to accommodate the center of gravity) in the deck that are to be used for the lifting purposes instead of the tie-down devices. The bar is shaped like a "dogbone" which is 5 in long and 3/4 in thick with a 1-in-wide reduced section and 1 1/2 in wide at each end with a 1/2-in-diameter bolt hole. It was bolted underneath the oblong hole that was cut in the treaded surface of the deck. The bar was fastened perpendicular to the long axis of the hole.

The pull tests were designed so that the lifting action on the bar in the roadway deck can be simulated on the testing machine. Two large aluminum sections were cut from the AVLB—one section from above

the center hinge area of the center panel assembly with three extruded deck panels still attached to the girder plates and the other section from the aluminum deck ramp area of the end panel assembly.

The large section with the deck panels was cut in such a manner that the surface of the roadway deck can be positioned at 45° on the testing machine. This setup will simulate the loading condition on the lifting bar in the deck when the legs of a lifting wire rope sling are used at 45° to lift the AVLB from four lifting points where the lifting bars are located in the roadway decks. A 3 1/2-in-diameter hole was machined in the side of both girder plates so that a round steel bar of the same diameter will go through the holes to attach the large section to the test jig fastened to the fixed crosshead of the testing machine. A large l-in-diameter egg-shaped steel ring was used around the lifting bar. The ring had to be bent to 20° offset in order to be paralleled to the loading axis. A large chain with a clevis hook was attached to the upper movable crosshead to pull on the steel ring, simulating the lifting action on the bar in the deck. A deflectometer was used to record the movement of the machine table during the test in order to determine when the lifting device (lifting bar) will deform and fail. The load was applied in tension to the bar until a failure occurred.

Figures 51–56 show the large section of the AVLB with the lifting bar in position in the testing machine; the bar bolted underneath the oblong hole in the extruded deck panel; the attachment of the ring, hook, and chain to the bar for the pull test; and the position of the deflectometer. Pull tests were performed on three lifting bar samples. For each pull test, a bar sample was fastened to the oblong hole in the deck panel of the same large AVLB section in the testing machine.

- First pull test: The lifting device with the original lifting bar failed at 20,250 lb by shearing out of the bolt holes in the deck panel at the oblong hole (see Figures 57–62). Apparently, with the steel ring against the upper edge of the oblong hole, the lifting bar was bending under the applied load, causing the bottom bolt to eventually shear the lower bolt hole in the deck panel. When that bolt hole sheared, then the bent lifting bar broke loose from the upper bolt hole of the deck panel by shearing also. Visual examination of the fractured surfaces of the sheared aluminum pieces from the bolt holes revealed small discolored areas which strongly indicated pre-existent cracks, probably caused by SCC, around the bolt holes in the deck panel prior to the pull test.

Preliminary stress calculation for the lifting device in the deck revealed that the failure load should have been higher than 20,250 lb at the time of the failure. Since the lifting bar bent into a U-shape during

the pull test, the strength of the steel bar may be inadequate for the proposed lifting application on the Class 70 Modified AVLB. A preliminary chemical analysis and hardness test on the bent bar indicated that the material was a mild carbon steel with about 67-ksi tensile strength, which conformed to ASTM A36 structural steel specified on the drawing for the lifting bar. The load defection obtained during the test revealed that something started to deform permanently at about 16,000 lb. It was suspected that the bar was bending during the test. The results of the chemical analysis and hardness test on the lifting steel bar from this pull test; tension and shear tests on the aluminum material of the extruded aluminum deck panel used in this test; and microstructural examination of the sheared aluminum pieces from around the bolt holes in the oblong hole of the panel are reported later in this report.

• Second pull test: This test was performed in the same manner as the first test except that a new stronger steel lifting bar was used and bolted to another aluminum deck panel that replaced the similar panel that was damaged during the first pull test. The new bar was machined from a stronger steel material known as "T-1" with a minimum yield strength of 100 ksi as compared to the specified ASTM A 36 with a minimum yield strength of 36 ksi. The deck panel with the new steel bar was bolted to the large AVLB section still attached to the testing machine (see Figure 51).

The lifting device with the new stronger lifting bar failed at 28,500 lb as compared to 20,250 lb in the first test. Cracks occurred at one end of the oblong hole to the end of the deck panel as well as in one of the bolt holes in the oblong hole to the edge of the panel (see Figures 63 and 64). According to the load-deflection curve obtained during this test, permanent deformation to the deck or lifting bar started at about 25,000 lb as compared to 16,000 lb in the first test. The lifting bar appeared to remain straight up to 25,000 lb before bending. As the load increased, a major crack occurred at one end of the oblong hole in the deck. The test was stopped after the crack propagated rapidly to the end of the panel.

The amounts of permanent bending in the lifting bars after both pull tests are shown in Figure 65. The new stronger bar did not bend as much at higher failure load as did the original mild steel bar at lower failure load. Visual examination of the fractured surfaces of the bolt holes that sheared in the oblong hole of the deck panel did not reveal the discolored areas that would indicate pre-existent cracks, as had happened in the bolt holes at the oblong hole in the panel used in the first test that may have contributed to the low failure load observed. The increase in the initial permanent deformation and failure loads observed during the second test may be contributed to the nonexistent cracks in the bolt holes.

• Third pull test: This test was performed on the lifting device with the original mild steel lifting bar in another deck panel in order to determine the maximum load at the time of the device failure, provided that no pre-existent cracks were present in the bolt holes at the oblong hole in the panel as had happened to the panel in the first test. The test was performed in the same manner as the previous two tests, still using the same large AVLB section attached to the testing machine. The lifting device with the original lifting bar failed at 23,500 lb maximum in this test as compared to 20,250 and 28,500 lb in the first and second tests, respectively. The bar had bent at the steel ring (see Figure 66).

According to the load-deflection curve obtained in this test, permanent deformation to the deck or bar started at about 21,000 lb as compared to 16,000 and 25,000 lb in the first and second tests, respectively, The first indication of the device failure in the deck panel took place in the lower bolt hole in the oblong hole by shearing on one side, and the crack continued to the edge of the panel. Then, upon further loading, a major crack occurred at one end of the oblong hole. The final failure occurred in shearing of a small section of the deck panel at the upper bolt hole in the oblong hole (see Figures 67 and 68). Before the final failure, the load was brought back to zero several times in order to permit examination of the area of the panel around the lifting device to locate the failures mentioned earlier. Visual examination of the fractured surfaces in the sheared areas around both bolt holes in the oblong hole of the panel used in this test did not reveal the discolored areas that would indicate pre-existent cracks, as had happened in the same bolt hole areas in the panel used in the first test. Again, chemical analysis and a hardness test on the original lifting steel bar used in this test were performed for comparison to the similar lifting bar used in the first test. The results are reported later in this report.

The next series of the pull tests performed was on the lifting device in the ramp deck section of the AVLB end panel assembly. In this case, a large section (30 in wide and 60 in long), containing the oblong hole with the lifting steel bar, was cut from a male end panel assembly to serve as a test specimen (see Figure 125 for the location of the section and Figures 69–71). The section contained three 6-in × 2 1/2-in aluminum channels in the longitudinal direction with both ends connected to the aluminum plates with the sections of aluminum and steel angles and aluminum buttonhead rivets in order to retain the integrity of the deck section for the pull tests of the lifting bar samples. The 1/2-in-thick aluminum tread floor plate was still fastened by aluminum countersunk head rivets to the flanges of the channels and angles on the ends. The oblong hole in the floor plate was between two channels.

A welded steel test jig was designed and fabricated. It was bolted to the bottom end of the large test section. In addition, steel straps were used to reinforce the end plate of the section to prevent it from flexing during the pull tests. The section was installed in position in the testing machine so that the lifting device would be pulled at an angle to the bottom plane of the floor deck of the AVLB end panel assembly (see Figures 72 and 73). This would simulate the loading condition on the lifting bar in the oblong hole when the legs of the lifting sling are at 45° to lift the AVLB. A large chain with a clevis hook was used to pull on the lifting bar in the test section. A deflectometer was used to record the movement of the testing machine table in order to observe when a component in the test section was deforming before the complete failure occurred.

A number of pull tests were made on several lifting steel bar samples, as follows:

- The original lifting bar in the large test section was pulled to 13,500 lb, which was stopped at this point when the deflectometer malfunctioned. The load was released, and the bar was inspected visually. It was already bent slightly in two directions—vertically and horizontally. The bar was pulled again, this time to 20,600 lb maximum. After the test, the bar was removed and inspected. It was bent more permanently than the first pull test.

- A new stronger lifting bar that was machined from T-1 steel material was installed in the test section and pulled to 25,000 lb. The load was released, and the bar was inspected visually. It was slightly bent. The new bar was pulled again, this time to about 27,000 lb when the deflectometer malfunctioned again. The load was lowered to 25,000 lb, and the deflectometer was repaired. The load was increased to about 28,000 lb when the chain slipped suddenly out of the gripping wedge jaws in the upper movable crosshead of the testing machine. The test was stopped, and the chain was attached more firmly in the jaws. The new bar again was pulled to 39,500 lb maximum when the test was stopped at this point because of the load limitation on the chain and hook. The load was released, and the bar was removed and inspected. It was bent slightly more in both directions. In addition, both countersunk head steel bolts that were used to fasten the bar under the oblong hole in the floor plate were slightly bent. Also, the countersunk bolt holes in both sides of the oblong hole were slightly elongated.

- Another original lifting steel bar was removed from the same AVLB end panel from which the large test section was cut. It was at location B in Figure 125. The bar was installed in the test section

and pulled to 30,000 lb maximum before the load was released. It was removed and inspected. It was bent more vertically and horizontally than the first original bar tested (see previous paragraph).

• The time at which the original lifting steel bar samples began to bend permanently during the pull tests could not be determined from their load-deflection curves recorded during their pull tests. Therefore, another original lifting bar was removed from an AVLB-extruded aluminum deck panel. The plan was to apply the loads in increments to the bar sample until permanent bend had occurred visually. The original bar sample was installed in the test section and pulled initially to 10,000 lb, and the load was released for visual inspection of the bar. It was observed to be already bent permanently after a load of 10,000 lb was applied.

Figures 74 and 75 show the extent of permanent bend in the lifting bar samples after their pull tests. One other observation was made on the test section during the pull tests. The area around the oblong hole in the floor plate would bulge during the pull test on the lifting bar where the bolted ends were pulled against the oblong hole from underneath the floor plate.

However, the oblong holes in the roadway decks of the AVLB will not allow the use of the four-leg lifting wire rope sling with hooks, currently used in the docking areas, to lift the modified bridge to be loaded for transportation. The hooks on the sling are too large to go in the oblong holes to grab the lifting bars to lift the whole bridge. To resolve this lifting problem, the new lifting device, similar to the configuration of the original tie-down device, was then designed to be made larger and stronger than the tie-down device now on the AVLBs. The new device would be bolted to the girder of the bridge in the same rivet holes after the old tie-down device was removed during the bridge modification. The testing of the new device is reported later in this report.

2.10 Failure Analysis of Small Pieces Sheared From the AVLB Extruded Aluminum Deck Panel. As mentioned earlier in this report, the first pull test performed on the lifting device in the AVLB extruded aluminum deck panel revealed pre-existent cracks in the counterbored bolt holes at the oblong hole in the panel for the lifting device (dogbone-shaped lifting steel bar). The bar broke loose during the test by shearing from both 1/2-in-diameter bolt holes at the oblong hole. Several small pieces (see Figures 59 and 60) of the deck panel also broke away from around both bolt holes. Preliminary visual examination of the broken pieces revealed the discolored areas in the fractured surfaces, indicative of pre-existence cracking around the bolt holes in the deck panel for the lifting bar prior to the pull test because of possible SCC. This was the reason for failure analysis.

Further visual examination of the pieces also revealed that the discolored areas had extended inward from the sharp fillet at the bottom of the counterbore made in both bolt holes in the deck panel (see Figure 76). Some exfoliation was observed on the surface at the bottom of the counterbore in the space between the bolt head and counterbore wall. Because of the protruded treads on the top surface of the extruded deck panel to provide the surface traction for the vehicles crossing the AVLB, the bolt holes in the panel for the lifting device had to be counterbored in order to provide the clearance needed for the bolt head and the socket tool (see Figure 77). This left a sharp fillet in the bottom of the counterbore of both bolt holes cut into the protruded treads, thus creating a stress raiser for the crack initiation. Figures 78–80 are the microstructures of a metallographic specimen of a broken piece with the discolored area showing evidence of intergranular corrosion and small intergranular cracks. This was indicative of SCC.

Apparently, over a period of time in the field, SCC occurred in the counterbored bolt holes where the dirt was trapped due to the traffic over the AVLB deck. The moisture or water was entrapped in the dirt, penetrating the paint coating and corroding the aluminum. Cracks were initiated in the sharp fillet of the counterbored hole. Since the extruded deck panels were made from aluminum alloy 2014-T6, this alloy was susceptible to SCC and exfoliation under certain corrosive environmental conditions encountered by the AVLB in the field.

In general, SCC and some exfoliation had occurred in the counterbored bolt holes in the AVLB-extruded deck panel at the oblong hole for the lifting device. The cracks had initiated in the sharp fillet (stress raiser) in the counterbored holes, resulting in lower failure load than expected during the pull test.

2.11 Tensile and Shear Properties of the AVLB Extruded Aluminum Alloy Deck Panel. Tensile and shear tests were conducted on the AVLB extruded aluminum alloy deck panel that contained the lifting device that was tested during the first pull test mentioned earlier in this report. The lifting bar broke loose from the deck panel by shearing from the bolt holes at the oblong hole in the panel. Also mentioned earlier, pre-existent cracks were present around the bolt holes. The aluminum alloy specified for the extruded deck panels on the AVLB was alloy 2014-T6, conforming to ASTM B 221 for aluminum and aluminum-alloy extruded bars, rods, wire shapes, and tubes.

Two standard 1/2-in-wide rectangular tension test specimens were cut from the 1/4-in-thick sidewall of the deck panel. Also, two subsize 1/4-in-wide rectangular tension test specimens were cut from between the rows of the protruded treads on the top surface of the panel. Two shear test specimens were cut from the

panel sidewall also. A shearing die apparatus with a 1-in-diameter opening was used in the shear tests to shear the specimens.

The results of the tensile and shear tests on the test specimens cut from the AVLB extruded aluminum deck panel are given in Table 4. The tensile properties obtained were above the minimum values for alloy 2014-T6 in ASTM B 221. The average shear strength obtained for the deck material was 46,800 psi as compared to 42,000 typical for alloy 2014-T6. Qualitative x-ray fluorescence analysis revealed that the deck material was a 2000 series aluminum alloy.

2.12 Composition and Hardness of Two Original Lifting Steel Bar Samples From AVLB Deck Panels. The composition and hardness were determined for two bent, dogbone-shaped original lifting steel bar samples—one of them was from the first pull test and the other from the third pull test on the lifting device in the oblong hole of the AVLB extruded aluminum deck panels. ASTM A 36 for structural steel was specified for the lifting bar (P/N 13211E7821). As an option, ASTM A 688, Class D for carbon and alloy steel forgings for general use, was also specified for the lifting bar.

Specimens were cut from both lifting bar samples, labeled as first bar from the first pull test and second bar from the third pull test, for chemical analysis, hardness tests, and microstructural examination.

The results of the chemical analysis and hardness test on the lifting bar samples are given in Table 5. Based on the composition, hardness, and approximate tensile strength, the steel material of both lifting bars conformed to ASTM A 36 as specified. Microstructural examination revealed that both bars were made from a mild carbon steel in the hot-rolled condition.

2.13 Metallurgical Evaluation and Mechanical Properties of Aluminum Huckbolt Fasteners. Because a few corroded hot-driven aluminum alloy 7277 rivets with the heads missing were found on a number of Class 60 AVLBs that were brought back to the United States from Southwest Asia after Operation Desert Storm for repairs and refurbishments, 3/4-in-diameter aluminum Huckbolt fasteners have been proposed for use on the AVLBs to replace the aluminum rivets, particularly in the critical areas such as the center hinges and bottom chords. "Huckbolt" is a registered trademark of Huck International, Inc. Figure 81 shows a two-piece aluminum C50L Huckbolt fastener which consists of a pin with the locking grooves and installation stem and a collar. With an appropriate installation tool, the collar is swaged on the locking grooves of the pin, and the stem is broken off like the familiar "pop" rivet (see

Figures 82–84). The Huckbolt fasteners will be used extensively when a number of Class 60 AVLBs will be modified to Class 70, thereby eliminating the need to heat the aluminum rivets prior to hot-driving. Most of the Huckbolt fasteners will be aluminum pin and collar, and a few of them will be steel pin with aluminum collar. Roundhead and countersunk head pins will be used on the AVLB where applicable during modification.

A number of tests were performed on aluminum Huckbolt fastener samples in order to obtain pertinent information about them for comparison to the hot-driven aluminum rivets. The Huck representatives had installed a number of 3/4-in-diameter aluminum buttonhead Huckbolt fasteners to fasten aluminum parts together to simulate certain AVLB components. This was done at ANAD during the demonstration of fastener installation.

The following fastener samples were received for evaluation:

- A new 3/4-in-diameter aluminum roundhead Huckbolt pin (P/N C50LR-C24-12) and aluminum flanged collar (P/N 3LC-F or I24). See Figure 81.

- Four Huckbolt-assembled aluminum shear test specimens:

  (1) Specimen A with a fully swaged collar (see Figure 83).

  (2) Specimen B with a fully swaged collar (see Figure 83).

  (3) Specimen C with a 1/2-swaged cinch-on collar.

  (4) Specimen D with a 1/4-swaged cinch-on collar.

Each shear test specimen is composed of two 3/8-in-thick aluminum angles fastened back to back to the 3/8-in-thick center plate that will serve as the plunger to shear the shank of the pin during the shear test.

- A section of two 5-in × 3/8-in-thick aluminum equal leg angles fastened back to back with three Huckbolt fasteners, each installed in a different manner.

  (1) Specimen E installed with two angles back to back in contact with each other with no space.

(2) Specimen F installed with two angles fastened together with two large flat washers between them.

(3) Specimen G installed with two 1/4-in-square steel bars to serve as spacers between two angles to form a 1/4-in gap (see Figure 85).

The following tests were performed:

- Shear test to shear the Huckbolt aluminum pin (see Figure 86 for the shear test setup).

- Push test to determine the load required to push the pin-locking groove end out of the swaged aluminum collar (see Figure 87 for the push-test setup).

- Hardness test (Brinell, Rockwell, or Knoop).

- Chemical analysis (x-ray spectrometric analysis of the aluminum collar).

- Tension tests.

In addition, radiographic inspection was performed on the collars swaged on the locking grooved end of the pins in order to determine the extent of the groove penetration into the interior wall of the collar after the swaging. This was done before and after the shear or push tests.

The results of chemical analysis and hardness tests on the aluminum collars are given in Table 6. The composition indicated that the collar was made of aluminum alloy 6061. The hardness of the new unswaged collar was 62HB (Brinell hardness), indicating typical hardness for 6061 in T4 temper condition. Qualitative x-ray analysis of the Huckbolt aluminum pin revealed that it was made from a 2000 series aluminum alloy such as alloy 2024. The hardness of the pin was 117HB, indicating typical hardness for alloy 2024 in T4 temper condition.

The results of the shear and push tests on the 3/4-in-diameter aluminum Huckbolt fasteners are given in Table 7. The average shear strength for the aluminum pins was 43,200 psi, which exceeded the minimum shear strength of 37,000 psi in ASTM B 316 for alloy 2024 in T4 temper condition. Based on similar shear tests conducted on the AVLB-corroded hot-driven buttonhead aluminum alloy 7277 rivets

and will be reported in a U.S. Army Research Laboratory (ARL) technical report,* their average shear strength was 47,670 psi as compared to 43,200 psi for the Huckbolt aluminum pins tested. Figure 88 shows a sheared pin where double shearing took place in the pin shank during the shear test. Figure 89 shows the elongated hole in the center aluminum plate plunger after the shear test.

The maximum loads required to push the locking grooved end of the Huckbolt aluminum pins out of the swaged aluminum collars ranged from 17,850 to 21,350 lb. A number of radiographs were obtained of the collars swaged on the pin-locking grooves to reveal the penetration of the grooved tips into the collar interior wall. Figure 90 shows the radiographic image of the new collar not swaged on the pin-locking grooves. Figures 91–93 show the number and penetration of the grooved tips into the interior wall of three swaged collars (fully, one-half, and one-quarter swaged) on the shear test specimens. The amount of grooved tip penetration into the swaged collar interior wall was about one-third deep, which was considered normal by the Huck representative of the installed large aluminum Huckbolt fasteners.

Figures 94 and 95 are radiographic images of fully swaged collars of Specimen G after the push test was stopped just after the maximum load of 21,350 lb was reached and before complete shearing of the collar interior wall occurred during the test. Figures 96 and 97 show the as-ground cross sections of the same swaged collar and pin (Specimen G) cut in half lengthwise to reveal the small amount of initial shearing that took place in the collar interior wall just after the maximum load was reached and the test was stopped then. The buildup of the penetrated wall material can be seen as the result of the tip of the pin-locking grooves pushing against the penetrated interior wall of the collar during the test.

Figures 98 and 99 show the etched microstructures of the swaged collars and pins from Specimens F and D. Deformed grain structure can be seen in the pin-locking grooves, indicating that the grooves were cold-rolled on a portion of the pin shank by the manufacturer. Figure 100 is the sketch of the hardness survey made across the portions of the swaged collar and grooved pin of Specimen F. The hardness was higher in the cold-rolled groove tip, which explained why the locking grooves were not damaged when they penetrated and sheared the interior wall of the swaged collar during the push test. The collar was softer than the pin to permit ease of swaging during the installation of the Huckbolt fastener. Partial penetration of the pin-locking grooves into the interior wall of the swaged collar instead of full penetration was sufficient for the clamping or holding purposes for the intended application.

---

*Horner, Howard E. "Failure Analysis and Mechanical Tests of Failed Aluminum Alloy 7277 Rivets on Armored Vehicle Launched Bridge." ARL report, U.S. Army Research Laboratory, Aberdeen Proving Ground, MD, to be published.

The yellow-gold color observed on the surface of the Huckbolt aluminum pin samples may indicate that they were anodized for protection against corrosion. Figure 101 shows the thin anodized coating on the surface of a locking groove of the Huckbolt pin (Specimen F). The thickness of the coating was 0.267 mil.

A special push test was performed on Specimen G with the 1/4-in gap in order to determine the amount of load required to deflect two vertical angle legs to the same deflection that occurred by the clamping force of the Huckbolt fastener installed during the demonstration at the Army depot. After the test to push out the grooved end of the pin from the swaged collar, Specimen G was set up again in the testing machine in a manner so that the two vertical legs separated by the same two 1/4-in-square steel bars could be compressed together by the same amount of deflection seen in Figure 85. With the aluminum collar in place above the hole of the top angle leg to simulate the clamping action, a load of 2,900 lb was required to compress the two angle legs together to 0.080-in deflection in the 1/4-in gap. This would be the approximate clamping force applied by the 3/4-in-diameter aluminum Huckbolt fastener during installation.

The following tensile tests were conducted on several 3/4-in-diameter Huckbolt fastener aluminum pin samples:

- Two pin samples in order to determine the load required to break off the installation stem at the large breakaway notch in the pin. The head of each sample was cut off first before the pin was placed in the gripping devices on the testing machine. The pin was then pulled apart until the stem broke off at the notch, as would happen during the installation of a Huckbolt fastener.

- A third pin sample that has a similar breakaway notch machined on the smooth pin shank (see Figure 102) in order to determine the effect of the notch in the base metal in the area that was not affected by cold rolling as had occurred in the original cold-rolled breakaway notch. The pin sample broke in the machined notch rather than in the cold-rolled notch.

- A fourth pin sample that has a reduced section machined to the same diameter of 0.419 in as the root of the cold-rolled notch, thereby forming a smooth section without the notch. The reduced section was 2 in long, with the location of the notch root in the middle. The tensile test on this pin was done in order to observe the effect that cold rolling had on the base metal in the area under the cold-rolled root of the notch. The pin broke in one necked-down region near one side of the notch root in the reduced section. The necking down of the reduced section occurred on both sides of the cold-rolled notch root

during the test, showing clearly the effect of cold rolling the breakaway notch on the pin by enhancing the surface mechanical properties.

- A 1/4-in-diameter subsize tension test specimen with 1-in gauge length in order to determine the basic tensile properties of the pin base material without the effect of surface cold rolling. It was machined from the broken section of the third pin sample in the previous paragraph.

The results of the tensile tests on the 3/4-in-diameter Huckbolt fastener aluminum pin samples are given in Table 8. The average load required to break off the installation stem at the large cold-rolled breakaway notch of two pin samples was 15,840 lb, which translated to 113,790-psi notch tensile strength. Meanwhile, the breaking load and notch tensile strength were 13,340 lb and 90,180 psi, respectively, for the machined notch in the smooth, not cold-rolled shank area of the third pin sample, confirming that the effect of cold rolling the large breakaway notch in the pin had resulted in higher tensile properties. The microstructural examination of the metallographic specimen containing the cross section of the large breakaway notch revealed the elongated grain structure in the notch area as the result of cold rolling as was normally done during the manufacture of the Huckbolt aluminum pins (see Figure 103).

The average properties obtained for both the reduced tension test specimen of the fourth pin sample (previously mentioned) and subsize tension test specimen of the broken third pin sample (previously mentioned) were 70,580-psi tensile strength and 45,130-psi yield strength. They met the minimum requirements specified for aluminum alloy 2024-T4 in ASTM B 316 for aluminum alloy wire and rod for manufacturing rivets and other similar items by cold-heading operations.

2.14 Pull Tests on New Lifting Devices (First Design) Proposed for the Class 70 Modified AVLB. Based on the findings as the results of the pull tests that were conducted on the tie-down devices on the girders and the lifting devices in the roadway decks of the current Class 60 AVLB, a new lifting device was designed stronger and larger as a replacement for the original tie-down device for use on the Class 70 Modified AVLB for the lifting purposes. As shown in Figure 104, the new device, which is a modification of the tie-down device, is composed of a 1 1/8-in-diameter steel bar that was formed into a 3-in inside diameter "U" shape with both ends inserted into the through holes in an 8-in × 7-in × 3/4-in steel plate. This will permit the use of the standard four-leg lifting slings currently used in the docking areas for the lifting of the modified AVLBs. Each end of the bar was welded in the hole on both sides of the plate (i.e., a groove weld on the bottom and a fillet weld on the top of the plate for each end of the bar). The U-shaped bar was orientated 30° from either side of the vertical axis of the plate so that it will

be more or less in line with the leg of the lifting sling that will be used to lift the folded modified AVLB at four lifting points on the bottom folded half of the bridge.

Four 7/8-in-diameter holes were made in the plate at the same locations as the rivet holes in the tie-down plate. This was done so that the hole locations in the new plate will match the rivet holes in the AVLB aluminum girder plates when the original tie-down devices will be removed to be replaced with the new lifting devices. A 1/2-in-thick steel plate of the same shape and size as the thicker plate of the new device will serve as the reinforcement back plate. Four 3/4-in-diameter SAE grade 8 steel bolts, nuts, and washers will be used to fasten the new device to the girder plate on the outside in the former rivet holes with the back plate on the inside.

Pull tests on the new devices were conducted in a manner similar to that described earlier in this report for the pull tests of the original tie-down devices. The tests attempted to simulate the lifting of the folded bridge with respect to different orientations of the new devices to three types of loading conditions with the lifting sling.

Six new lifting devices were made of ASTM A 36 structural steel round bars and plates. They were fabricated and welded at the Belvoir Machine Shop. Large sections of the AVLB aluminum plate were cut from the AVLB end and center panel assemblies to serve as the test plates to which the new devices can be fastened with bolts for the pull tests. A special test jig that was used in the previous pull tests of the tie-down devices was slightly modified and used for testing of the new devices. For each pull test, a new device was bolted to the girder test plate with 3/4-in-diameter steel bolts (see Figure 105). The girder plate, in turn, was bolted to the test jig, which was placed in position under the lower fixed crosshead of the testing machine (see Figure 106). A large chain with a clevis hook was used to hook the new device in a manner similar to lifting the bridge at a lifting point. Where applicable, a deflectometer was positioned on the test jig to measure the movement of the U-shaped bar under applied load in order to determine approximately when permanent deformation of the device occurred during loading. Load-displacement curves were recorded during the pull test.

Three types of the pull tests on the new lifting devices (two per test type) were conducted as follows:

(1) Straight-out pull test (Nos. 1 and 2) whereby the load was applied to the U-shaped bar of the lifting device in such a manner that the bar will be pulled straight out from the plate (see Figure 107 for the test setup). A maximum load of 40,000 lb was applied to the device in the pull test so as not to

exceed the load limitations of the chain and hook. No apparent permanent damage to the bar and 3/4-in-thick front steel plate was observed; however, the 1/2-in-thick back steel plate did bend permanently.

(2) Perpendicular pull tests (Nos. 3 and 4) whereby the load was applied to the U-shaped bar, which was in the horizontal position in the testing machine (see Figures 108 and 109 for the test setup). This will cause the bar to be bent upward with the load (see Figures 110–112 on the results of this type of the pull test on the new lifting device). According to the load-defection curves obtained during the tests, the bars of two new devices tested started to bend permanently at about 6,000–6,500 lb. It continued to bend as the load increased, even to the point that the cracks occurred in the upper toe of the fillet welds around both bar legs in one of two devices tested. The maximum load reached was 26,150 lb when the load started to drop as the result of the crack. The test was stopped after a load of 35,000 lb was reached on the other device tested.

(3) Parallel pull tests (Nos. 5 and 6) whereby the load was applied to the U-shaped bar which was in the vertical position in the testing machine (see Figures 113 and 114 for the test setup). This will cause the upper leg of the bar with the hook under it to be under load up to 40,000 lb maximum. Figure 115 shows the extent of permanent damage to the leg under the hook after the pull tests. According to the load-deflection curves obtained, the upper leg of two devices tested started to bend permanently at about 22,000–23,000 lb.

No significant damage was noted on the three aluminum girder test plates used in the pull tests. This indicated that the girder plates on the AVLB would be able to withstand the lifting loads at the lifting points that were the same locations as the original tie-down devices.

The new lifting device at each lifting point on the girder plate of the bridge will have the orientation (30° on either side of the vertical axis) of the U-shaped bar more or less in line with the leg of the four-leg lifting sling. The worst possible scenario would be to lift the folded bridge using the new devices on the upper folded half and with the ramp ends tied together with a chain to prevent unfolding of the bridge during lifting. In this case, the loading of the lifting devices on the bridge during the lifting would be similar to the perpendicular pull test. As stated before in regard to the result of this type pull test, the bar began to bend permanently at about 6,000 lb. Since about 7,500 lb or more will be exerted on each lifting device when the bridge, which weighs 30,000 lb, is lifted in the scenario described previously, the bars may bend slightly and permanently at 7,500 lb, but they will not fail catastrophically, as verified at higher loads in the pull tests. Nevertheless, a stronger steel material for the U-shaped bar as well as the back

plate is needed, based on the results of the different types of pull tests conducted on the new lifting devices proposed for the Class 70 Modified AVLB.

2.15 Hardness of the New Steel Lifting Device (Second Design) Proposed for the Class 70 Modified AVLB. Hardness tests were conducted on three components of a new lifting device of the second design proposed for use on the Class 70 Modified AVLB. The second design was based on the results of the pull tests performed on the previous new lifting devices of the first design. The main differences between the first and second designs are the use of alloy steel UNS G41300 instead of weaker ASTM A 36 structural steel, a thicker and larger back plate, larger front plate, and two more 7/8-in-diameter holes in both plates. Three components of the new device are to be heat treated after welding. The new devices of the second design will replace the tie-down devices at the same locations on the girder plates of the modified AVLBs.

A number of the new lifting devices of the new design were fabricated at the Belvoir Machine Shop to be installed on an AVLB for the lifting tests to evaluate their performance. When no 3/4-in plate made of steel alloy UNS G4130 was available in the shop, an ASTM A 36 structure steel plate of the same thickness was used in its place for the two plates of the new design. The 1 1/8-in-diameter U-shaped bar that was made of annealed UNS 4130 alloy steel was welded to the front plate. The welded components of the new device were then heat treated to increase the strength of the bar. The 3/4-in-thick back steel plates for the new devices were not heat treated. A set of the new devices was selected after the heat treatment for the hardness test on three steel components. A portable Brinell hardness tester with a 10-mm steel ball and 3,000-kg load was used for the tests.

The results of the hardness tests on three steel components of the new lifting device of the second design are as follows:

(1)	1 1/8-in-diameter U-shaped bar: (heat-treated UNS G4130 alloy steel)	340 HB equivalent to 36 HRC (Approx. 159,000-psi tensile strength)
(2)	3/4-in-thick front plate: (heat-treated ASTM A 36 steel)	183 HB equivalent to 90 HRB (Approx. 89,000-psi tensile strength)

(3)	3/4-in-thick back plate: (ASTM A 36 steel, not heat treated)	149 HB equivalent to 81 HRB (Approx. 75,000-psi tensile strength)

NOTE: HB is Brinell hardness, HRB is Rockwell B hardness, and HRC is Rockwell C hardness.

Since ASTM A 36 material is a mild carbon steel, the increase in hardness obtained for the heat-treated front plate may be due to the surface-hardening effect with the core being softer because of the plate thickness.

The new lifting devices were then installed on an AVLB in the same locations as the tie-down devices, which were removed to serve as the lifting points. They performed satisfactorily under various lifting conditions when the bridge was lifted during the lifting tests.

2.16 Inspection and Testing of Two Class 70 Modified AVLBS. Again, based on the findings of the various tests performed at Belvoir by this laboratory during the Class 70 AVLB modification program, ANAD had modified two current Class 60 AVLBs to Class 70 for tests and performance evaluation (see Figure 116). The following modifications were made on both AVLBs at the depot:

- Larger center hinges to be made of stronger forged aluminum alloy 7050-T7452 to replace alloy 2014-T6 (see Figure 117). Because the hinge forgings would not be available during the modification of two bridges, the hinges at that time were machined from large alloy 7050 plates or forged billets.

- Larger and stronger bottom chord aluminum alloy 7050-T76511 angles in place of original alloy 2014-T6 angles. The angles were long enough to join the center and end panel assemblies permanently to form one bridge section after the forged bottom aluminum connectors were removed entirely. Alloy 7050 flat bars were used as reinforcements at the joints (see Figure 118).

- Larger and stronger aluminum alloy 7050-T76511 angle splices at the joint where the steel ramp end section was spliced to the aluminum section of the end panel assembly (see Figures 119 and 120). Also, a 1/4-in-thick T-1 steel bottom plate was used in place of alloy 2014-T6 at the splice joints.

- Roundhead and countersunk head Huckbolt aluminum fasteners were used in the center hinges, bottom chord angles, and splices. A few Huckbolt steel fasteners with aluminum collars also were used

where applicable. The Huckbolt fasteners replaced the hot-driven aluminum alloy 7277 rivets in the bottom chords.

- New larger lifting devices made entirely of heat-treated steel alloy UNS G41300 were bolted in the same rivet holes in the AVLB girder aluminum plates after the riveted steel tie-down devices were removed.

The prototype No. 1 Class 70 Modified AVLB was sent from ANAD to APG for the crossing fatigue tests in the field. Several pull tests were conducted on the new lifting devices on the bridge at APG. Two of them failed in the tests at about 30,000 lb. The U-shaped steel bar of one device was pulled out of the plate holes. Visual examination of this failed device revealed that the sizes of the groove and fillet welds were too small, even though meeting the partial joint penetration groove weld design on the drawing. However, for future Class 70 AVLB modification, the weld-joint design was changed to full joint penetration weld for welding both ends of the U-shaped bar in the holes of the front plate.

After the 2,000 M1A1 armored tank crossings on the bridge at APG, the bridge was sent to Belvoir for additional simulated crossings. Before the fatigue testing under the load frame at the Belvoir Bridge Hangar, the bridge was inspected visually for visible cracks. One minor crack was found at the bottom of an inboard vertical aluminum structural angle of one interior cross brace. The bridge was inspected several times during a series of simulated crossing fatigue tests. After a total of 1,000 simulated crossings under three different loading conditions (midspan, two-third span, and quarter span), no new cracks were found, and the minor crack had remained the same.

The prototype No. 2 Class 70 Modified AVLB arrived at Belvoir from ANAD for static overload tests and the ultimate failure test. It was inspected for visible cracks before and after the overload tests. No cracks were found before and after the 131-, 145-, and 158-ton overload tests. For the ultimate failure, the loads, starting above the maximum overload load, were applied at 10-ton increments for 10 min each at the midspan until the bridge failure occurred. While the load was increasing from 180 tons to 190 tons, the modified bridge buckled suddenly at about 190 tons (more than twice the Class 70 load) in the top chords of both female bridge sections, causing the girder aluminum plates also to buckle outward or inward from top to bottom (see Figures 121–124). The buckling occurred near the outer or middle footpads of the special loading device on each treadway at the midspan of the bridge. Other damages observed after the failure were the following: a 6-in-long crack in the inside corner at the bottom of an inboard vertical aluminum structural angle of the center interior cross brace inside the center panel of one female bridge section; a broken upper corner of the aluminum plate in two transverse braces; cracks at

top of the long and short outer inboard vertical aluminum angles that a transverse brace was attached to at the upper corner; extensive cracks in a number of extruded aluminum deck panels above the buckled areas of the failed bridge; bent vertical legs of the bottom chord aluminum angles due to the buckling in the girder plates; and a pushed steel pin for the lateral brace. In addition, the steel curbs that were bolted at the outer edge of the treadways on top of the deck panels with long steel bolts through the outer horizontal leg of the top chords broke loose at the buckled areas. Several bolts broke or were pulled through the bolt holes in the angle legs. All those damages were caused by the secondary effects of the bridge buckling at the time of the failure.

Except for the bent bottom chord angles at the buckled areas, the modified bottom chords, center hinges, and splices in four bridge sections did not fail by cracking during the ultimate failure test. The Class 70 modifications to the bottom chords, including the center hinges, splices, permanent joining of both the center and the end panel assemblies, and the use of the Huckbolt fasteners, were successful. The Class 70 Modified AVLB will be capable of carrying Class 70 tracked and wheeled loads over a 60-ft-wide gap.

3. CONCLUSIONS

Based on the results of limited mechanical and special tests, failure analyses, and visual inspections performed on the modified AVLBs during the Class 70 modification program, it is concluded that:

- The sharp fillets machined in the forged aluminum center hinges and bottom connectors acted as stress raisers (stress concentration) where small fatigue cracks had initiated that led to catastrophic failures in either part when the modified bridges were undergoing fatigue tests. Because of a potential failure in the bottom connectors, a modification will involve elimination of them entirely and include permanent joining of both the end and the center panel assemblies to form a bridge section with continuous and stronger bottom chord aluminum angles. The Class 70 Modified AVLB will be composed of four bridge sections (two females and two males) instead of eight panel assemblies (four ends and four centers) for the current Class 60 AVLB.

- Current aluminum alloy 2014-T6 structural angles for the bottom chords and splices will be replaced by stronger and larger alloy 7050-T76511 angles. The modified splices will not have a sharp corner to act as a stress raiser as did the original splice.

• The forged aluminum center hinges will be made larger and stronger with smooth contours (no sharp machined fillets). Stronger alloy 7050 forgings will replace original alloy 2014-T6 forgings.

• A 1/4-in-thick T-1 steel plate will replace the aluminum plate on the bottom of the bottom chord at the splices.

• The original steel tie-down devices on the girder plates and the lifting devices in the deck treadways were not suitable for lifting of the entire Class 70 Modified AVLB. A larger and stronger lifting device made entirely of heat-treated steel alloy UNS G4130 was designed to replace the tie-down device which will be removed and replaced with the new lifting device in the same rivet holes in the girder plate.

• The Huckbolt aluminum and steel fasteners in place of the hot-driven aluminum alloy 7277 rivets were considered suitable for use in the modified bottom chords, including the center hinges and splices. Therefore, the ovens needed for heating the aluminum rivets and the hot-driving riveting process were eliminated.

• Based on the fatigue tests done at this time on the prototype No. 1 Class 70 Modified AVLB, and based on the overload tests and results of the deliberate failure on the prototype No. 2 Class 70 Modified AVLB, the modifications proposed and made on those bridges were deemed satisfactory for conversion of current AVLB from Class 60 to Class 70 to continue with the production of 53 Class 70 Modified AVLBs by ANAD for the Army.

The Marine Corps also plans to convert 55 of its AVLBs from Class 60 to Class 70 at its depot. It will use similar modifications proposed by the Army based on the data obtained during the Class 70 modification program at Belvoir.

4. RECOMMENDATIONS

With extensive modifications proposed for the bottom chords, including the center hinges and splices, the Class 70 AVLB modification program was a success. One recommendation is that a procedure for welding the ends of the U-shaped alloy 4130 steel bar in the holes of the front alloy 4130 steel plate of the new lifting device be established to include preheating of both parts to avoid potential cracking in the toe of the fillet welds on top of the plate. As mentioned earlier in the report, the weld joint design for

the new lifting device was changed from partial to complete joint penetration welds of the bar legs in the holes of the 3/4-in-thick plate.

One of the observations that was made about both Class 70 Modified AVLBs was the overtightening of the long bolts through the top chord angle leg to fasten the steel curbs to the top of the deck panels, causing the leg to bend at those bolts. In addition, it was known that when the curbs were sometimes hit hard by the vehicles crossing the bridge, the deck panels as well as the top chord angle legs were damaged at the long bolts, even causing the bolts to shear through the bolt holes in the angle legs and deck panels. One recommendation that should be considered is to fasten the steel curbs directly to the deck panels only, not with the bolts through the panels to the top chord angles. This way, when the curb should happen to break loose, the damage will be restricted to the deck panels where the curb was bolted. The damaged panels can easily be replaced, and the top chord angles will remain intact.

The aluminum pins of the Huckbolt fasteners that were tested and evaluated as the replacement for the hot-driven aluminum rivets in the bottom chords were anodized. It is well known that the fatigue life of the anodized aluminum parts can be shortened. Because of the dynamic cyclic loadings that can occur in the AVLB during the crossings of the heavy vehicles, the aluminum pins of the Huckbolt fasteners should not be anodized for use in the modified bottom chords. Nonanodized Huckbolt aluminum fasteners were used in both prototype Class 70 Modified AVLBs that were fabricated for tests and performance evaluation.

In the event the new Class 70 Modified AVLB should be damaged in the field as extensively as had occurred to the prototype No. 2 Class 70 Modified AVLB during the bridge failure test, such as buckling in the top chords and girder plates, it should not, as a precaution, be used again for vehicle crossings. The uncertainty on the extent of the bridge damages makes it necessary for safety reasons to prevent personal injuries, death, and loss of the equipment.

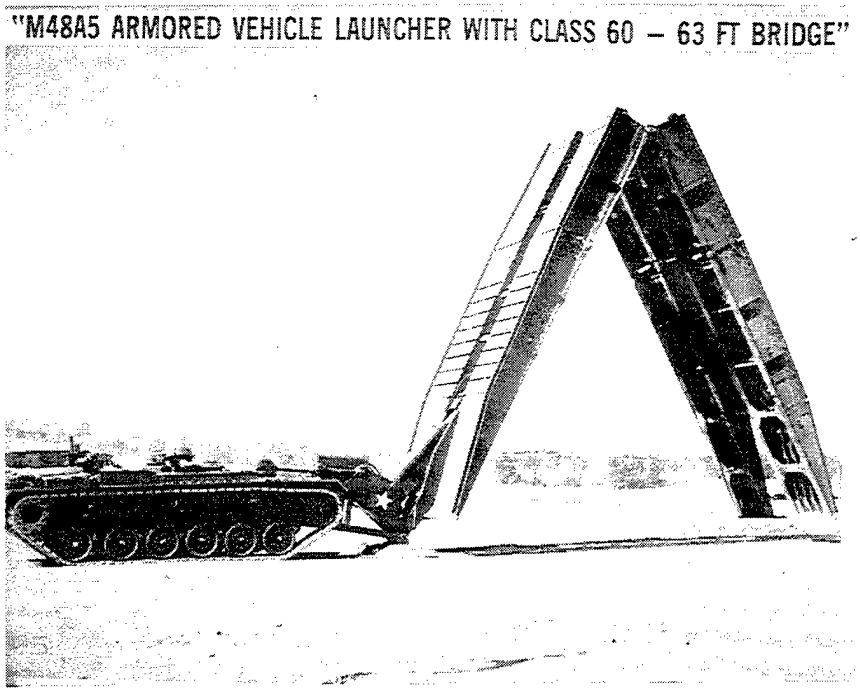

Figure 1. The AVLB at right in the scissoring formation from the bridge launcher at left.

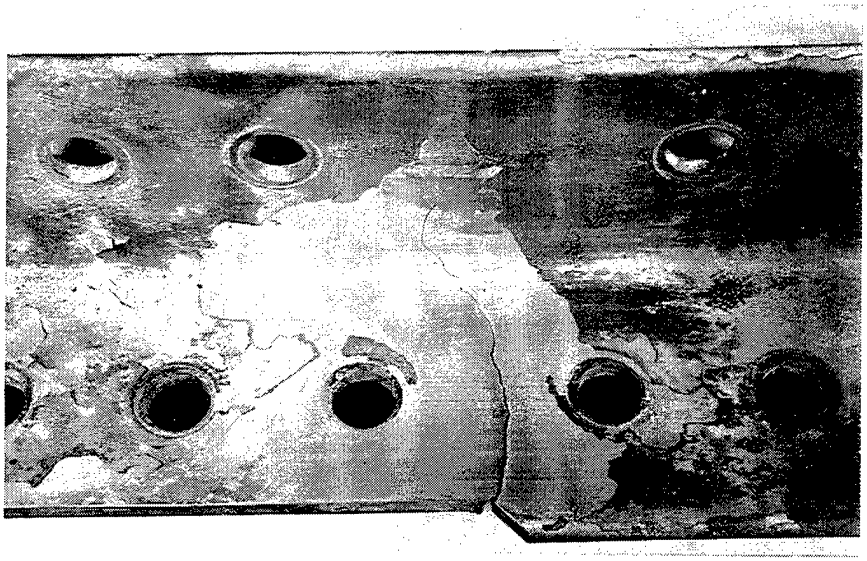

Figure 2. A view of the front side of the cracked inner splice aluminum angle showing the crack, which had initiated at a sharp corner in the angular notch, extending across the horizontal leg and 4/5th of the way up the vertical leg. Note that a portion of the edge was already machined from the leg edge, resulting in an angular notch with a sharp corner that can serve as a stress raiser (stress concentration). Magnification: Approx. 0.4×.

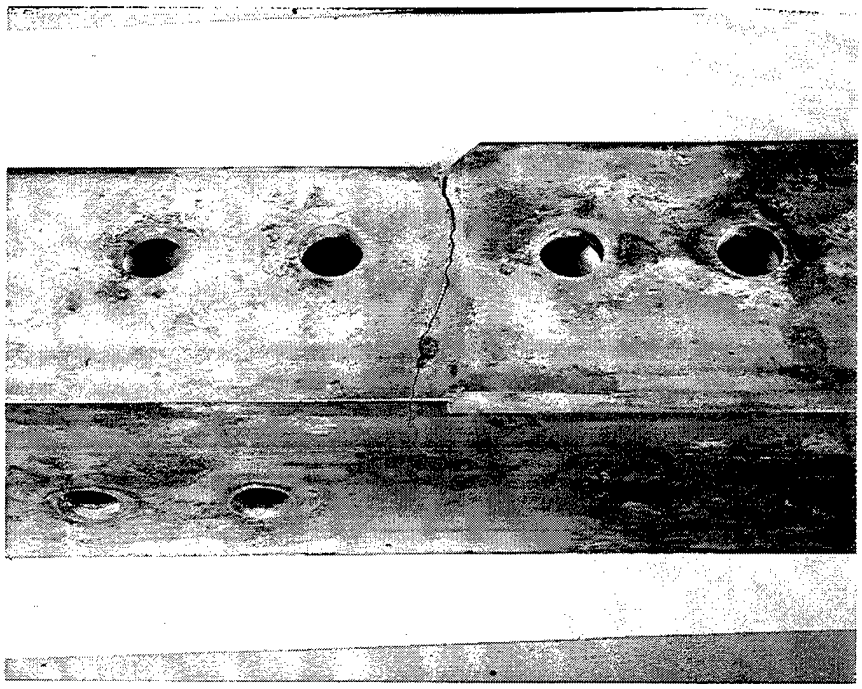

Figure 3. A view of the back side of the same angle in Figure 2. Areas of white corrosion products can be seen on the back sides that were not painted, indicating intrusion of the moisture in the gaps of the spliced joint. Magnification: Approx. 0.4×.

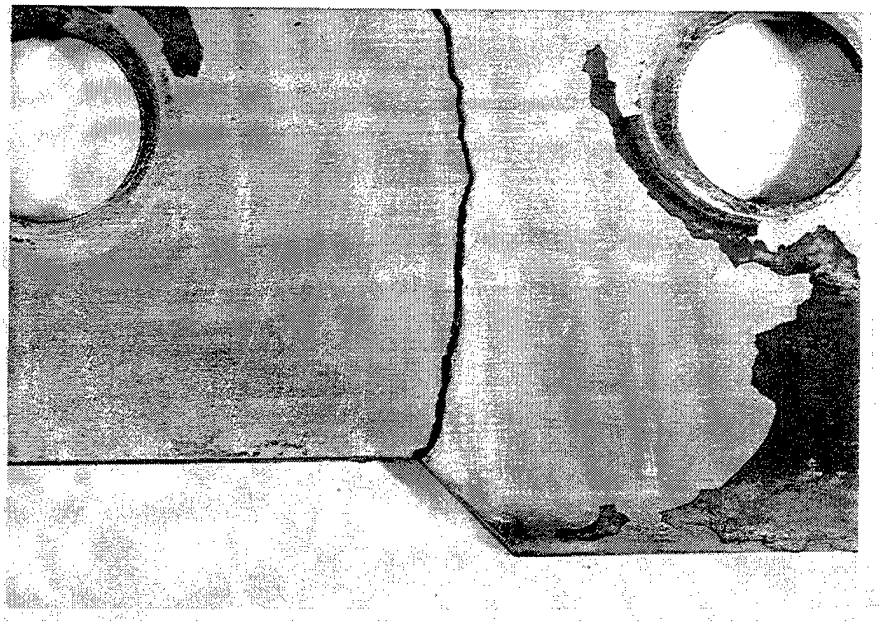

Figure 4. A close-up view of the machined angular notch with a sharp corner that acted as a stress raiser where the crack initiated. Same angle as in Figure 2. Magnification: 1 1/3×.

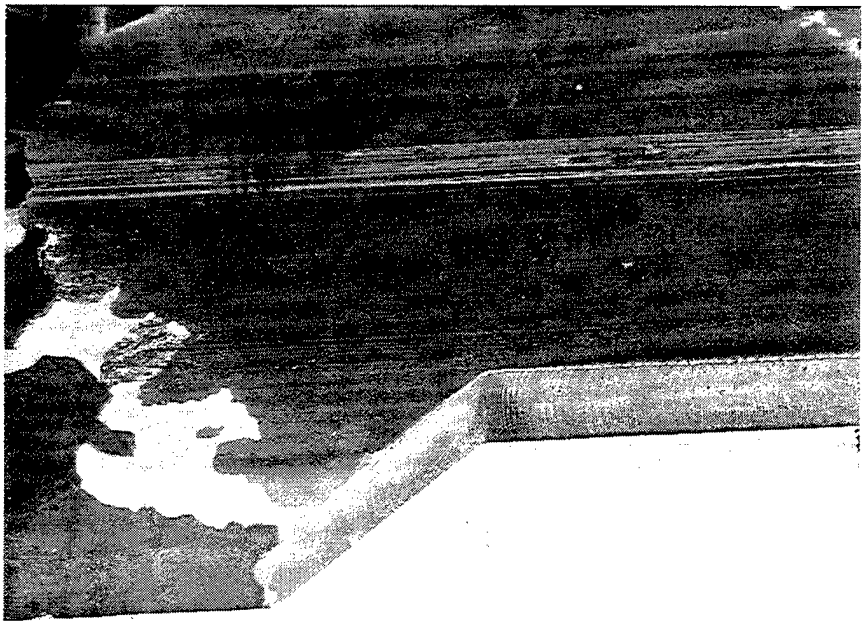

Figure 5. A close-up view of the machined angular notch with a sharp corner in the outer splice angle with no crack. Note the machining of the edge from the angle leg. Magnification: 1 1/3×.

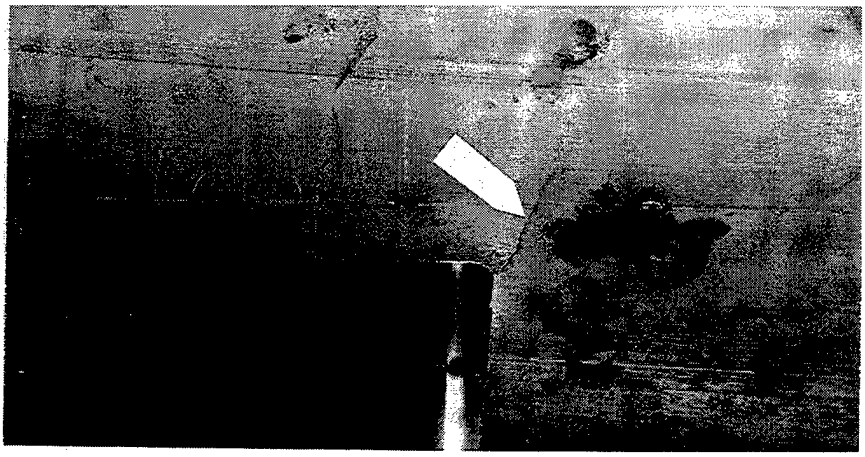

Figure 6. A close-up view of a crack (arrow) at the corner radius of the bottom chord inner aluminum angle where its horizontal leg was cut off to accommodate the thicker bottom flange (dark area in lower left-hand corner of the photograph of the inboard steel beam girder. Magnification: 1.28×.

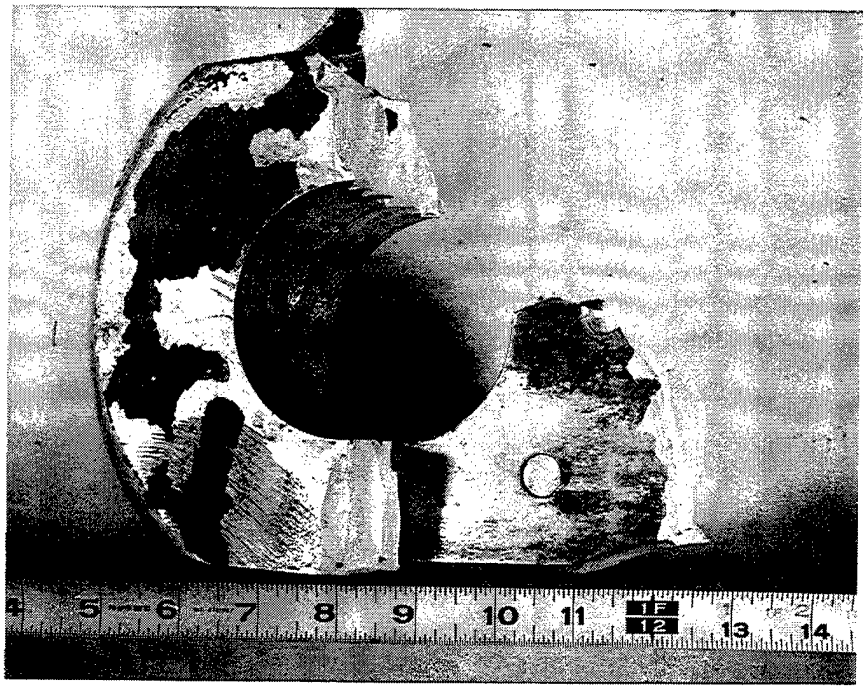

Figure 7. A view of the broken eyehole section from the failed male bottom connector.

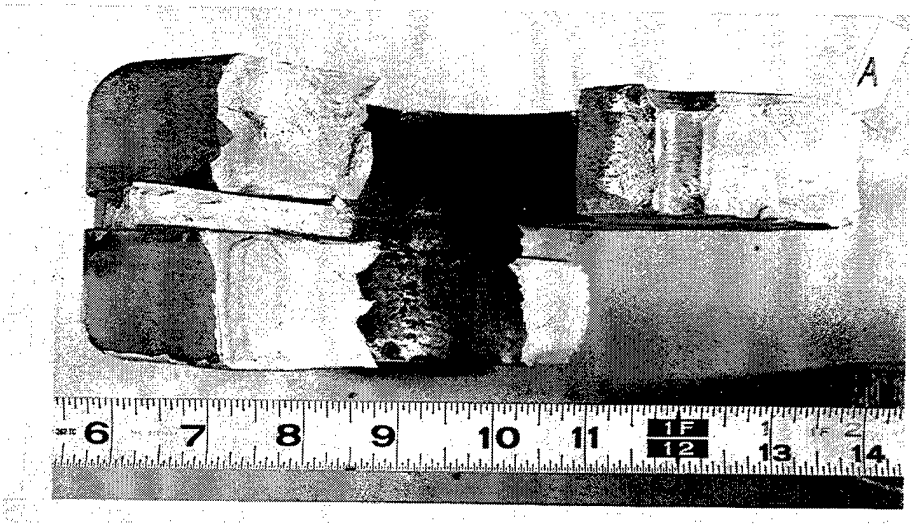

Figure 8. Top view of the broken section in Figure 7, showing the fractured surfaces. Two forged aluminum connector parts were riveted to a 3/8-in-thick inboard girder web aluminum plate (between the forged parts). The top broken piece is a section of the forged inboard connector part, whereas the bottom piece is a section of the outboard connector part. The location at A is the origin of the brittle failure.

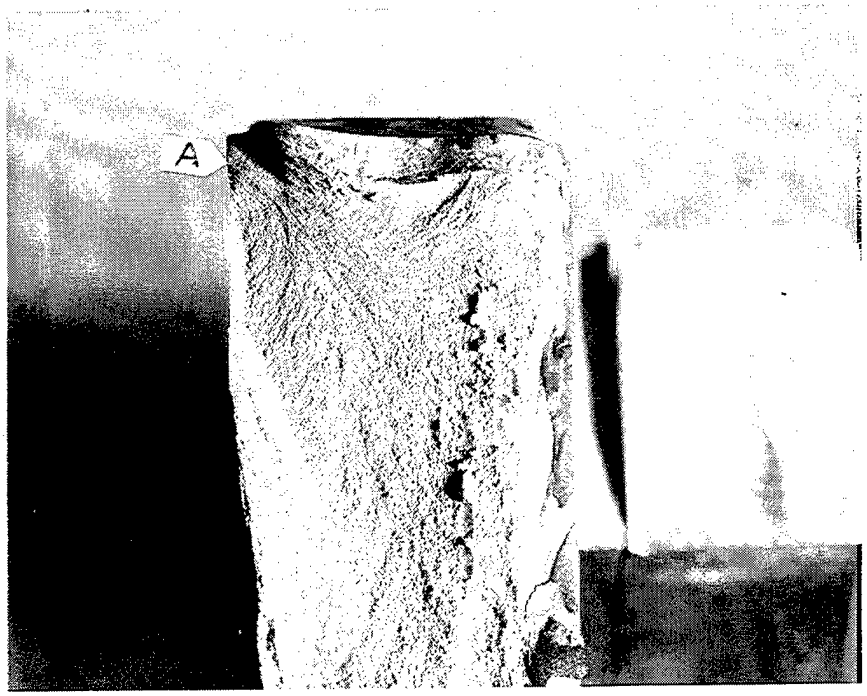

Figure 9. Close-up view of the fracture at location (A) in Figure 8. The features of the fractured surface point toward the failure origin. Magnification: Approx. 1.5×.

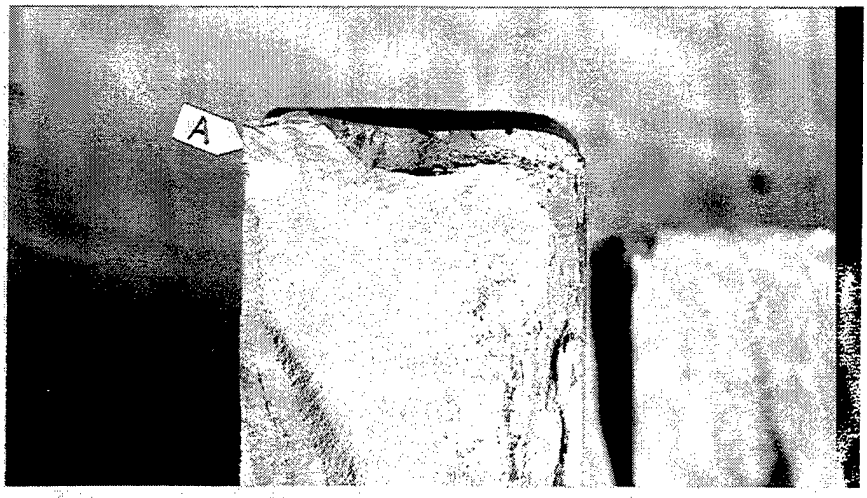

Figure 10. Close-up view of the same area in Figure 9, but under a different lighting condition to show the light-discolored area at the failure origin (A), indicating a fatigue crack. Magnification: Approx. 1.5×.

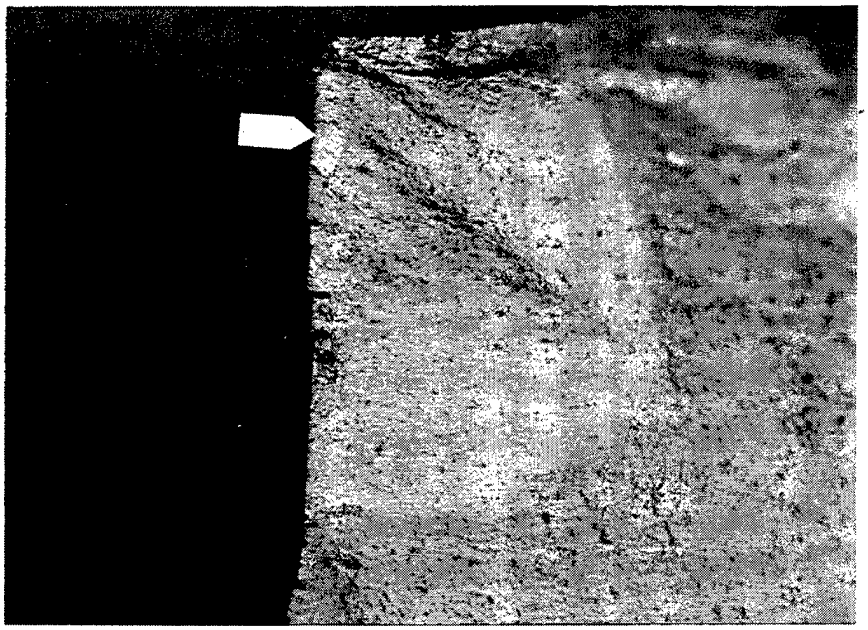

Figure 11. Close-up view of the same area in Figure 10, but at a higher magnification to show smaller fatigue cracks at the edge of the vertical machined sharp notch that cannot be seen in this photograph. Magnification: Approx. 4.3×.

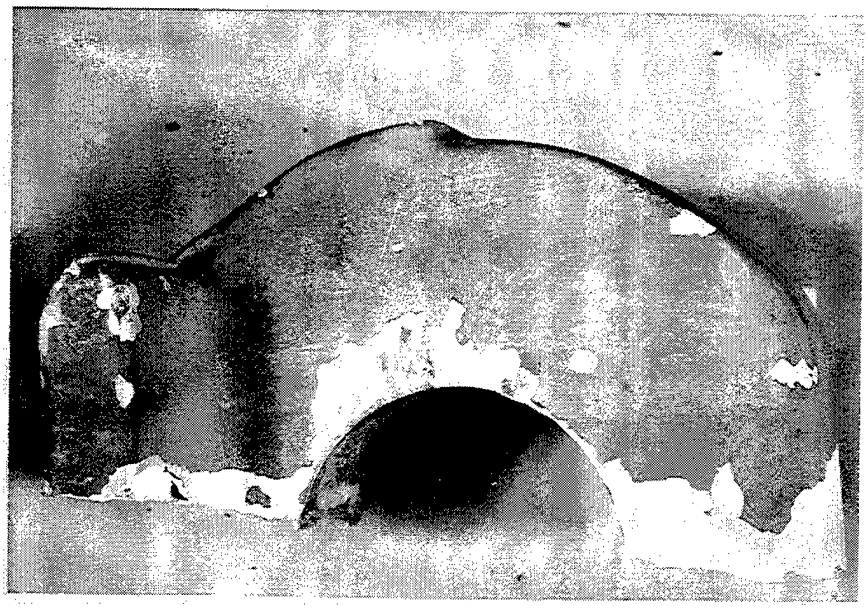

Figure 12. A side view of the broken eyehole section from the failed outboard female bottom connector (outboard forged part). It was removed from a female center panel assembly of the No. 2 Modified AVLB after the bridge's second failure during the fatigue tests. The connector part broke across the 3-in-diameter eyehole for the connector steel pin.

Figure 13. Same broken eyehole section in Figure 12, showing the fractured surfaces.

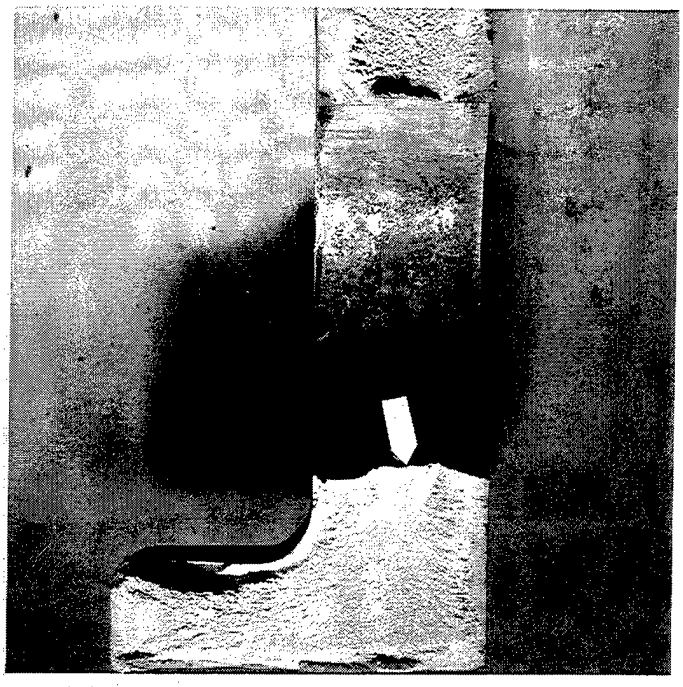

Figure 14. A view of the fractured surfaces of the broken section in Figure 13, showing the location of the failure origin (arrow) at the bottom edge of the 3-in-diameter eyehole. It reveals the characteristic feature of a fatigue crack. Although not clearly seen in the photograph, the corrosion products were observed on the internal bare surface of the eyehole, indicative of corrosion. The eyehole was slightly worn by the steel pin rubbing against it, removing most of the paint to produce bare areas to corrosion.

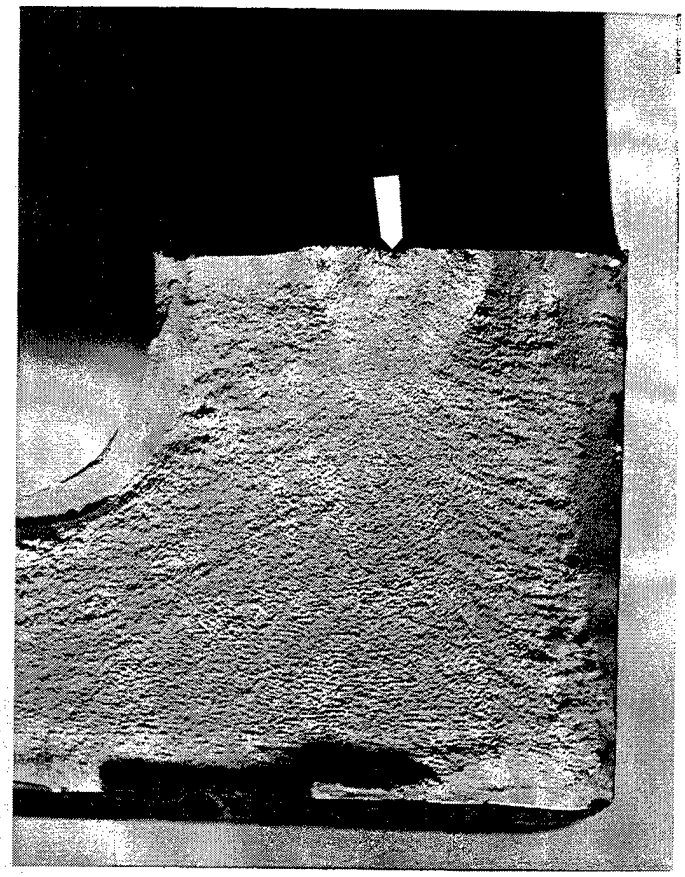

Figure 15. Close-up view of the origin failure (arrow) in Figure 14. Although not clearly seen in the photograph, a small area of discoloration that may be indicative of corrosion was observed in the fatigue crack at the eyehole edge. This was where the fatigue crack had initiated, growing to the critical size during fatigue cyclic loadings to the point of brittle fracture in the forged bottom connector across the eyehole section.

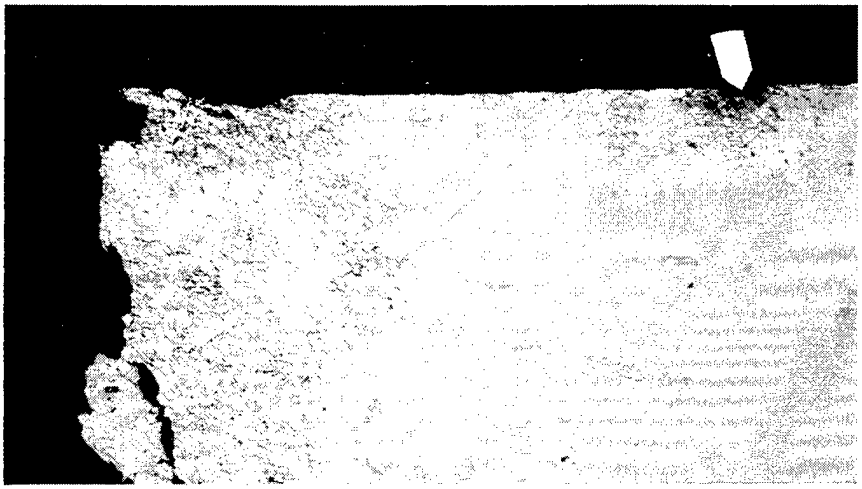

Figure 16. As-polished microstructure of the intergranular corrosion adjacent to the primary fracture (left side) and at a small surface corrosion pit (arrow) in the surface of the eyehole. The metallographic specimen was cut from the failure origin containing the fatigue crack. Magnification: 185×. Unetched.

Figure 17. Same area in Figure 16, but at a higher magnification. Magnification: 365×. Unetched.

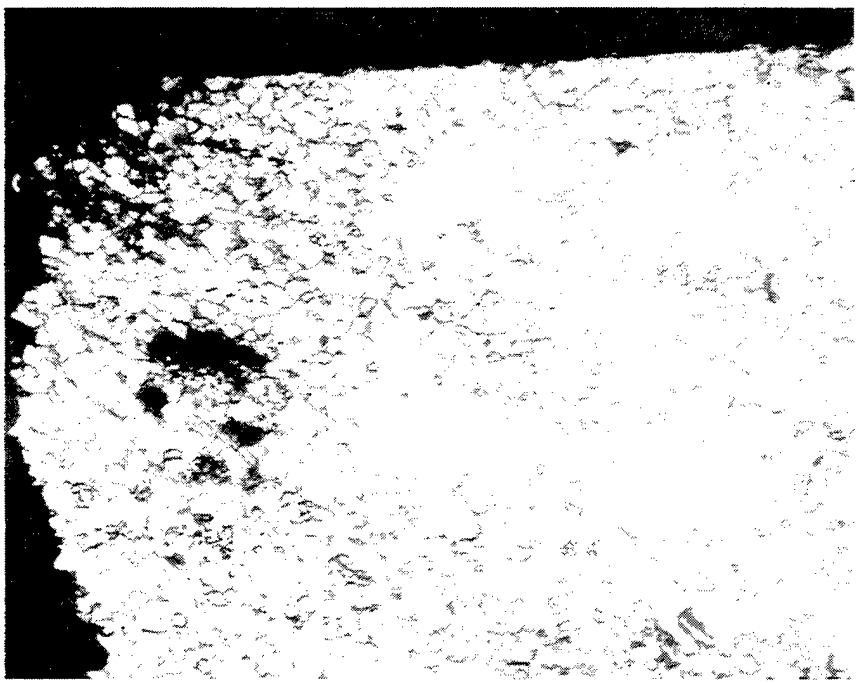

Figure 18. Same area in Figure 17, but etched to reveal the grain structure. Magnification: 365×. Keller etchant.

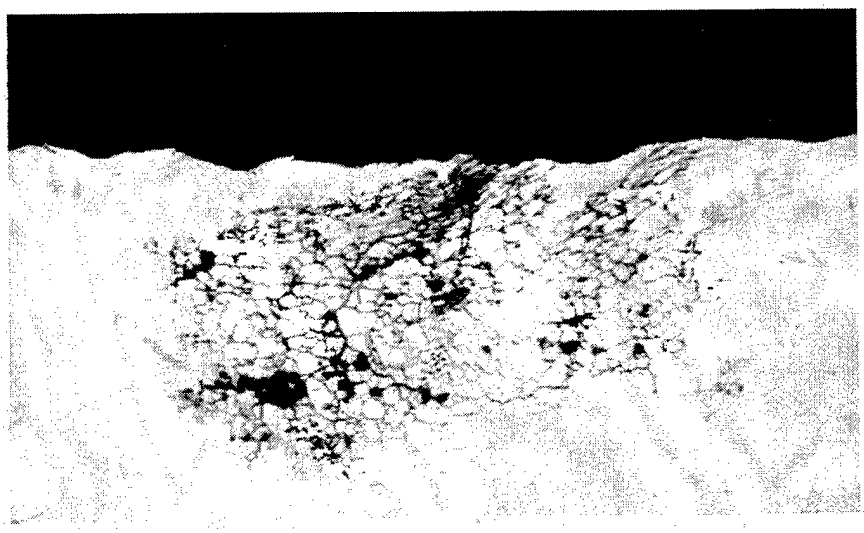

Figure 19. Enlarged view of the intergranular corrosion in a small corrosion pit in Figure 16. A small pit was started in the worn, bare surface of the eyehole, whereby integranular corrosion spread out internally. Magnification: 365×. Unetched.

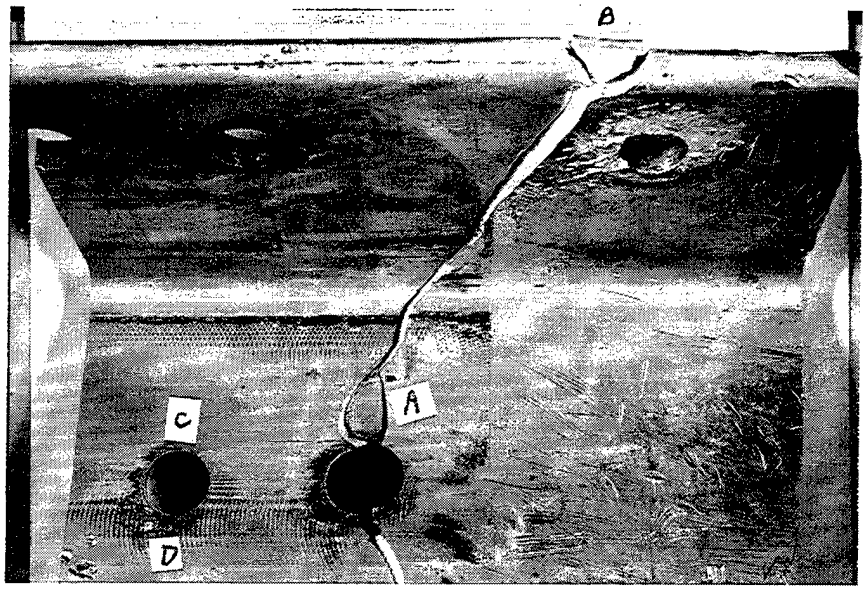

Figure 20. Top view of the broken angle section of the failed bottom chord on the female center panel assembly of the No. 2 Modified AVLB. The crack went across the countersunk rivet hole in the horizontal leg. Note the blackened areas at the edge of the holes in the horizontal leg and along the inside corner of the angle in addition to the outlines of the machined marks from the bottom of the forged center hinge in contact with the top surface of the angle. Two small pieces (A and B) probably broke off during the removal of the broken section. Two small cracks (C and D) were observed 180° apart in the edge of the second rivet hole in the horizontal leg. One-half actual size.

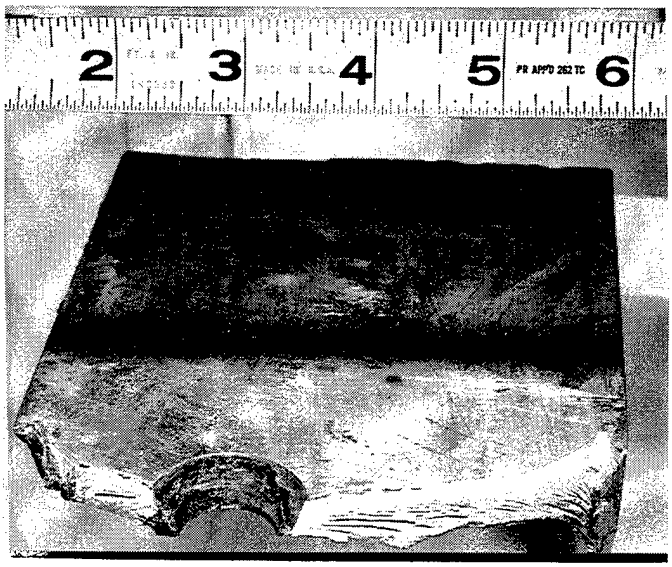

Figure 21. A view of the fractured surfaces of the right section of the broken angle in Figure 20.

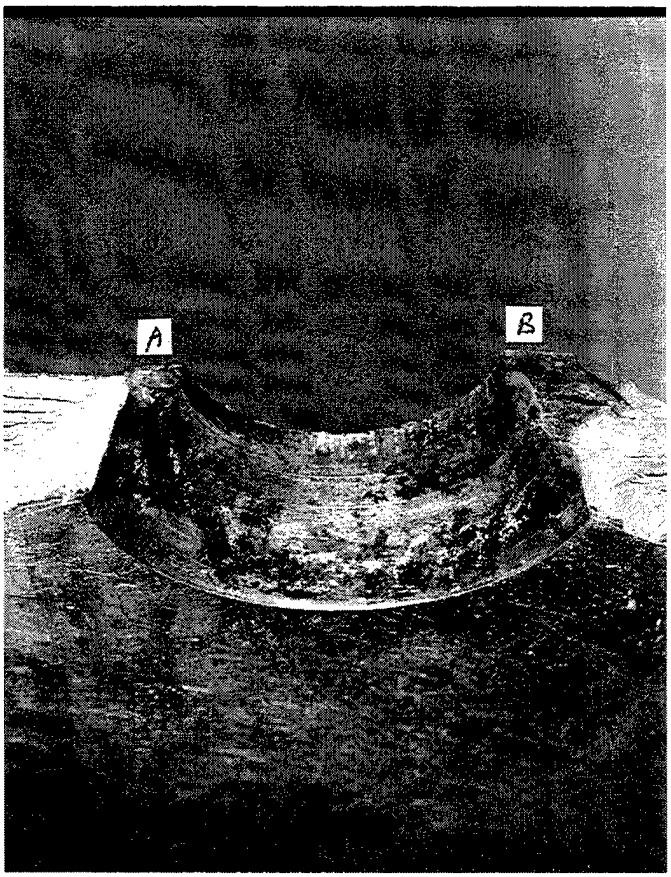

Figure 22. Enlarged view of the fractured countersunk rivet hole in Figure 21, viewing the hole from the bottom surface of the angle. The discolored areas at locations A and B and fatigue beach marks at both corners of the hole were the origin sites of the brittle failure in the bottom chord angle. Magnification: 2.2×.

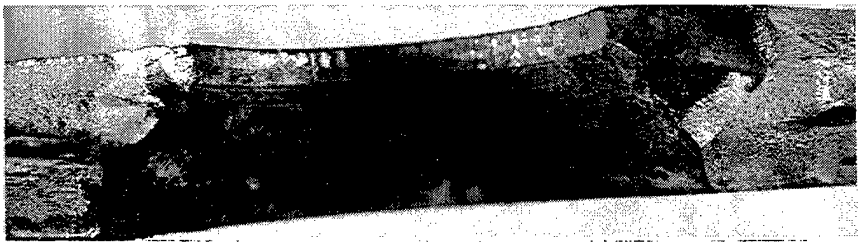

Figure 23. Same area of the fractured rivet hole in Figure 22 with a perpendicular view. Magnification: 2.9×.

Figure 24. Enlarged view of the rivet hole edge with a crack (arrow) in the small angle piece (A) in Figure 20. Magnification: 15×.

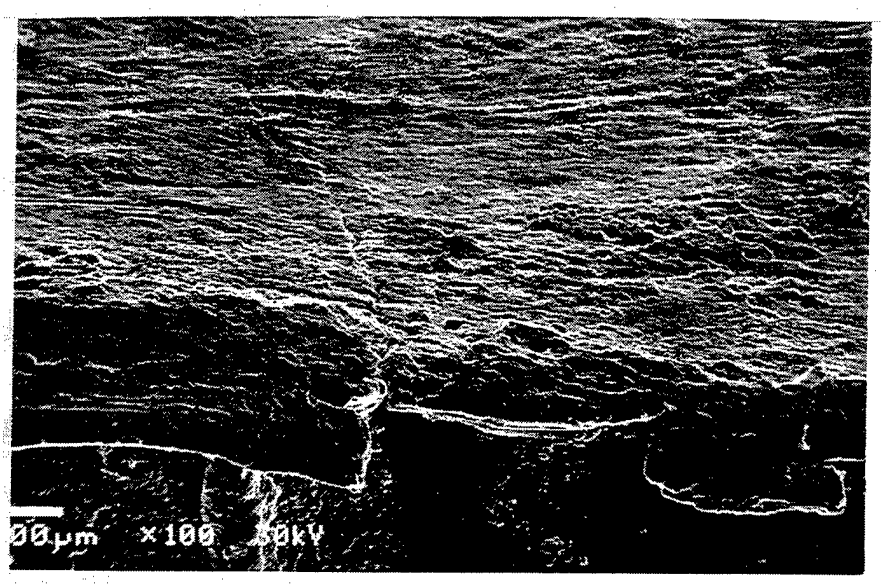

Figure 25. Electron scanning microscope view of the small crack in Figure 24 along the top surface at the hole edge of the small-angle piece. Magnification: 100×.

Figure 26. As-polished specimen with the crack seen in the small angle piece in Figure 24. The crack extended from the top surface halfway down the land edge of the countersunk rivet hole. Magnification: 40×.

Figure 27. Same area in Figure 26 except etched to reveal the microstructure. The wide light-colored band in the top surface is the recrystallized layer as the result of the angle extrusion process. Magnification: 40×. Keller's etchant.

Figure 28. A view of the etched microstructure about 3/4 of the way down the crack in Figure 27. Some branching of the crack is seen. Note that the crack is transgranular since it went across the grains. The grains are elongated as the result of the angle extrusion process. Magnification: 360×.

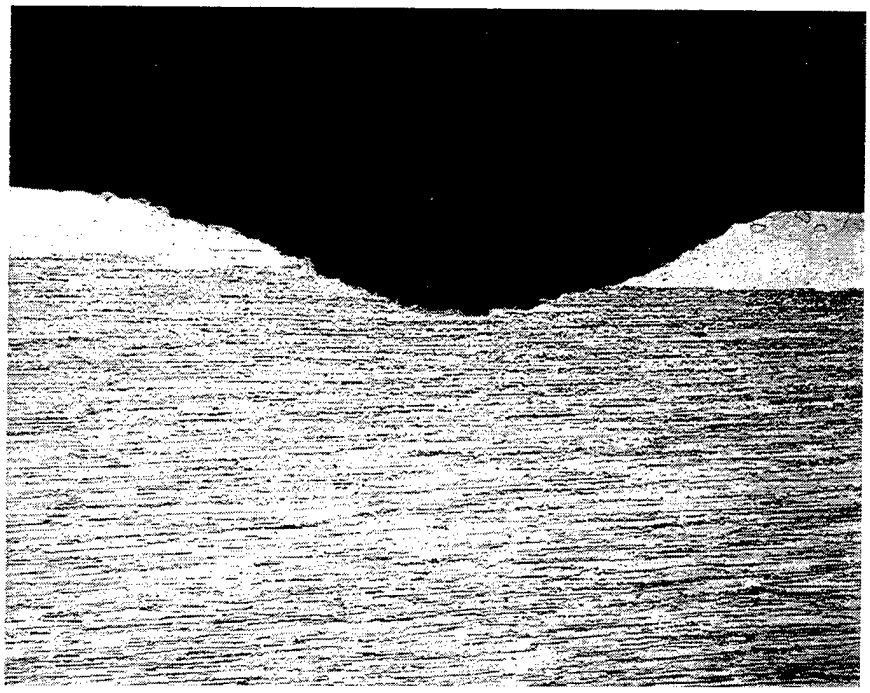

Figure 29. A view of a surface corrosion pit in the top surface of the broken angle. The cross section is through the blackened area in the inside corner of the angle in Figure 20. Magnification: 40×. Keller's etchant.

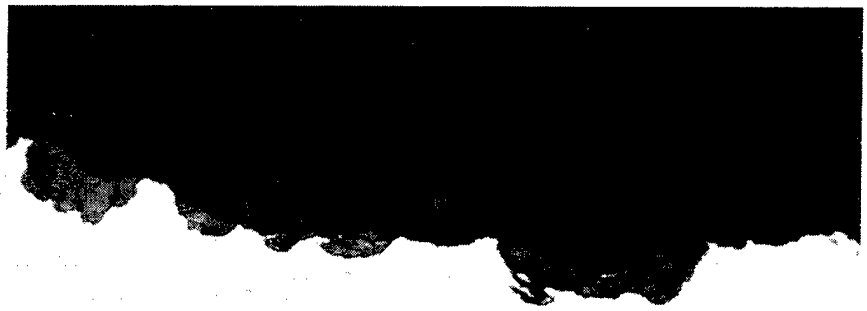

Figure 30. The bottom of the surface pit in Figure 29. The dark gray corrosion products embedded in the bottom, which account for the black color on the top surface of the angle. Magnification: 280×. Unetched.

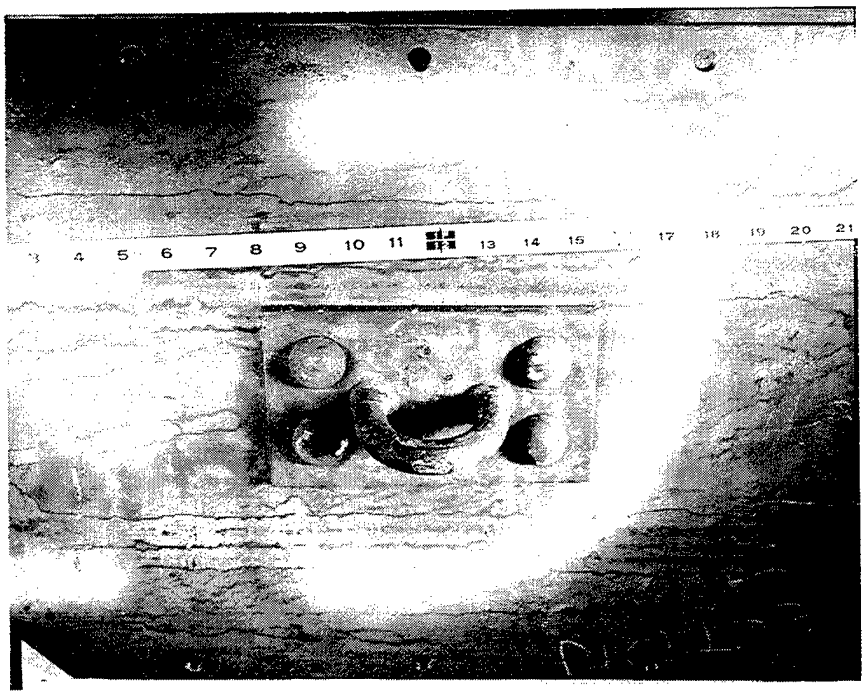

Figure 31. A view of the girder test plate with the tie-down device that was fastened to the plate with four buttonhead aluminum rivets.

Figure 32. A view of the girder test plate bolted to the special test jig. The tie-down U-shaped steel bar is in the vertical orientation (parallel to the tension load) for the pull test.

Figure 33. The back view of the girder test plate bolted to the back of the test jig. Note the tie-down reinforcement steel plate fastened to the backside of the girder plate.

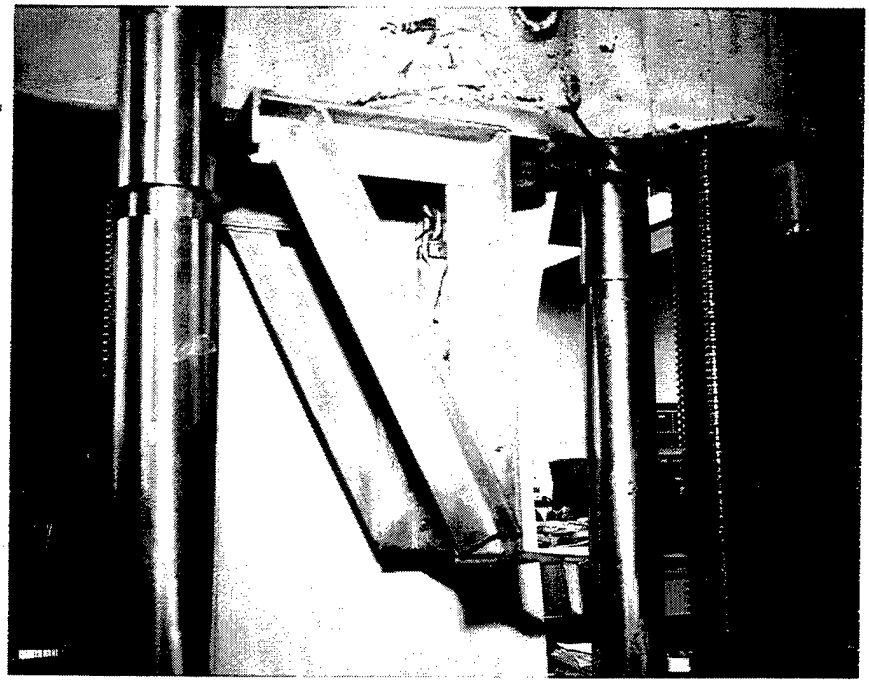

Figure 34. A view of the test jig in position underneath the fixed crosshead of the testing machine.

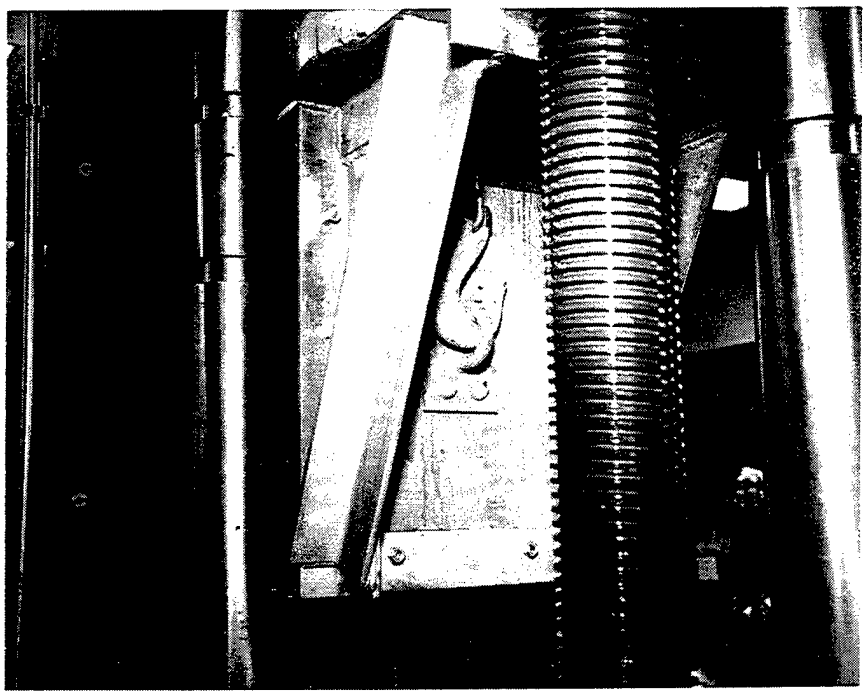

Figure 35. Another view of the test jig in Figure 34. Note the steel hook in the U-shaped bar for pulling against the upper leg of the tie-down device for the vertical pull test.

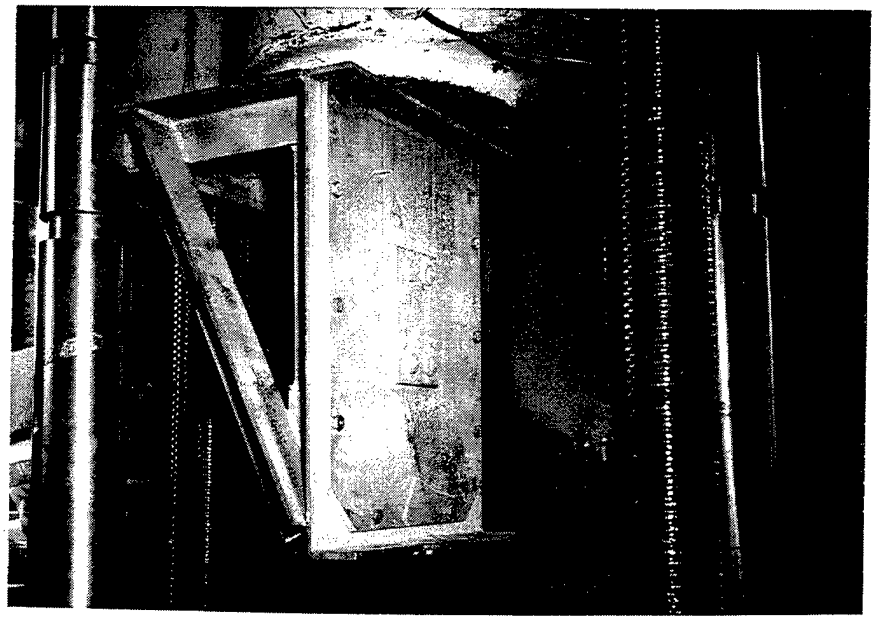

Figure 36. The back view of the test jig in Figure 34.

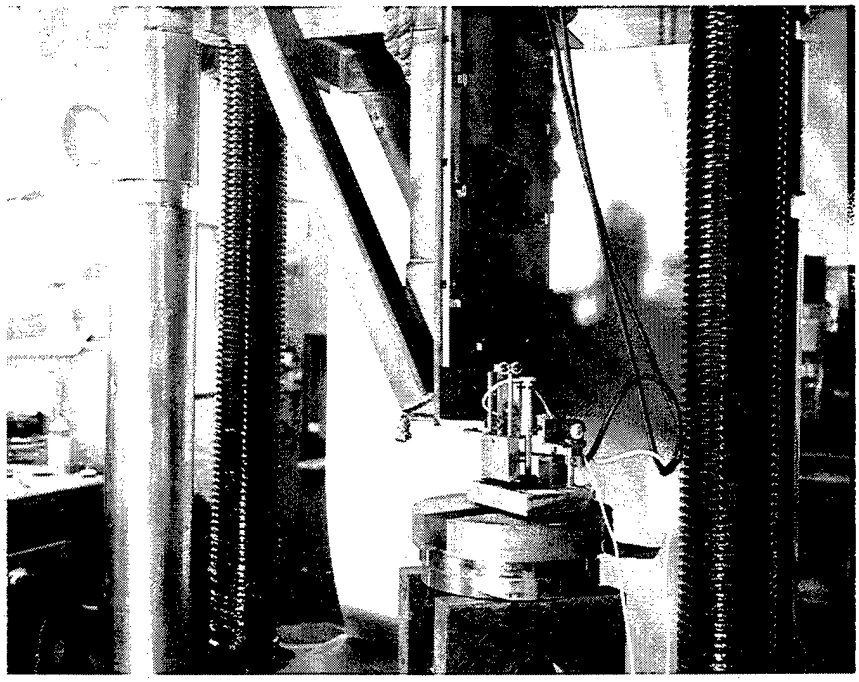

Figure 37. A view of a typical pull test setup to show the deflectometer in position at the bottom of the test jig to record the movement of the crosshead to which the jig is attached.

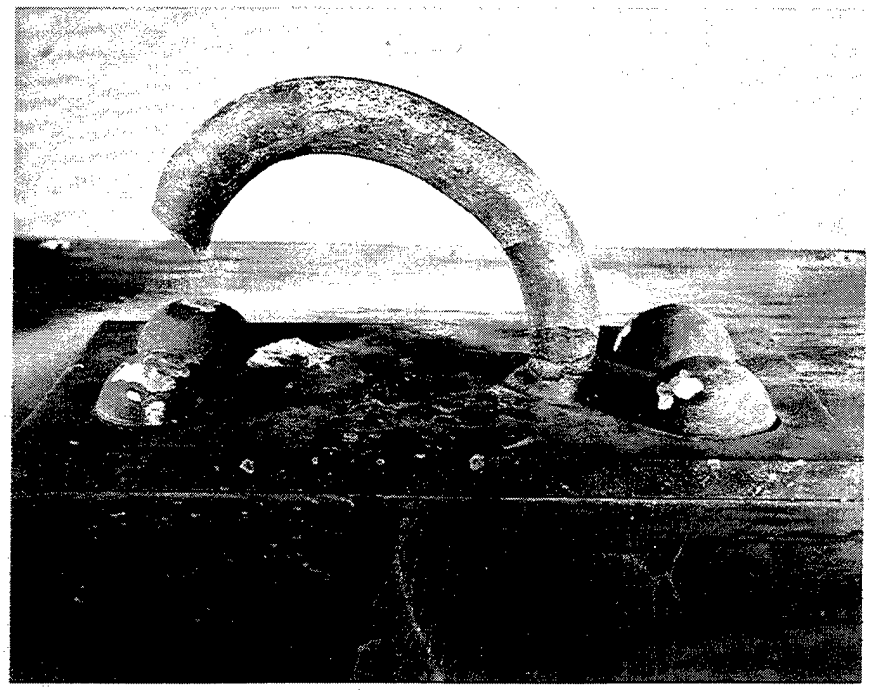

Figure 38. The failure of the AVLB tie-down device after the pull test. The broken end of the steel bar failed under the hook by shearing in the bevel-fillet weld.

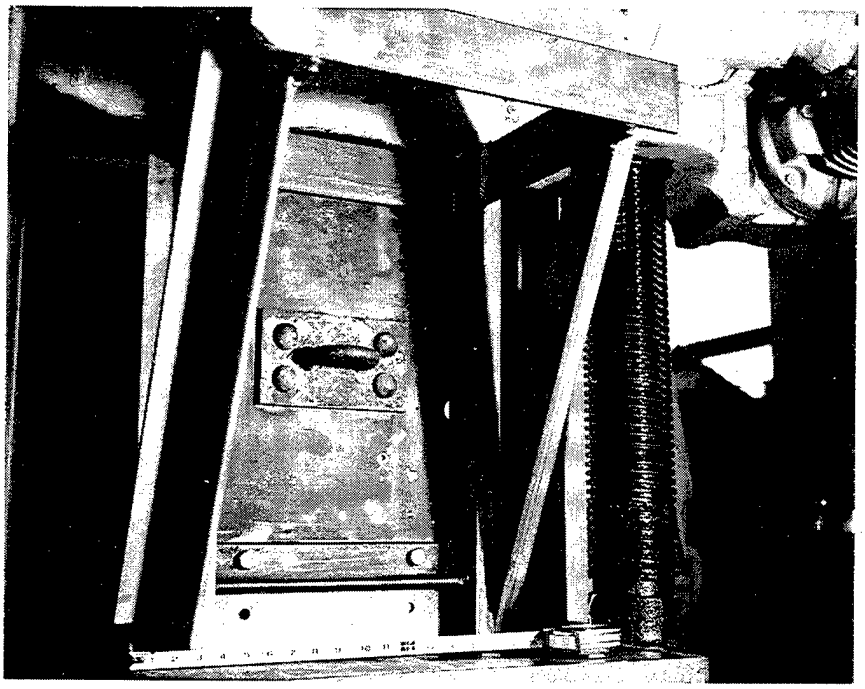

Figure 39. A view of the girder test plate bolted to the test jig with the tie-down U-shaped steel bar in the horizontal orientation (perpendicular to the tension load) for the pull test.

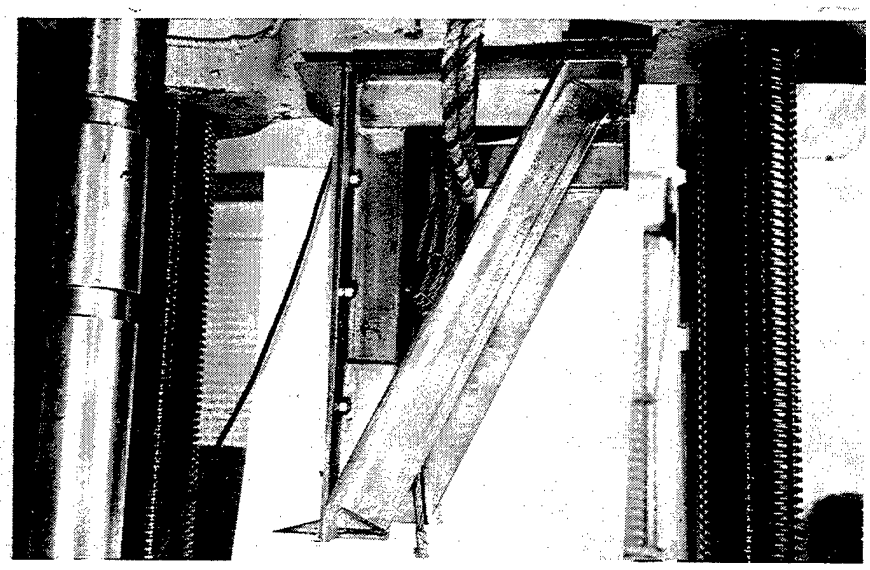

Figure 40. A view of the test jig showing the 1/2-in-diameter wire rope that was looped five times around the U-shaped steel bar of the tie-down device to pull on it during the horizontal pull test.

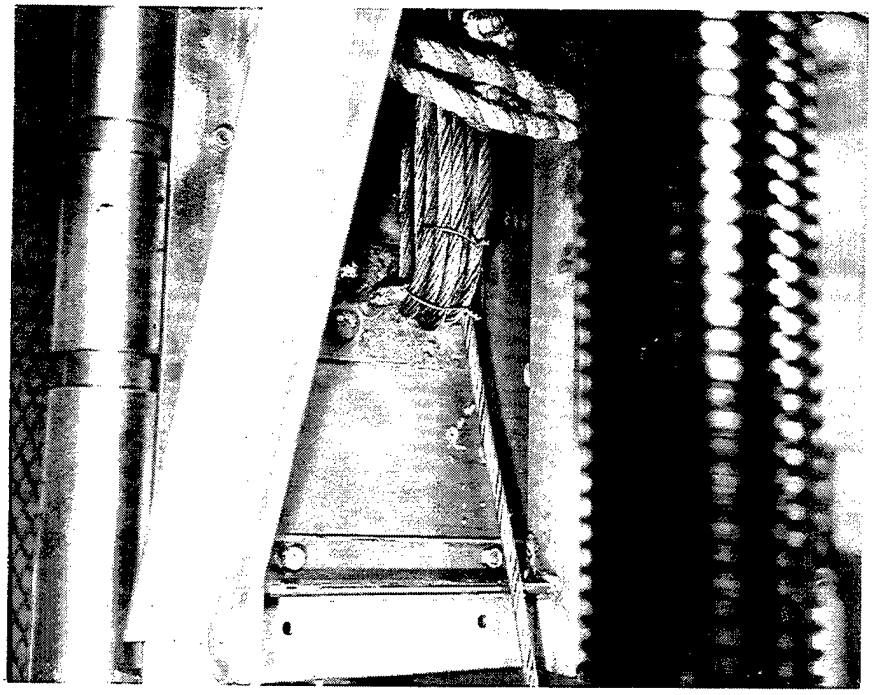

Figure 41. A close-up view of the test jig and device in Figure 40.

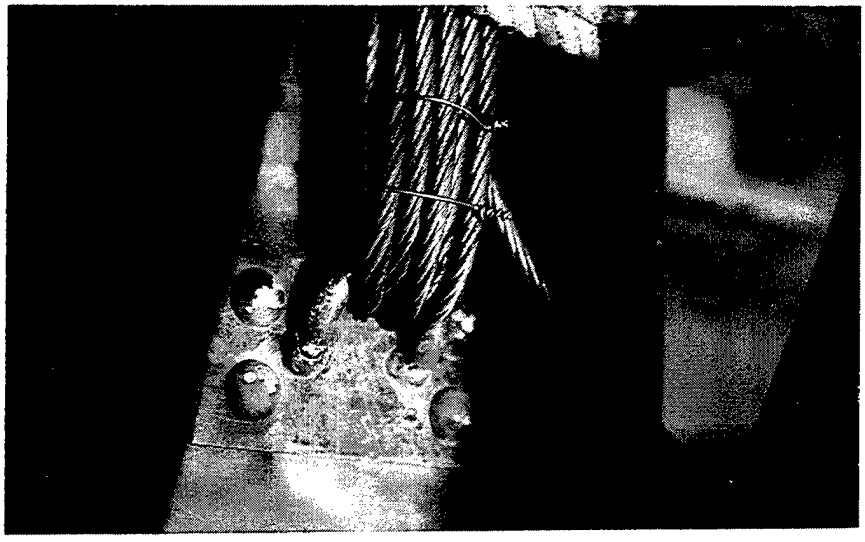

Figure 42. A view of the tie-down device after the pull test to show the mode of the failure of the U-shaped bar by bending and cracking at the welded joints.

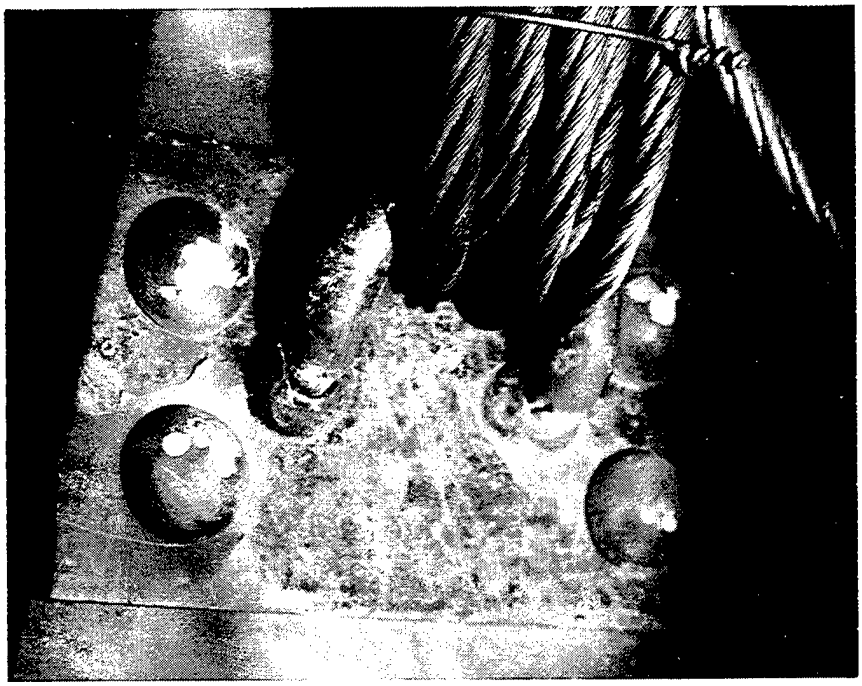

Figure 43. Enlarged view of the failed tie-down device in Figure 42. Note that the failure occurred in the upper toe of both welds.

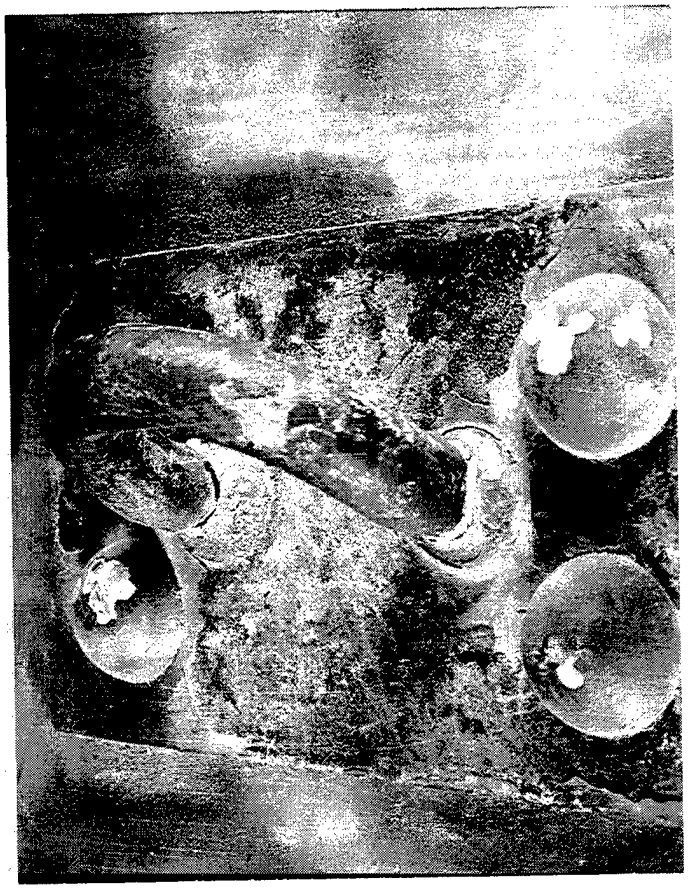

Figure 44. Close-up view of the failed tie-down device in Figure 43 after the removal of the wire rope for a clearer view.

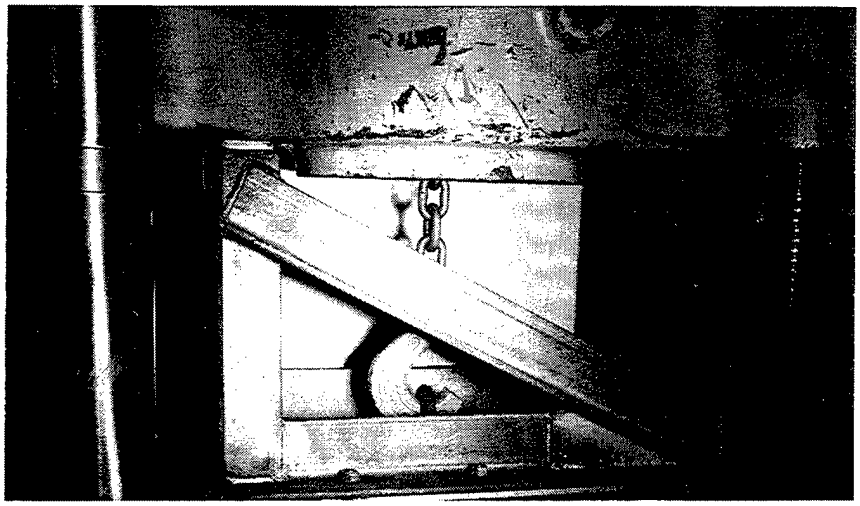

Figure 45. A view of the test jig in position underneath the fixed crosshead of the testing machine, showing the hook on the U-shaped bar of the tie-down for the straight pull out test.

Figure 46. Close-up view of the test jig and device in Figure 45.

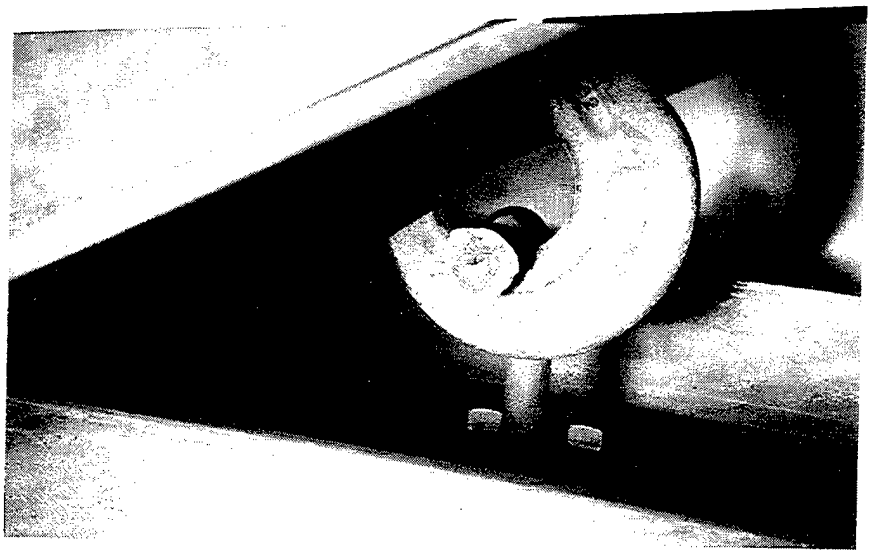

Figure 47. Close-up view of the failed welded end of the U-shaped bar of the third tie-down device tested after the pull test.

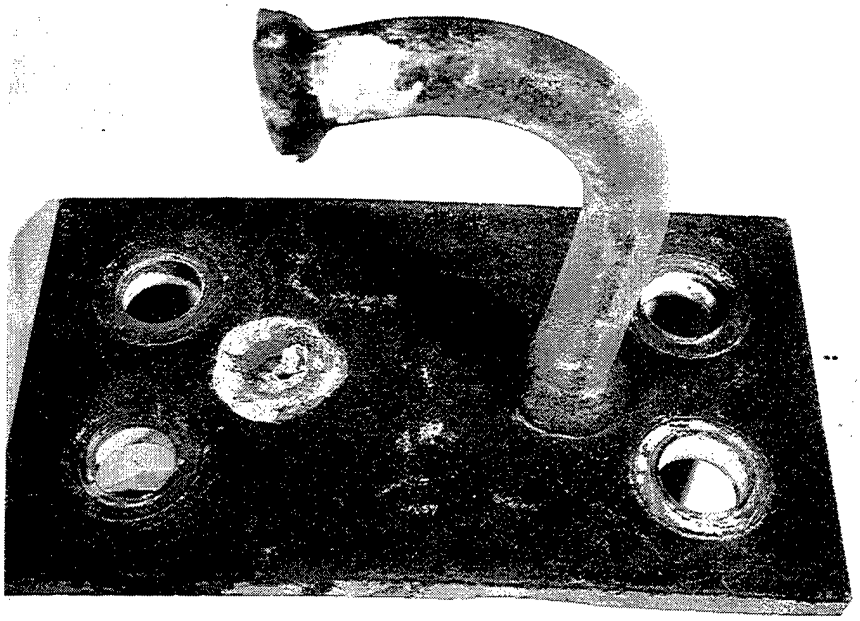

Figure 48. A view of the failed tie-down device after its removal from the test jig in Figure 47.

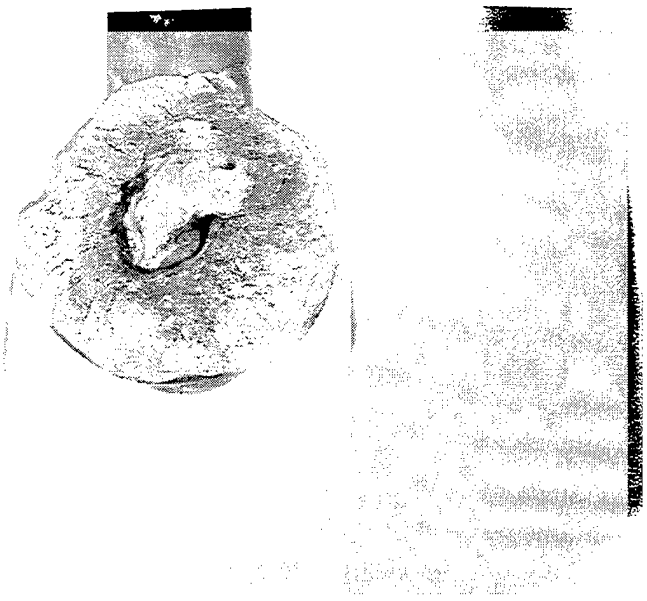

Figure 49. Enlarged view of the weld fracture of the failed end of the bar in Figure 48. Only the central portion of the bar end was truly fused to the base plate. The remaining area of the fracture was essentially cold fusion with very little weld penetration into the base plate.

Figure 50. Enlarged view of the weld fracture in the tie-down base plate where the welded end of the bar broke loose.

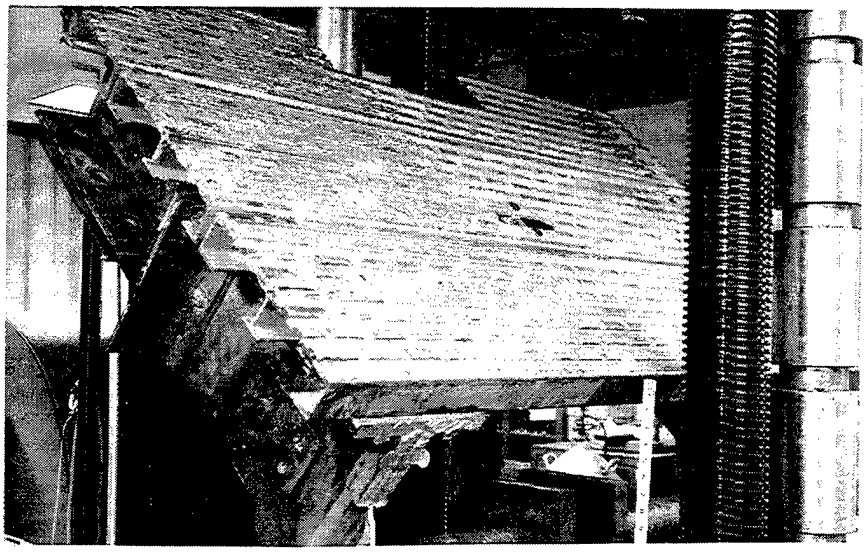

Figure 51. A large section of the AVLB deck in position on the testing machine. A large round steel bar was through the holes of the girder plates to attach the section to the test jig fastened to the crosshead of the testing machine. The section is positioned at a 45° angle to the load axis. The lifting device (lifting steel bar) is in the oblong hole of the center deck panel.

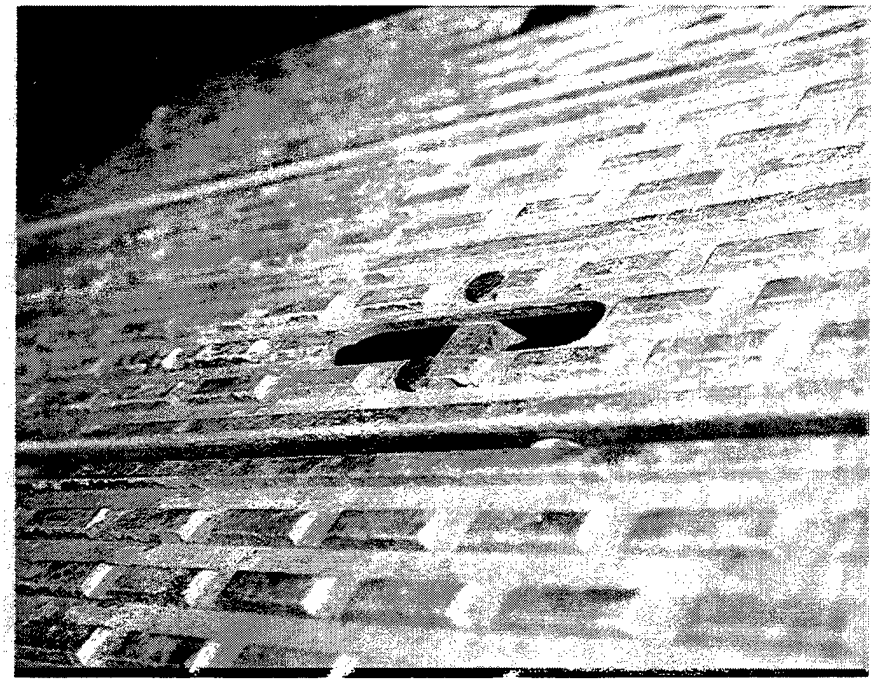

Figure 52. Close-up view of the lifting device showing the lifting steel bar bolted underneath the oblong hole. Note that the bar is perpendicular to the long axis of the hole.

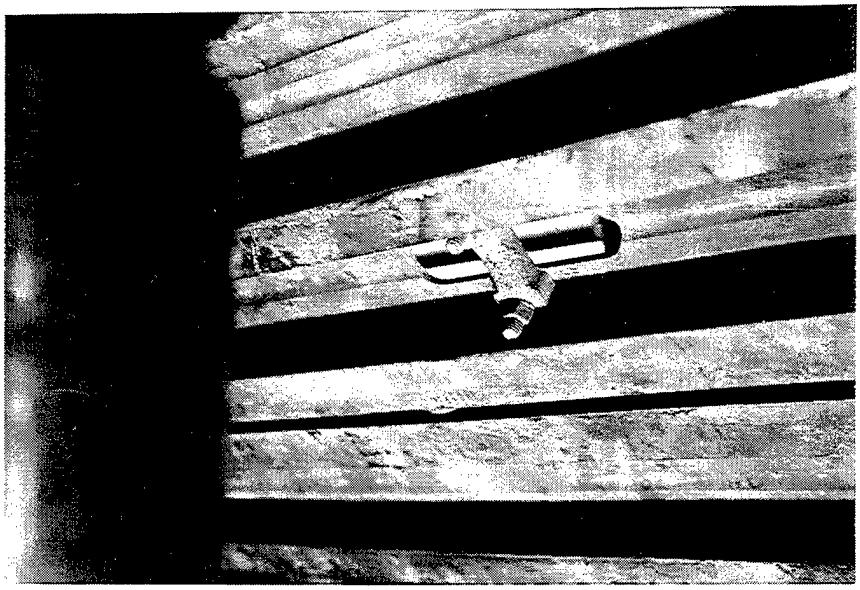

Figure 53. A view of the lifting steel bar underneath the oblong hole in Figure 52.

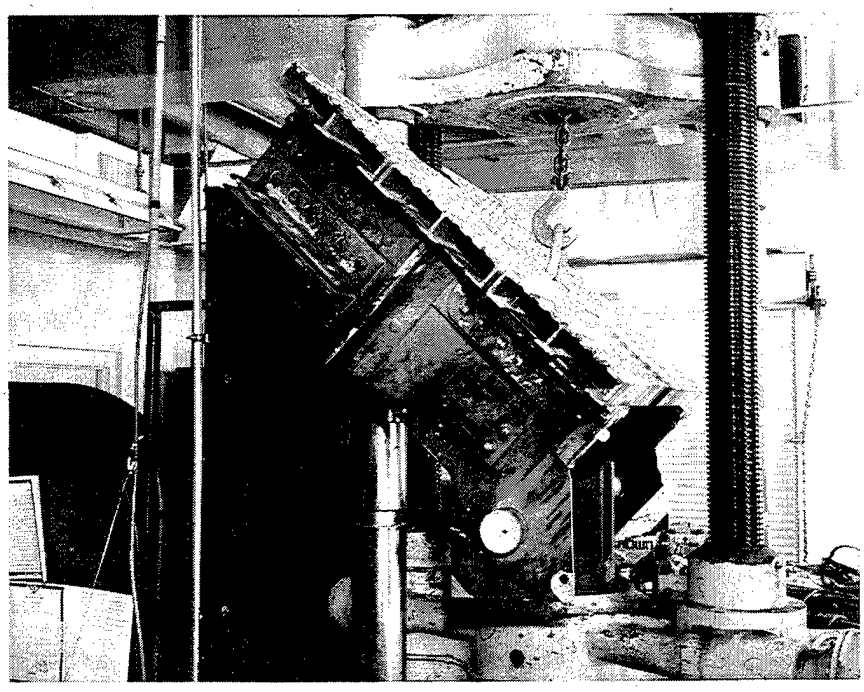

Figure 54. A side view of the large AVLB deck section in position at 45° on the lifting machine. A large chain with a clevis hook was used to pull on the steel ring that was around the lifting bar in the deck panel.

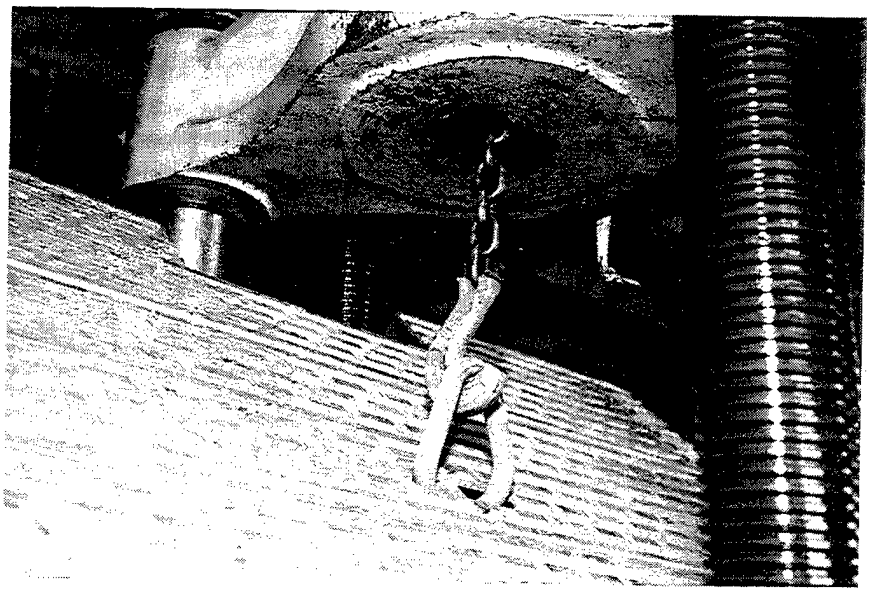

Figure 55. A close-up view of the egg-shaped steel ring around the lifting bar in the deck panel. The ring had to be bent to 20° offset in order to be parallel to the loading axis of the chain and hook. The bent ring was against the upper edge of the oblong hole.

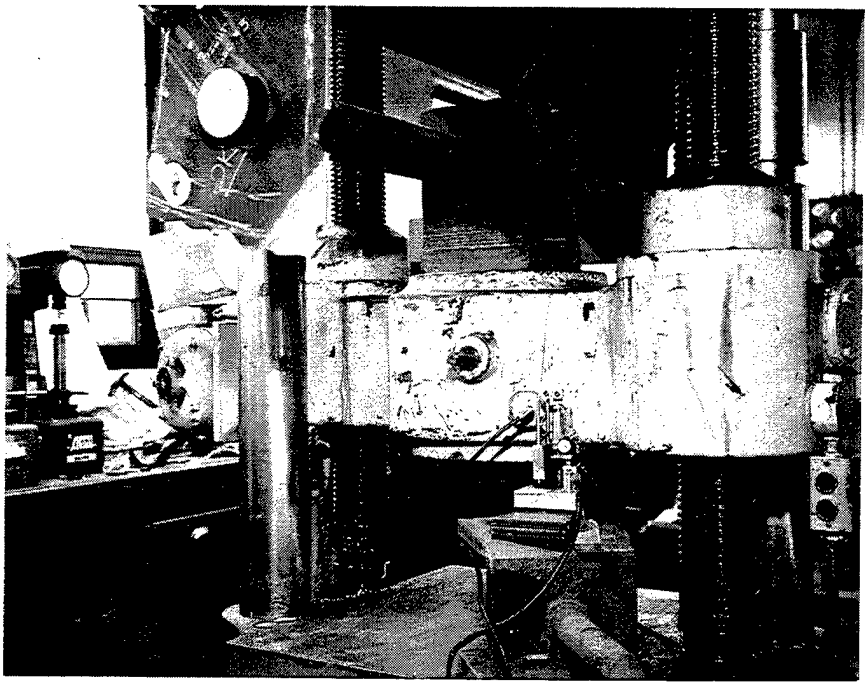

Figure 56. A view of the testing machine showing the deflectometer in position to measure the movement of the table during the pull test.

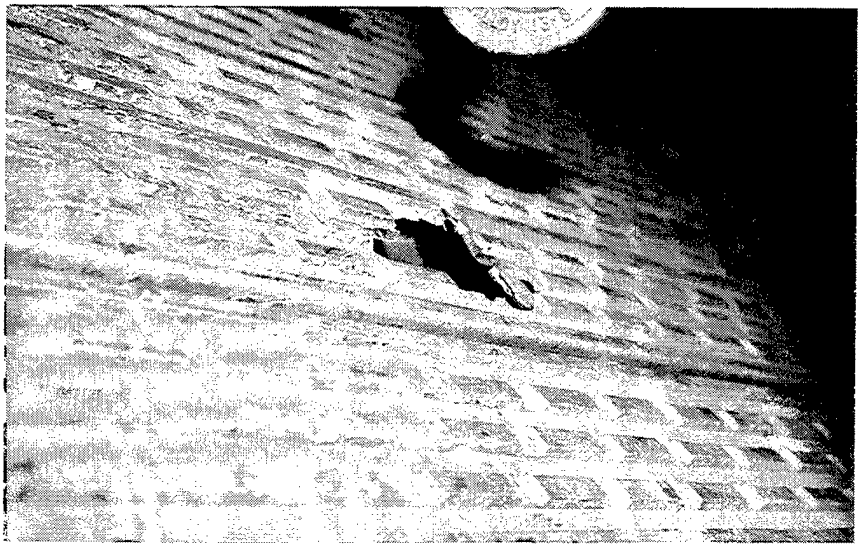

Figure 57. Damage to the oblong hole in the deck panel after the lifting steel bar was pulled out during the first pull test.

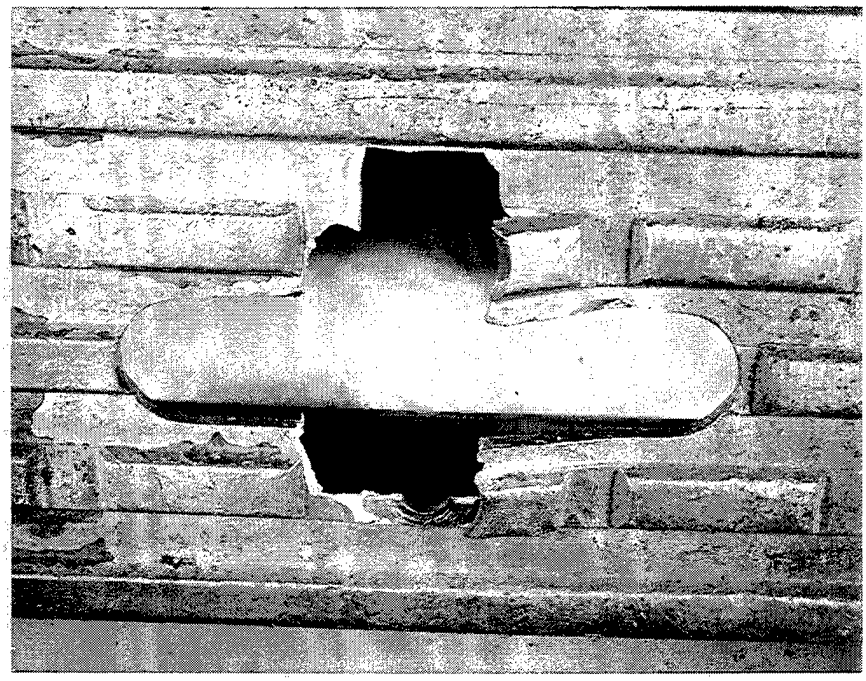

Figure 58. Close-up view of the damaged oblong hole in Figure 57.

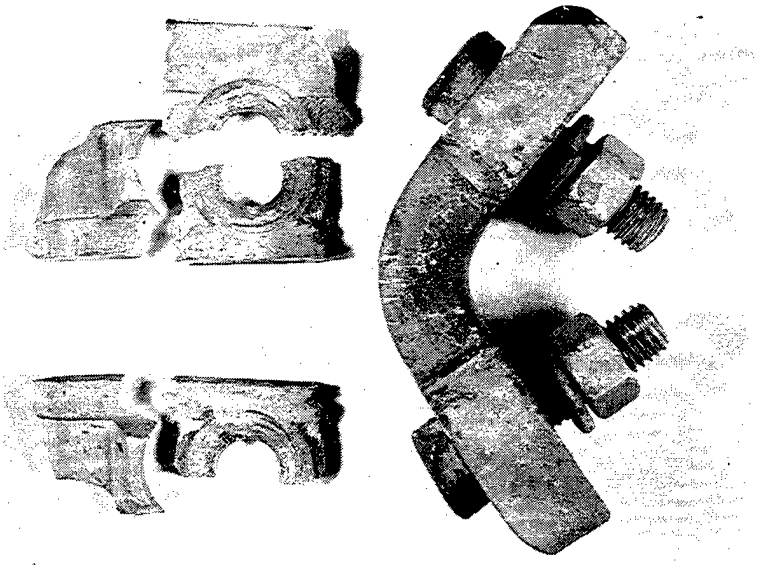

Figure 59. Broken pieces from the bolt holes at the oblong hole in the deck panel plus the bent lifting bar as the result of the pull test. Although not clearly seen in the photograph, discolored areas were observed in the fractured surfaces of the pieces.

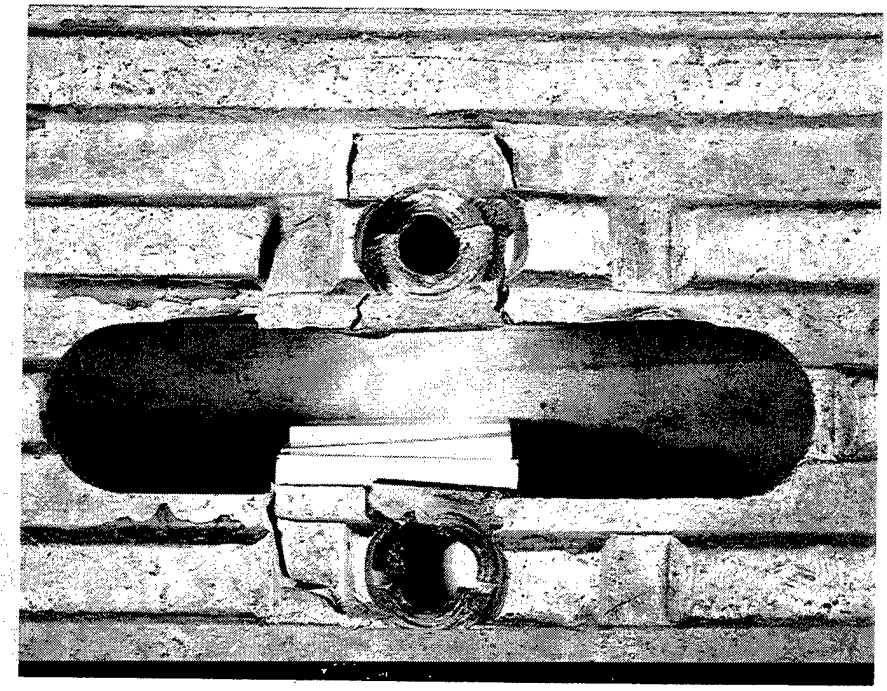

Figure 60. Broken deck panel pieces put back in place in the damaged oblong hole in Figure 58.

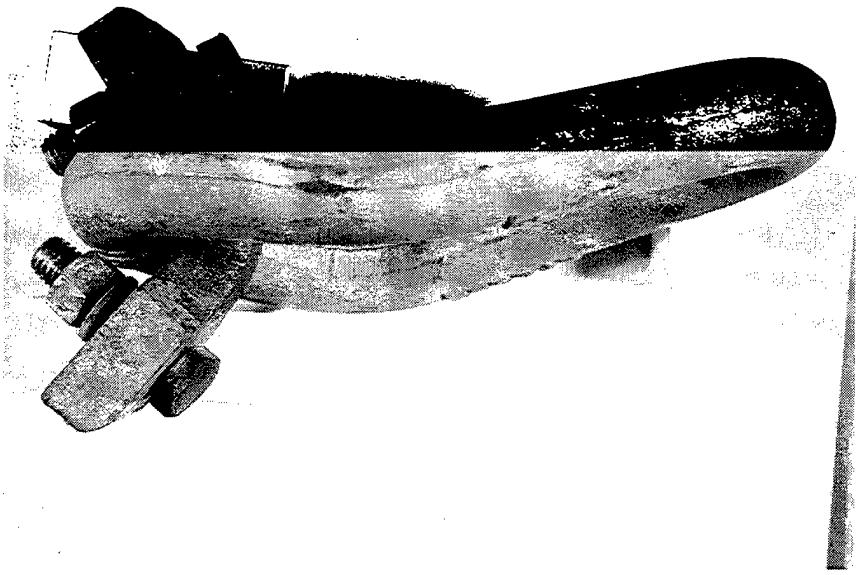

Figure 61. Close-up view of the lifting bar that had bent around the egg-shaped ring during the pull test. Note the 20° offset bend in the ring that had to be bent to be paralleled to the loading axis.

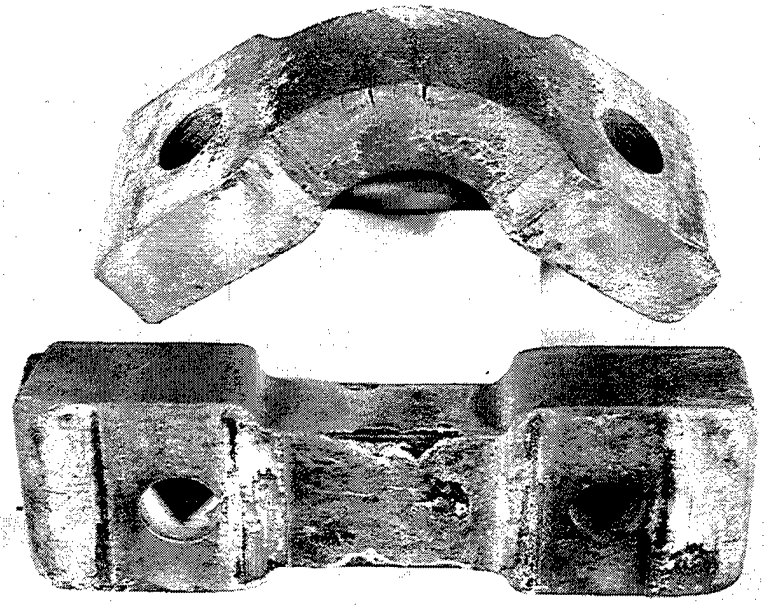

Figure 62. Comparison of the bent lifting bar (top) after the pull test to the straight bar. Note the "dogbone" shape of the lifting bar.

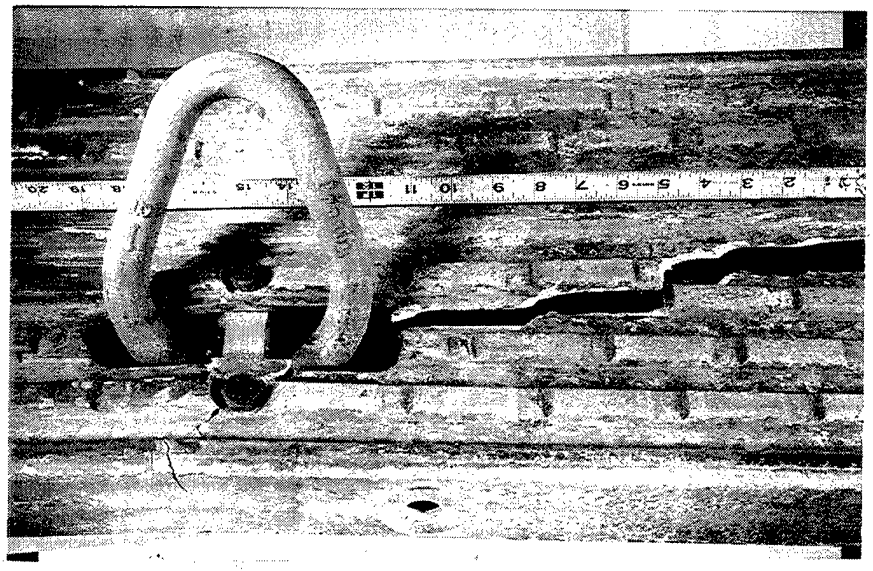

Figure 63. Damages to the extruded aluminum deck panel with the new stronger lifting device bolted to the oblong hole in the panel as the result of the second pull test. Note that the crack started from one end of the oblong hole (right) and continued to the end of the panel (not seen in the photograph). Also, note the smaller cracks at the lower bolt hole of the oblong hole. The bolt hole was sheared and the crack continued to the edge of the panel. The steel ring was used to pull on the lifting bar in the panel during the test.

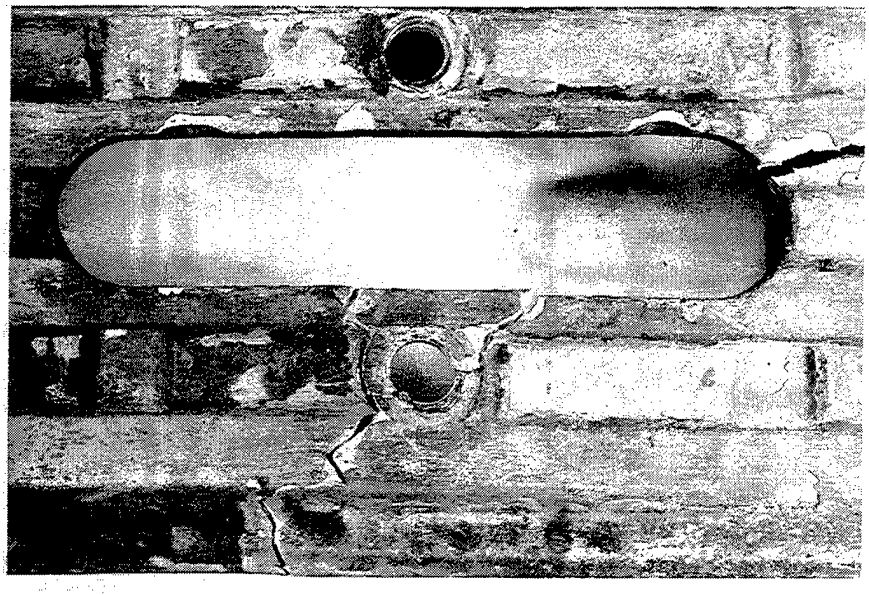

Figure 64. Close-up view of the damaged oblong hole in the deck panel in Figure 63 after the removal of the lifting bar, bolts, and steel ring. Although not clearly seen in the photograph, a small crack was observed in the upper bolt hole.

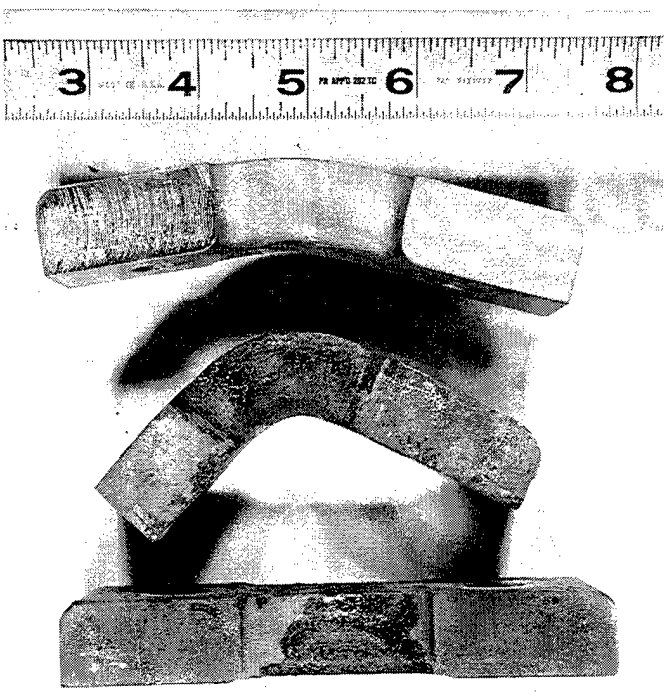

Figure 65. Edge view of the lifting steel bars revealing the extent of bending to the top two bars after the pull tests. The bottom bar served as the reference part that had not been tested for comparison. The middle bar was the original bar made of specified ASTM A 36 structural steel. It was used in the first test that went to 20,250 lb maximum at the time of the failure. The top bar was the new stronger bar made of T-1 steel material. It was used in the second test that went to 28,500 lb maximum at the time of the failure.

Figure 66. Damage to the original lifting device at the oblong hole in the AVLB deck panel after the third pull test. Note that the lifting steel bar was bent slightly around the egg-shaped steel ring.

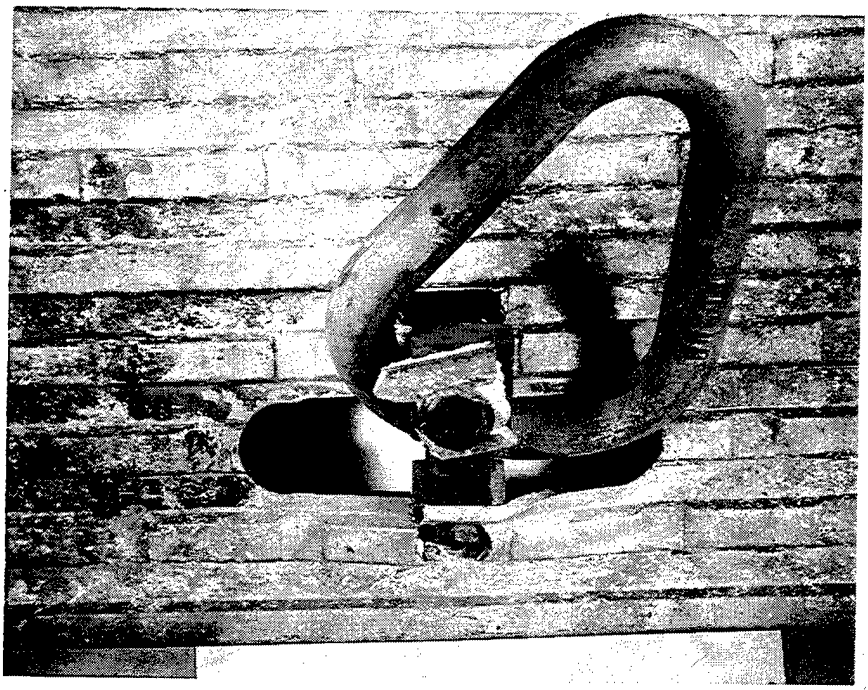

Figure 67. Close-up view of the damaged lifting device at the oblong hole in Figure 66 after removal from the testing machine. Note a small section of the deck panel sheared from the upper edge of the oblong hole, where the final failure of the lifting device occurred.

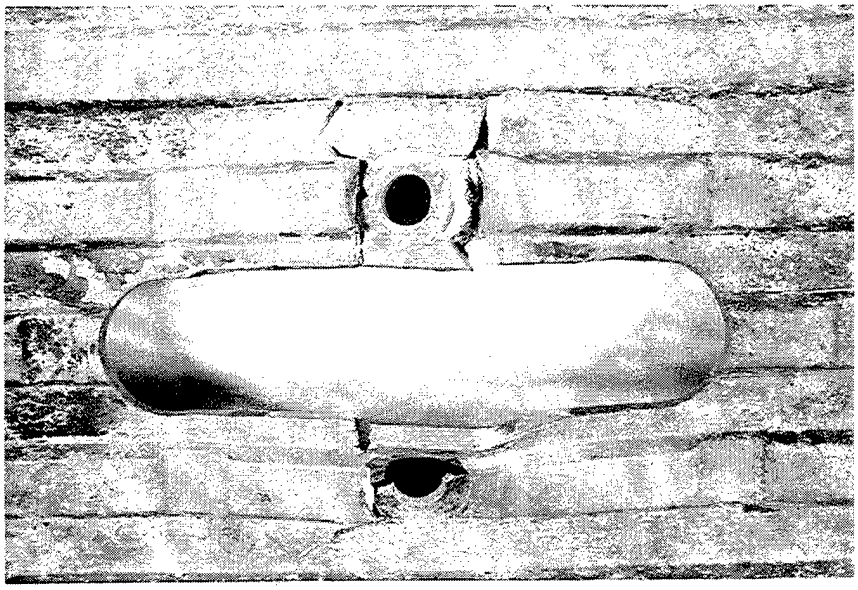

Figure 68. Same close-up view of the damaged oblong hole in Figure 67 after the removal of the lifting bar, bolts, and steel ring.

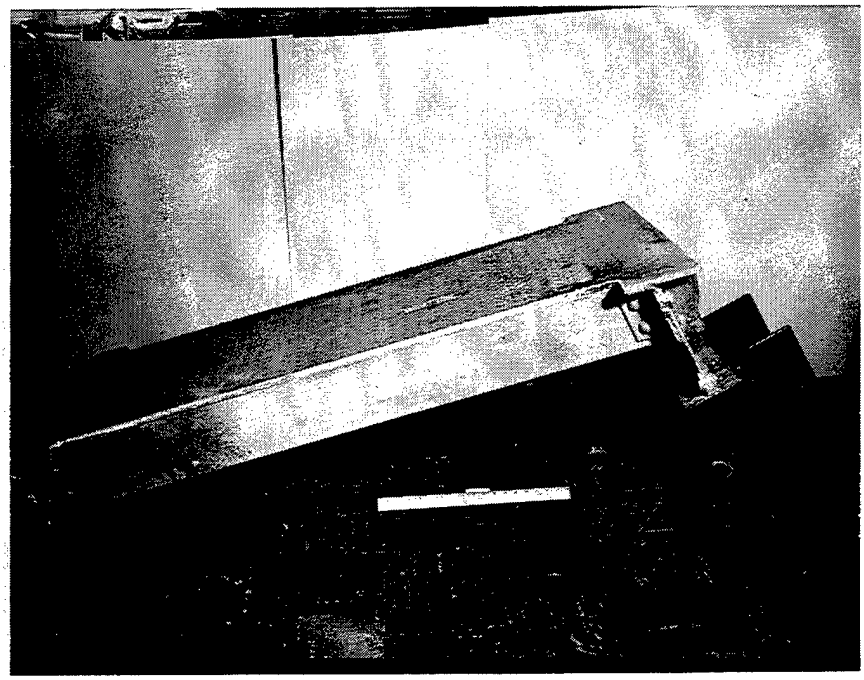

Figure 69. Side view of the large test section cut from the ramp deck end of the AVLB male end panel assembly. The special test jig was already bolted to the bottom of the end plate at right.

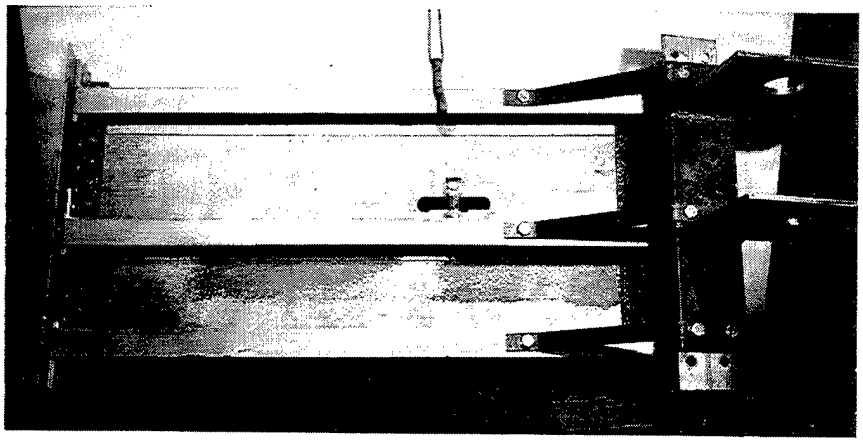

Figure 70. Underside view of the test section in Figure 69. Three aluminum channels can be seen in a longitudinal direction with both ends riveted to the aluminum end plates. Steel straps were bolted to the test jig at right and to the channel flanges to reinforce the end plate to prevent flexing during the pull tests. Note the lifting steel bar bolted at the oblong hole in the aluminum floor plate.

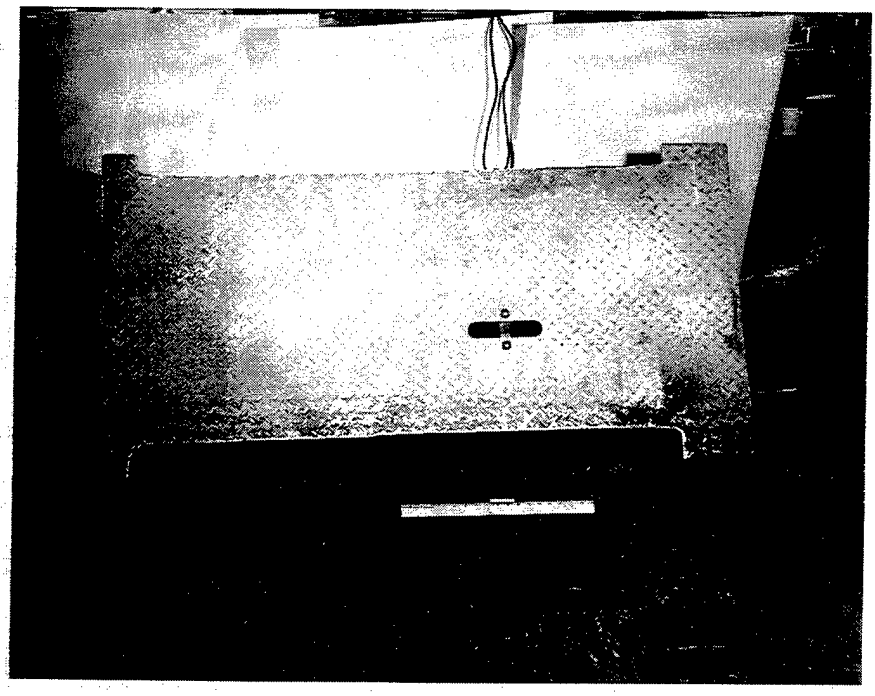

Figure 71. Top view of the surface deck of the test section in Figure 69. See the rolled raised figure for skid resistance on the surface. Note the lifting bar bolted underneath the oblong hole in the aluminum floor plate.

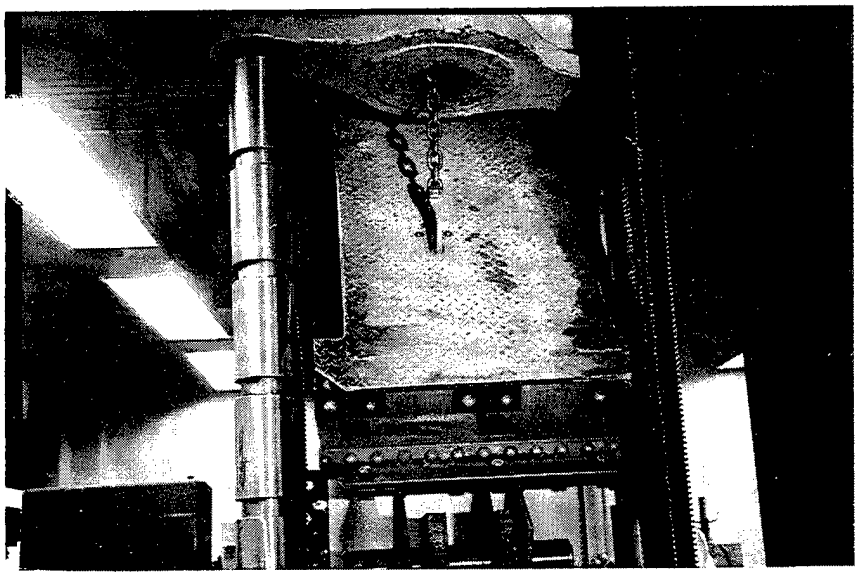

Figure 72. Front view of the large AVLB test section in position in the testing machine for the pull test. The test jig bolted to the bottom of the section is connected by a large round steel bar to another test jig fastened to the lower fixed crosshead. A large chain with the clevis hook around the lifting steel bar in the oblong hole in the floor plate is attached to the upper movable crosshead.

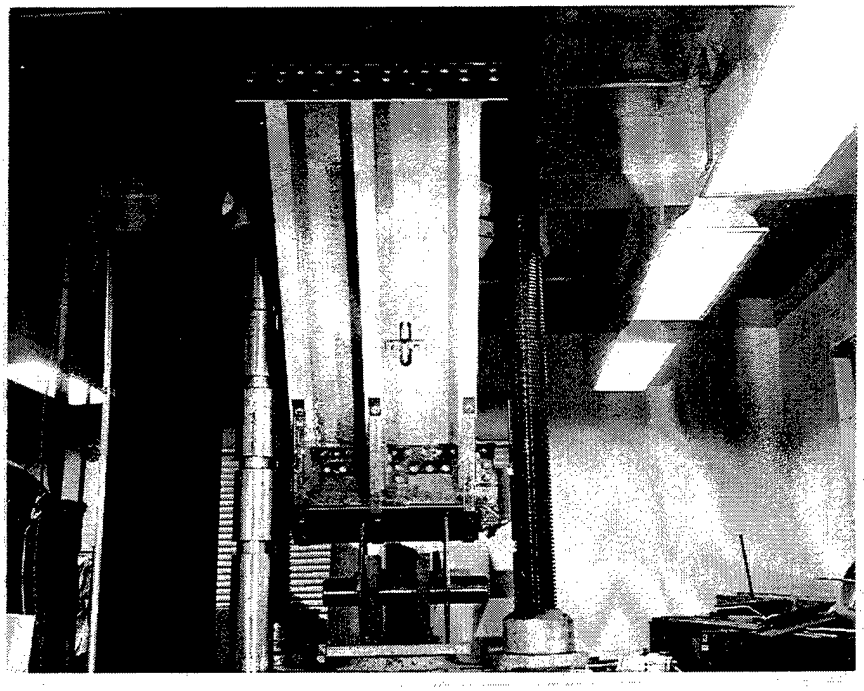

Figure 73. Back view of the test section in Figure 72. The section is positioned in such a manner that the lifting bar bolted at the oblong hole would be loaded at 45° to simulate the loading condition when the lifting sling with legs at 45° to the lifting points is used to lift the AVLB.

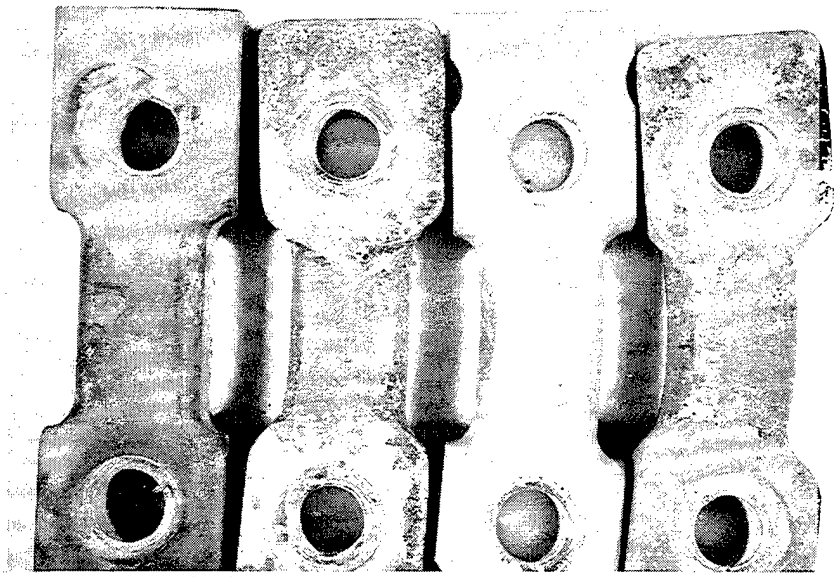

Figure 74. Top view of the lifting steel bar samples after their pull tests. The amounts of bend observed in three samples on the right were compared to the untested straight bar on the left. The first original bar (second from left) was pulled to 20,600 lbs maximum, the stronger bar made from T-1 steel material (third from left) to 39,500 lbs maximum, and the second original bar on right to 30,000 lb. Those three bars were permanently bent horizontally.

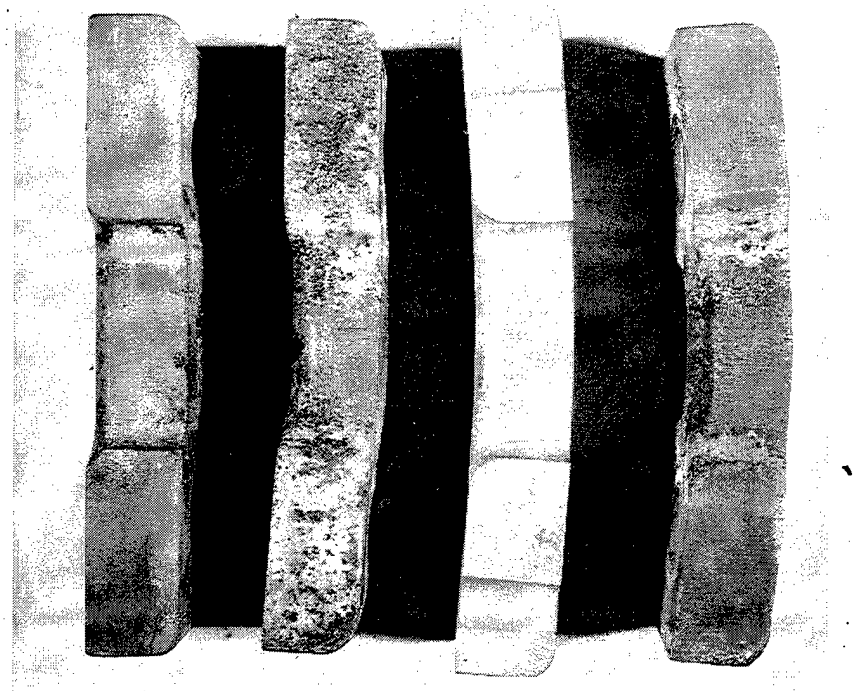

Figure 75. Side view of the same lifting steel bar samples in Figure 74. The three bars on the right were permanently bent vertically.

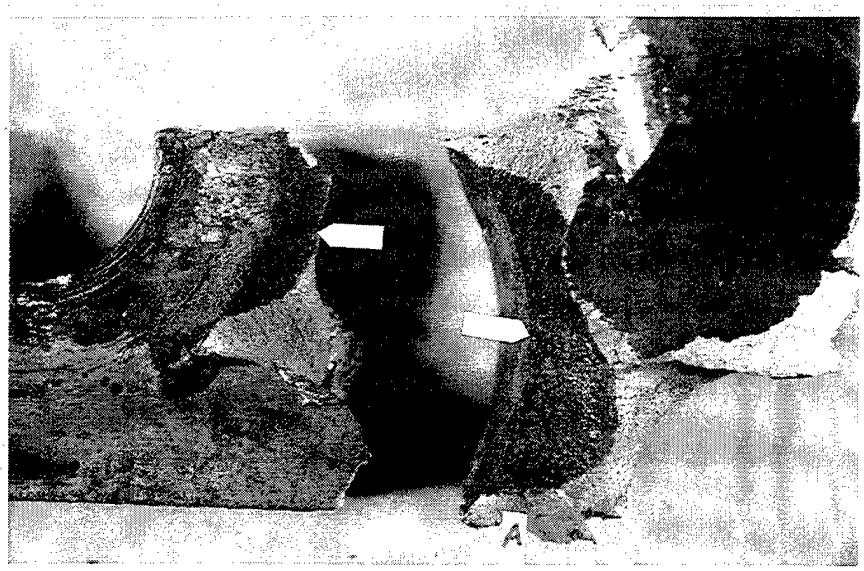

Figure 76. Two small aluminum pieces broken from a 1/2-inch-diameter bolt hole in the AVLB extruded deck panel containing the lifting device that was tested during the first pull test. The arrows point to the matching discolored (dark) areas in the fractured surfaces of both pieces. The curvature seen in the right piece (A) is the wall surface of the counterbore that cut into a protruded tread on the top surface of the deck panel to provide the clearance for the bolt head and socket tool. The pieces are seen in Figures 59 and 60. A small metallographic specimen was cut from the right piece for microstructural examination. Magnification: 2 1/4×.

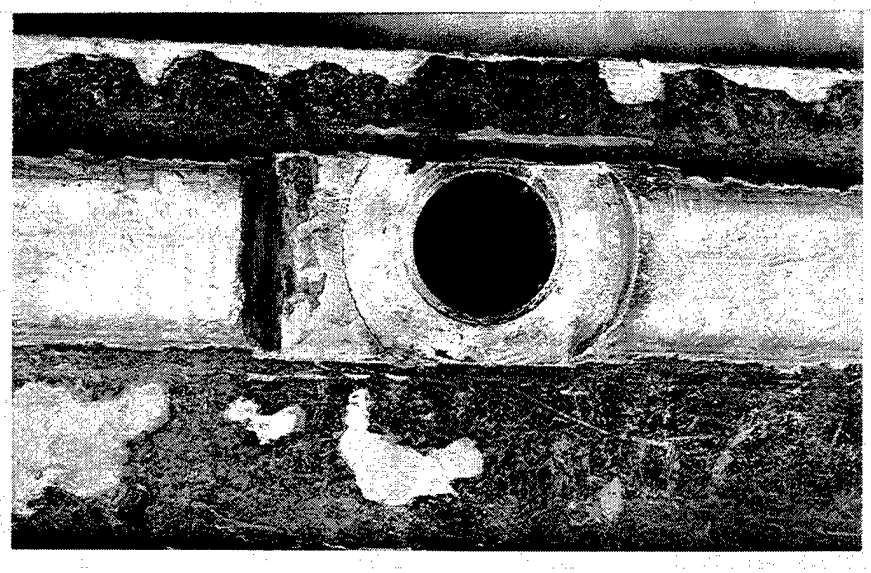

Figure 77. An example of a counterbored bolt hole made on top of the AVLB extruded aluminum deck panel. Note that counterboring had cut into the protruded tread on the right, leaving a sharp fillet at the bottom of the counterbored hole. The fillet can act as a stress raiser for the crack initiation.

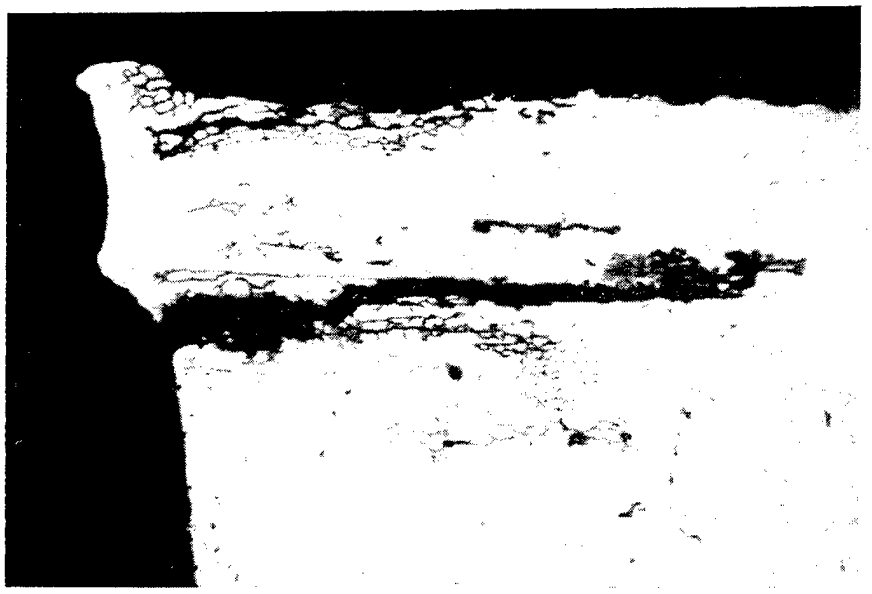

Figure 78. As-polished microstructure showing intergranular corrosion and cracks adjacent to the fracture at top. The vertical side on the left of the microstructure is the wall surface of the counterbore hole, and the slight curvature at the upper left is a portion of the sharp fillet at the bottom of the hole where a crack was initiated because the sharp fillet acted as a stress raiser. Magnification: 380×.

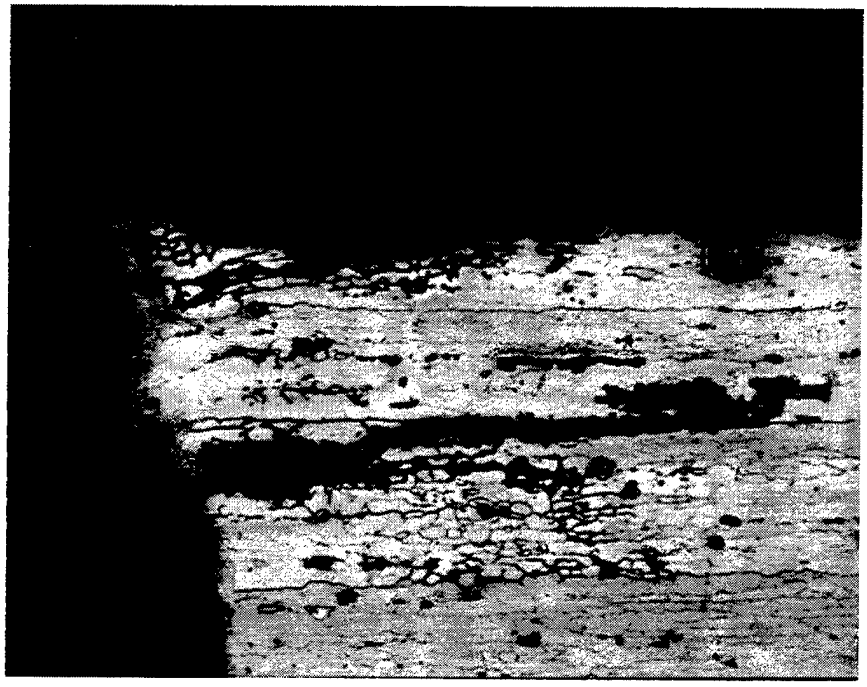

Figure 79. Etched microstructure of the same area in Figure 78. Magnification: 380×. Keller's etchant.

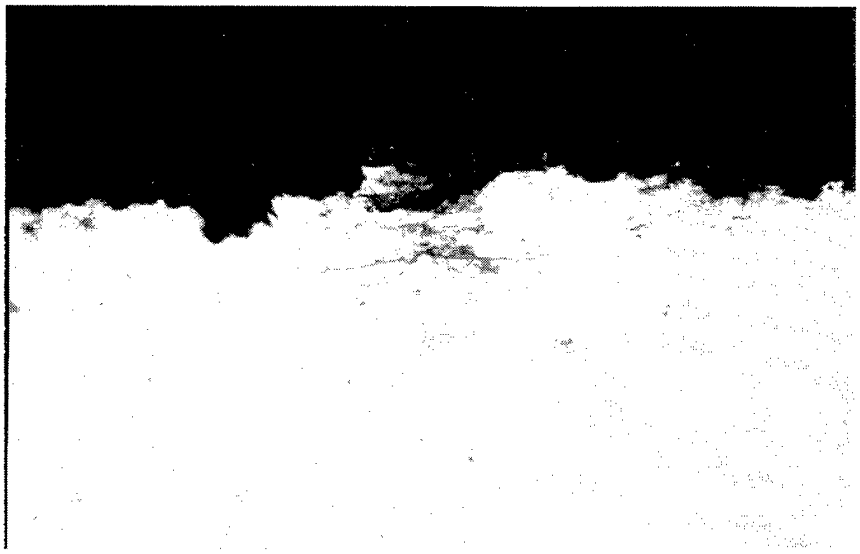

Figure 80: As-polished microstructure showing intergranular corrosion and small cracks in the fractured surface at top at a different location from the one shown in Figure 78. Magnification: 380×.

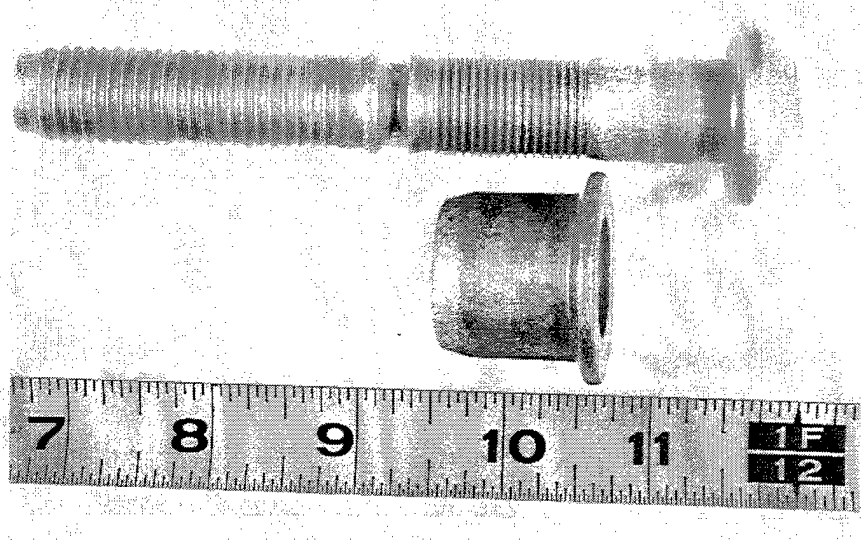

Figure 81. A typical roundhead aluminum Huckbolt fastener consisting of the 3/4-in diameter aluminum pin with the locking grooves next to the smooth shank, the grip stem at the end of the pin, and the flanged aluminum collar. Note the large notch in the center of the pin where the stem will break during the installation of the fastener like a "pop" rivet.

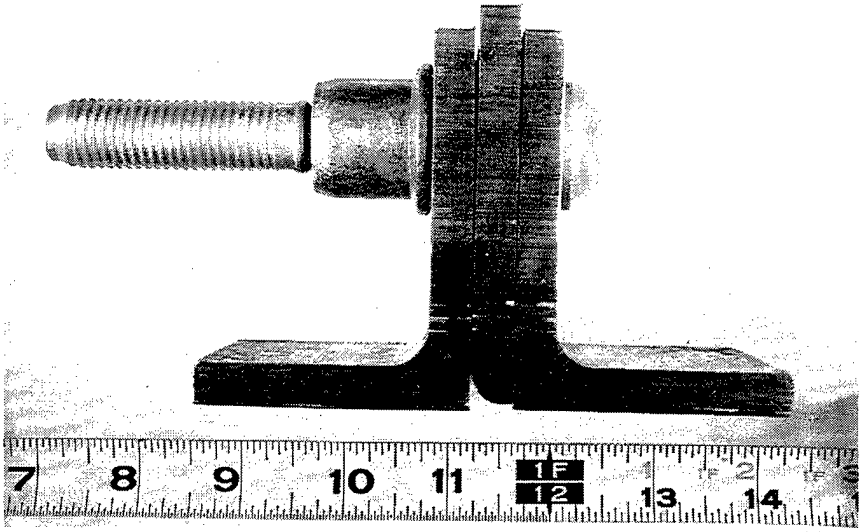

Figure 82. Shear test specimen with a Huckbolt fastener prior to swaging of the collar. The grip stem will be grabbed by the installation tool and broken off after the collar is swaged onto the locking groove section of the pin by the anvil of the tool.

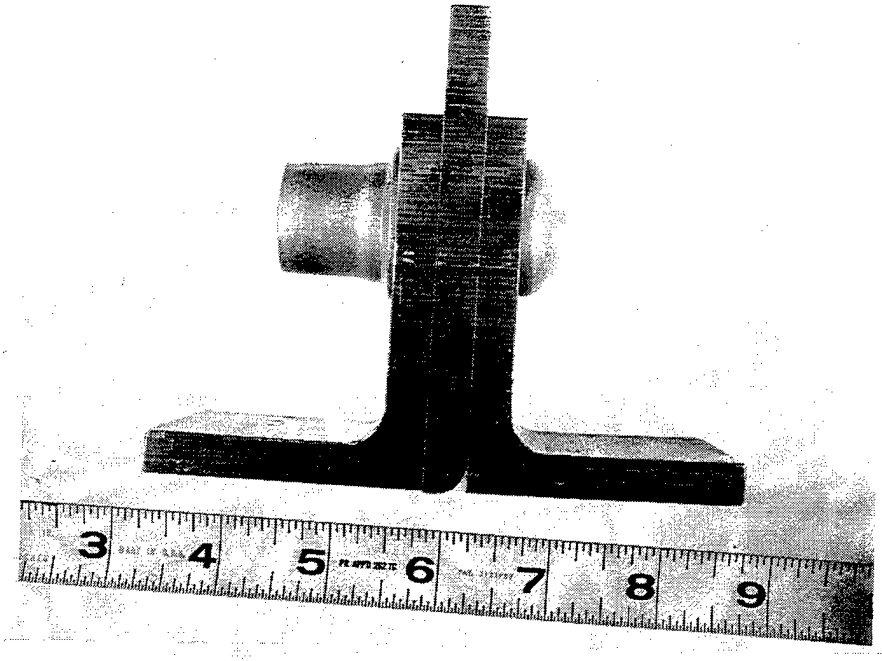

Figure 83. Shear test specimen with the Huckbolt fastener. The center piece will serve as a plunger to shear the shank of the pin during the test. The collar is fully swaged. Note the amount of deformation that had occurred on the outside wall of the collar during the swaging process by the tool anvil.

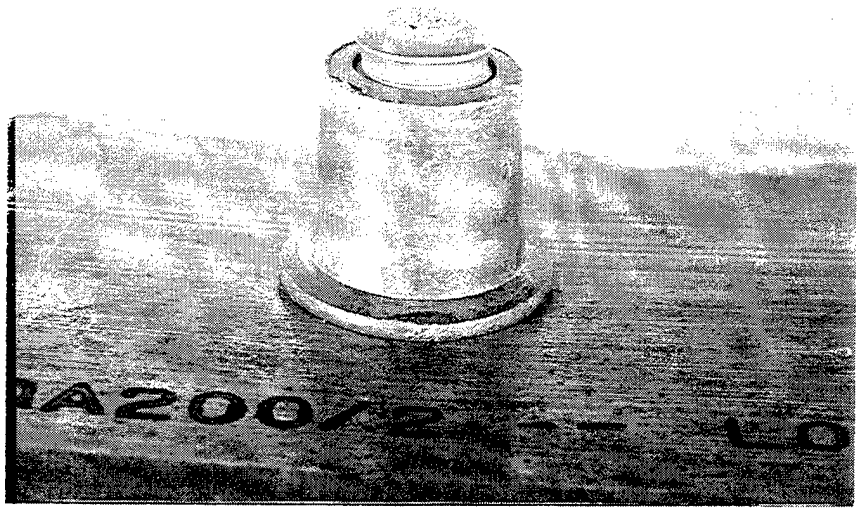

Figure 84. Fully swaged collar of the Huckbolt fastener after the installation. Note that the grip stem portion of the pin was already broken off at the end. (Test Specimen G)

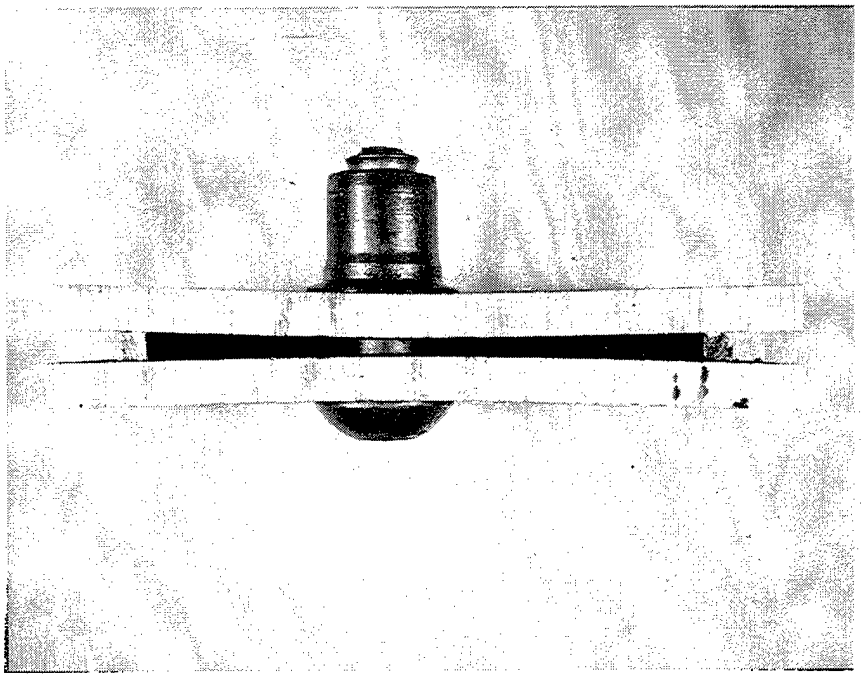

Figure 85. Edge view of the Huckbolt assembly test Specimen G. Two 1/4-in steel bars were used as spacers to form the 1/4-in gap between the angle legs. Note the amount of deflection in both legs when the fastener was installed to show the clamping action during the installation.

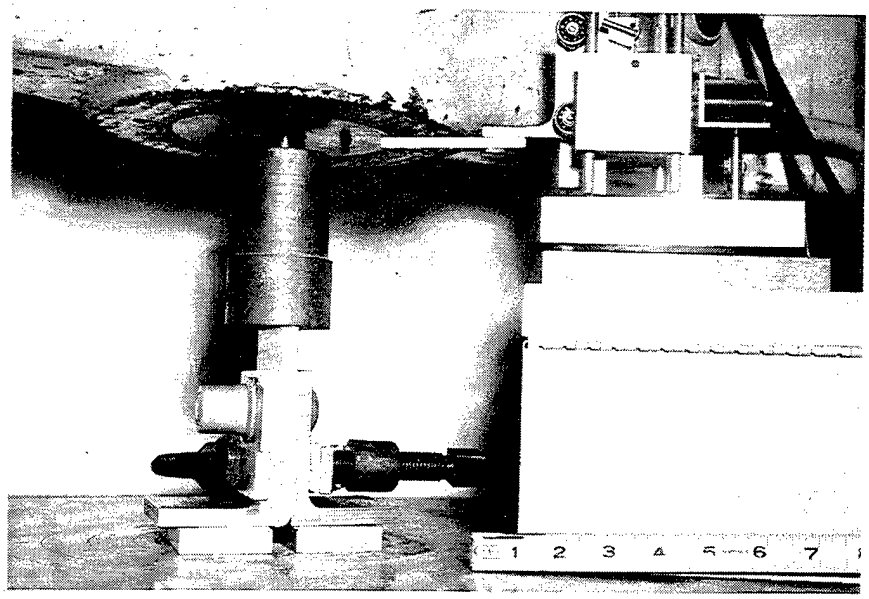

Figure 86. A typical shear test setup of the Huckbolt assembled test Specimen B for double shearing in the pin shank. The specimen was set on 1/2-in-thick blocks to permit the bottom end of the plunger (center piece) to extend beyond the bottom of the angle horizontal legs. A deflectometer was placed in position on the testing machine to measure the movement of the machine table to obtain the load-deflection curve. A clamp was used below the fastener to prevent the spreading of the angle vertical legs at the bottom during the test.

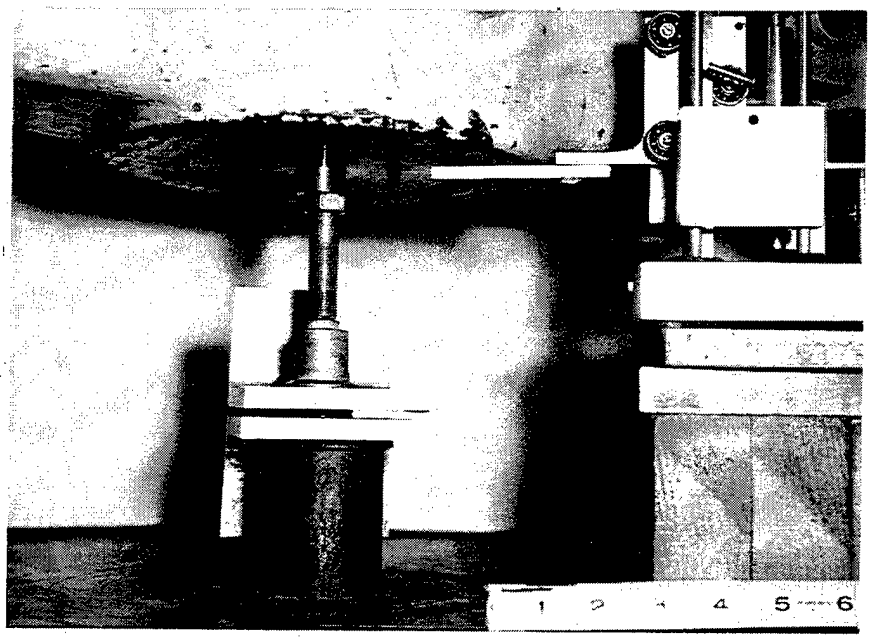

Figure 87. A typical push test setup of the Huckbolt assembled test Specimen F. An SAE grade 8 steel bolt served as a plunger on the end to push the pin through the swaged collar. The round head of the pin was placed in the steel tube at the bottom. The test specimen contained two large flat washers to serve as the spacer between two angles that were assembled back to back with the Huckbolt fastener. A deflectometer was used to obtain the load-deflection curve.

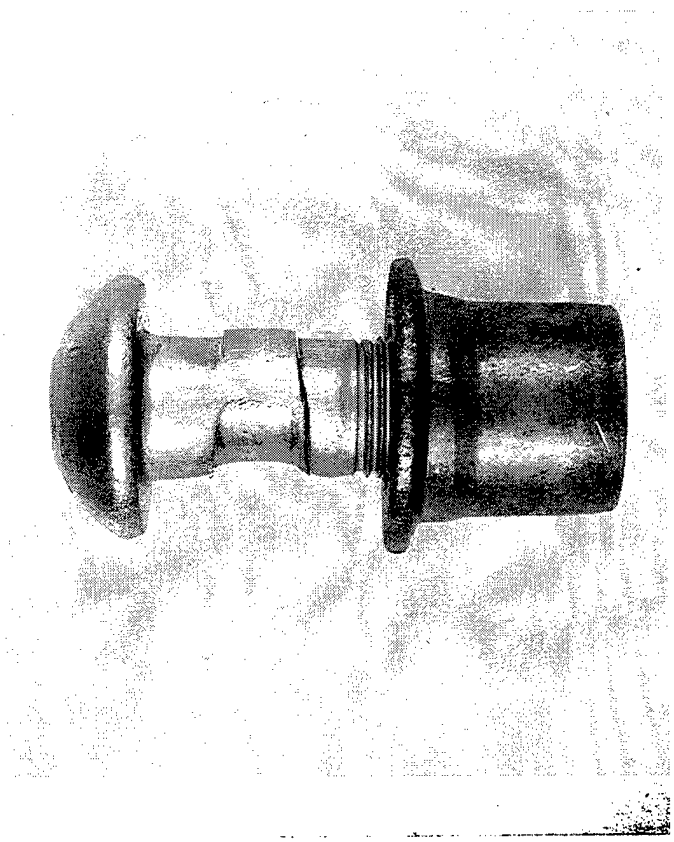

Figure 88. Double-sheared Huckbolt fastener from shear test Specimen A after the shear test. The collar was fully swaged. Actual size.

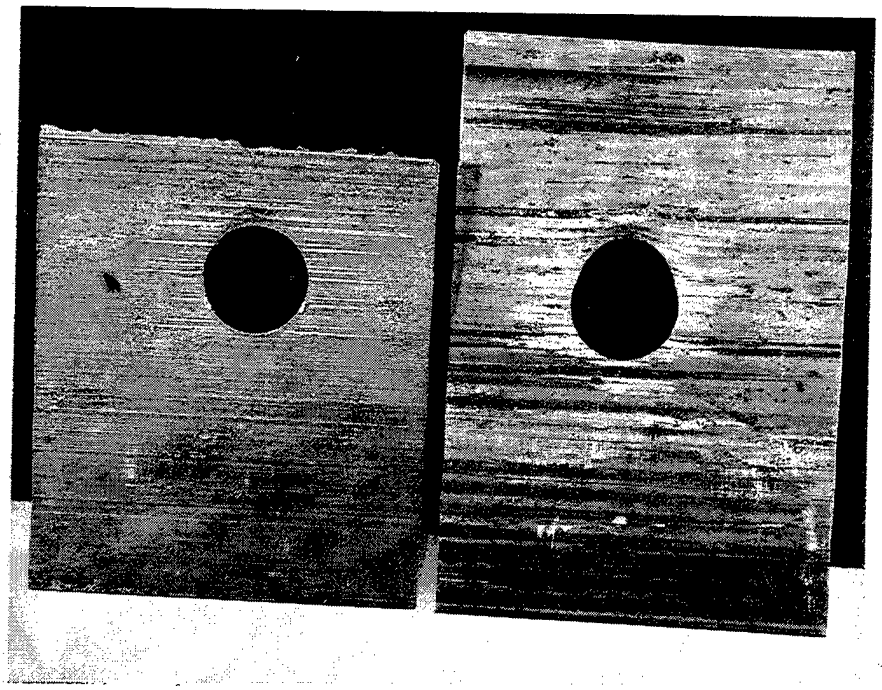

Figure 89. The effect of the shear test on the holes in shear test Specimen A. Note the elongated hole in the center piece (plunger) on right and very little elongation in the hole of the angle leg on left.

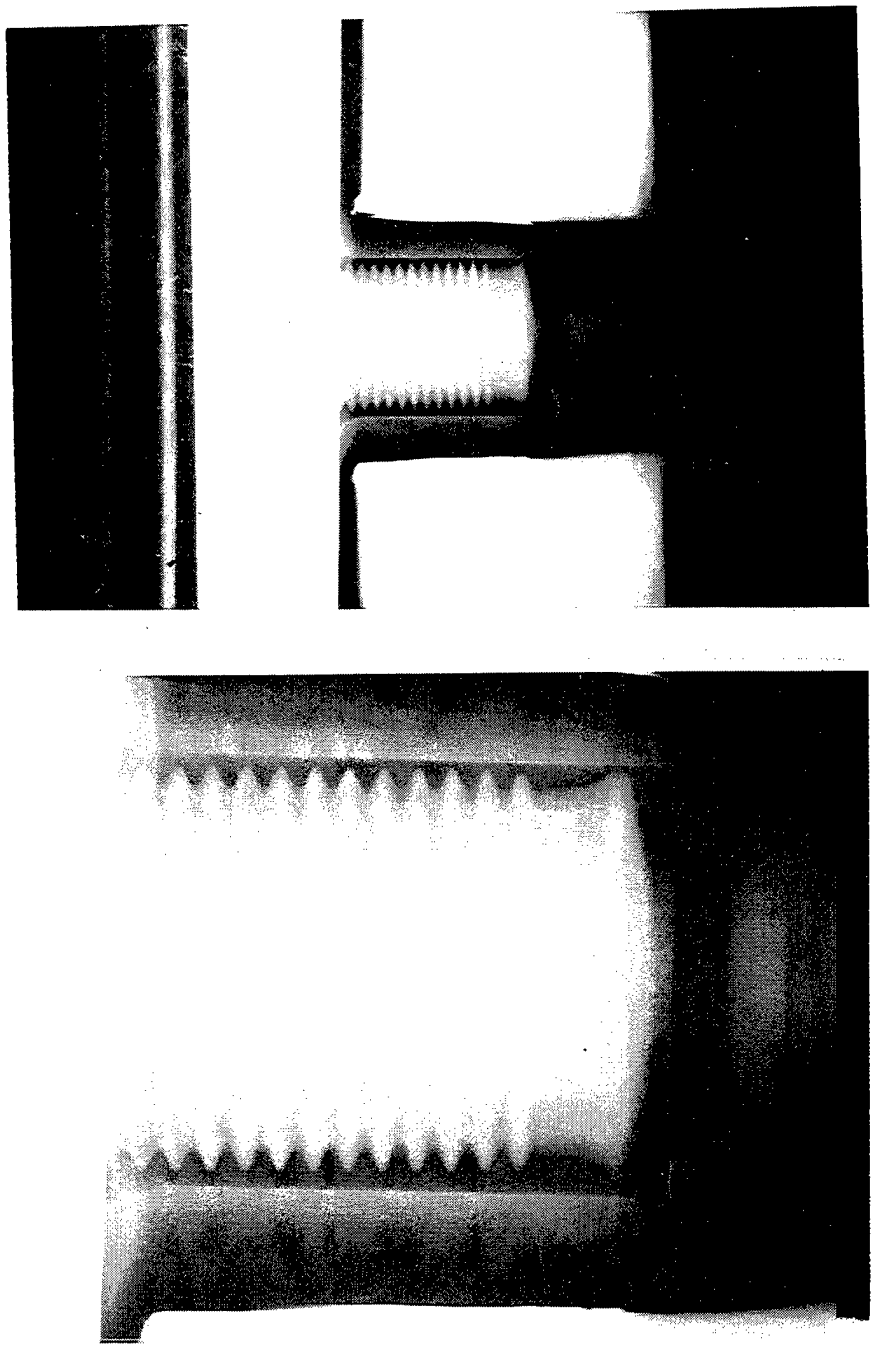

Figure 90. Photographs of a radiographic image of the collar not yet swaged onto the locking groove portion of the Huckbolt fastener pin. Actual size (top). Magnification: 2 2/3× (bottom).

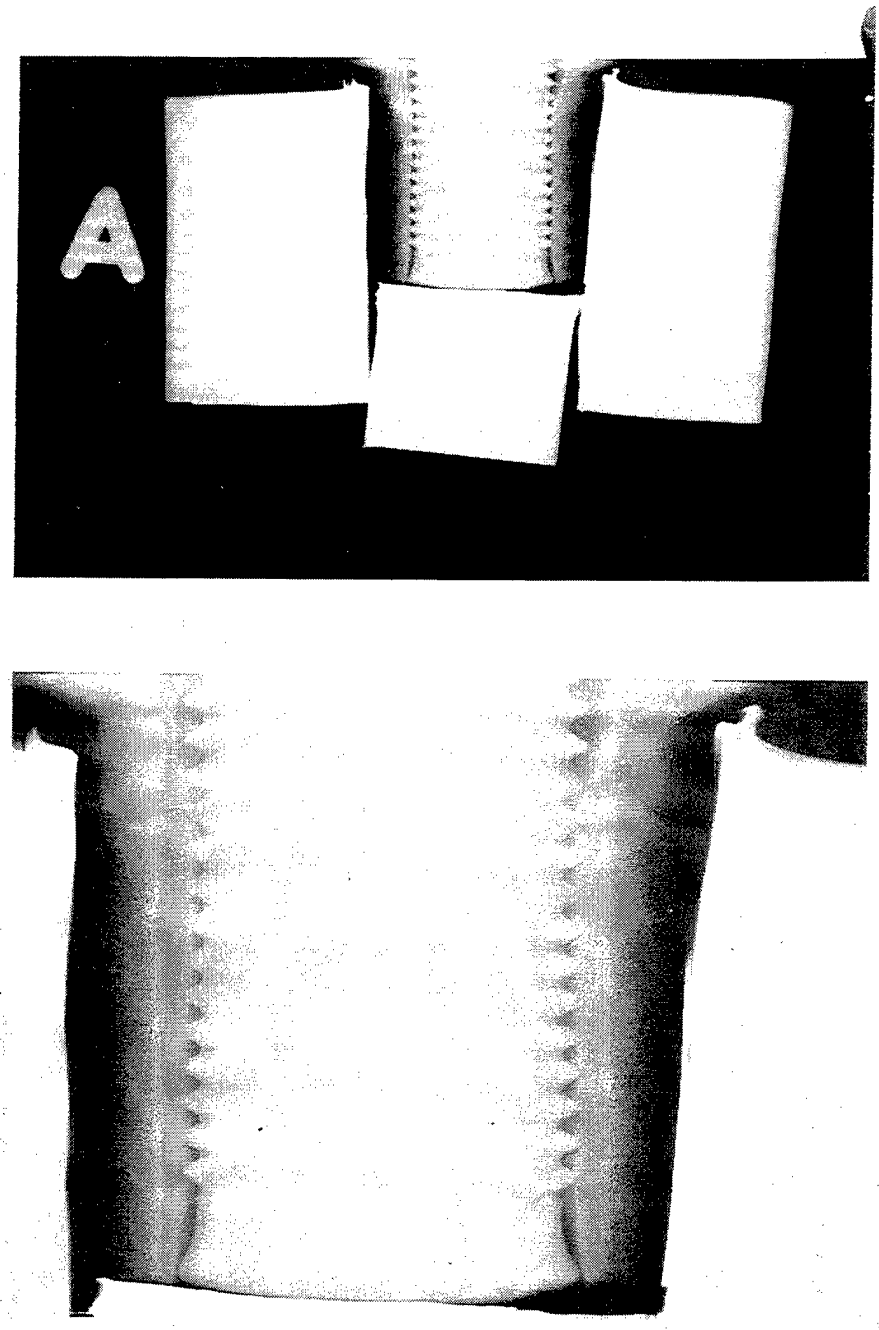

Figure 91. Photographs of a radiographic image of the collar fully swaged on the locking groove portion of the Huckbolt fastener pin. Shear test Specimen A. Actual size (top). Magnification: 2 2/3× (bottom).

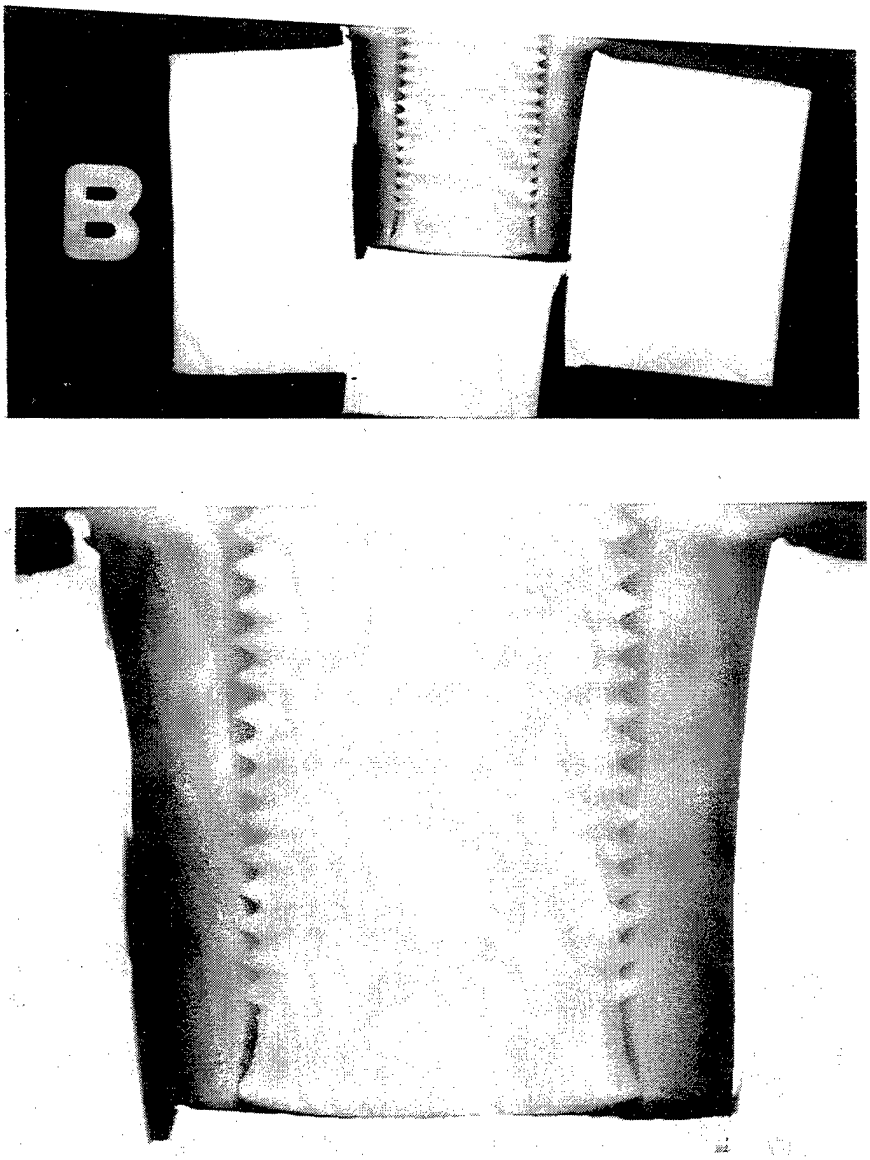

Figure 92. Photographs of a radiographic image of the collar half swaged on the locking groove portion of the Huckbolt fastener pin. Shear test Specimen C. Actual size (top). Magnification: 2 2/3× (bottom).

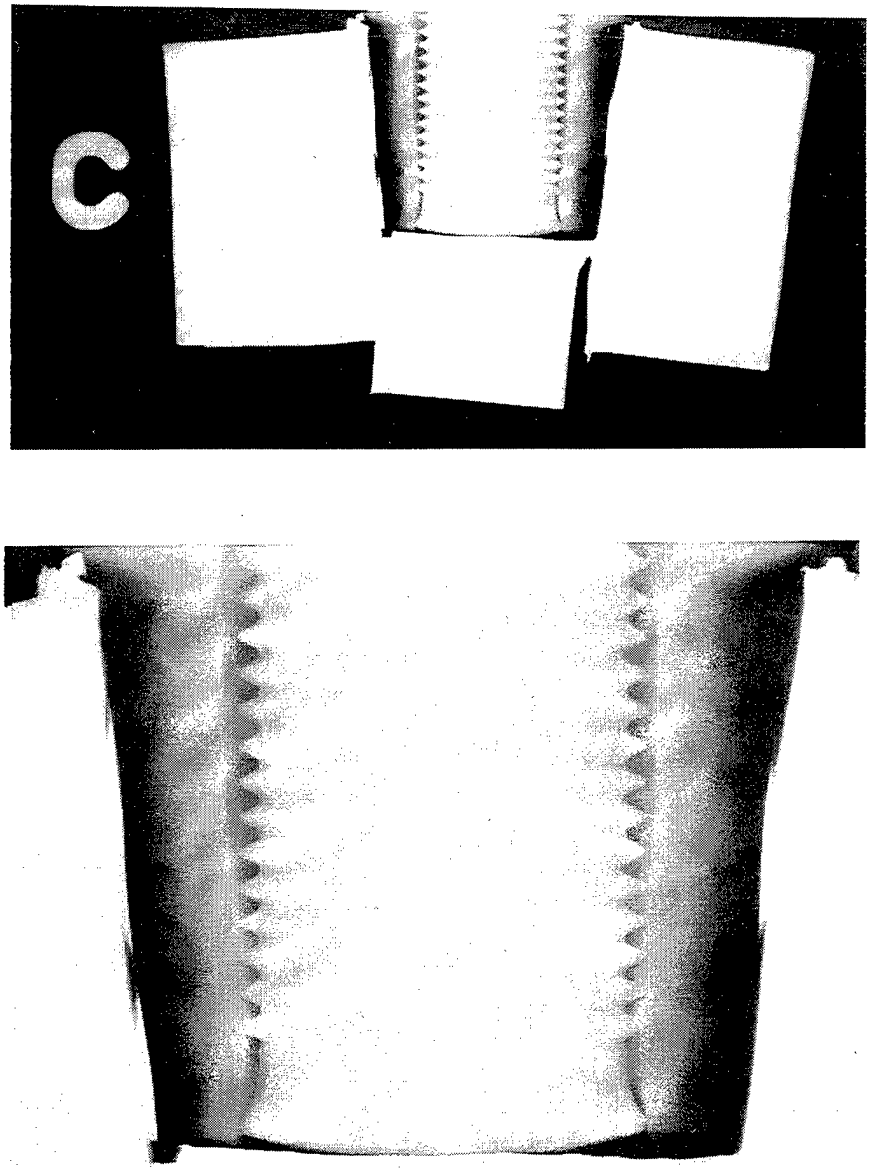

Figure 93. Photographs of a radiographic image of the collar quarter swaged on the locking groove portion of the Huckbolt fastener pin. Shear test Specimen D. Actual size (top). Magnification: 2 2/3× (bottom).

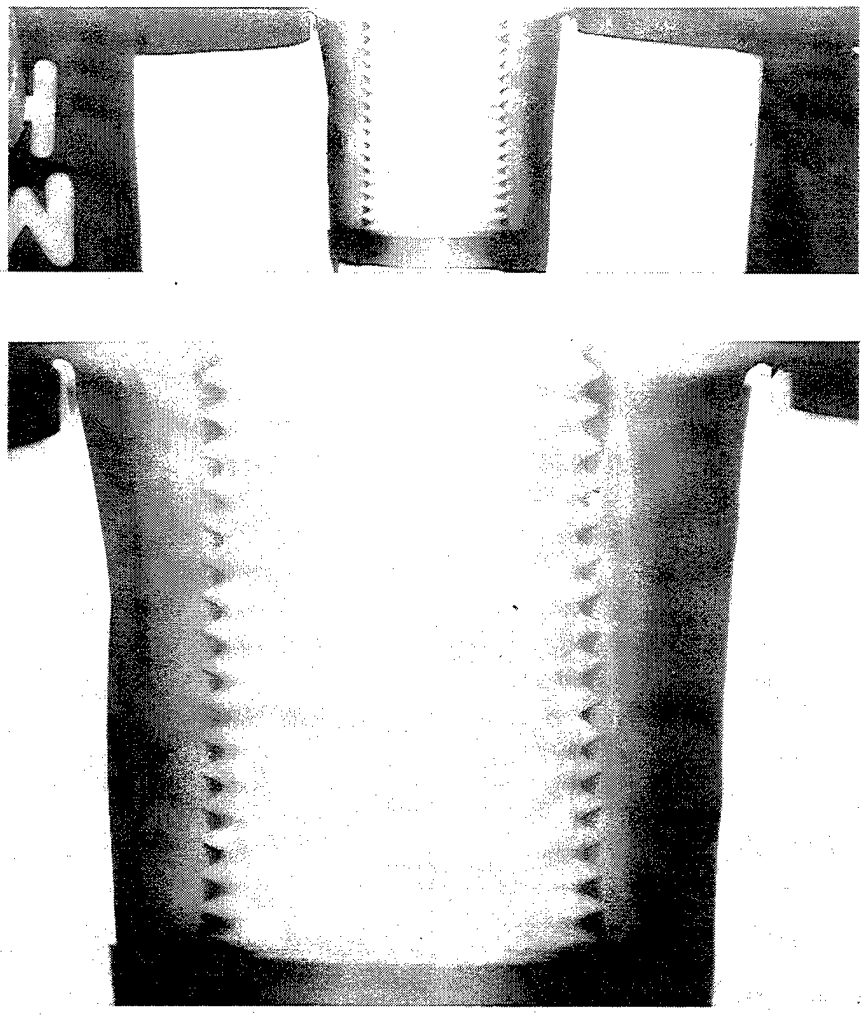

Figure 94. Photographs of a radiographic image of the collar fully swaged on the locking groove portion of the Huckbolt fastener pin. Shear test Specimen F. The push test was stopped at a 21,350-lb maximum load before the complete shearing of the collar interior wall. Note partial shearing of the wall in the image. Actual size (top). Magnification: 2 2/3×.

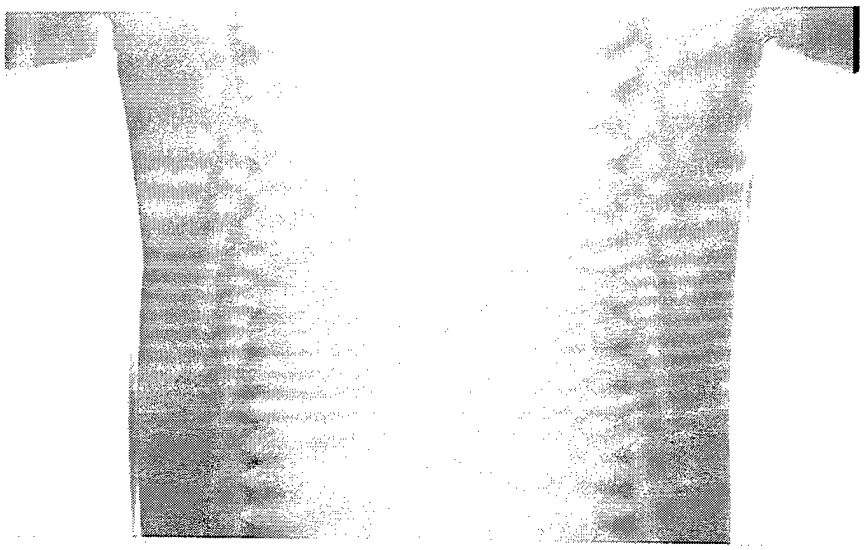

Figure 95. Photograph of a radiographic image of the fully swaged collar on the locking groove portion of the Huckbolt fastener pin before the push test for comparison to Figure 94. Specimen G. Magnification: 2 2/3×.

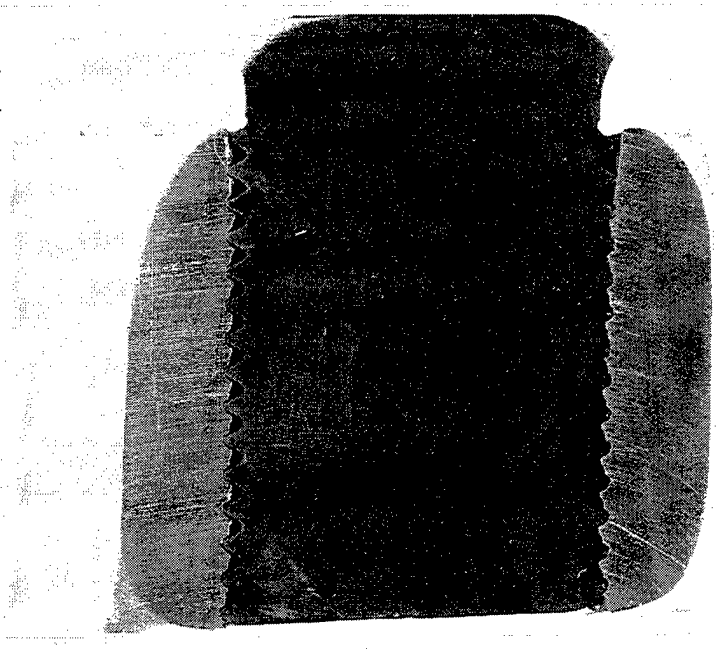

Figure 96. Cross sections of the Huckbolt pin with the locking grooves and the fully swaged collar showing the initial deformation in the collar interior wall penetrated by the tips of the locking groves. The push test of Specimen F was stopped after the maximum load of 21,350 lb was reached and before the indented interior wall was to be stripped completely by the pin-locking grooves. See Figure 97 for the enlarged view. Magnification: 2.7×. 600-grit surface finish.

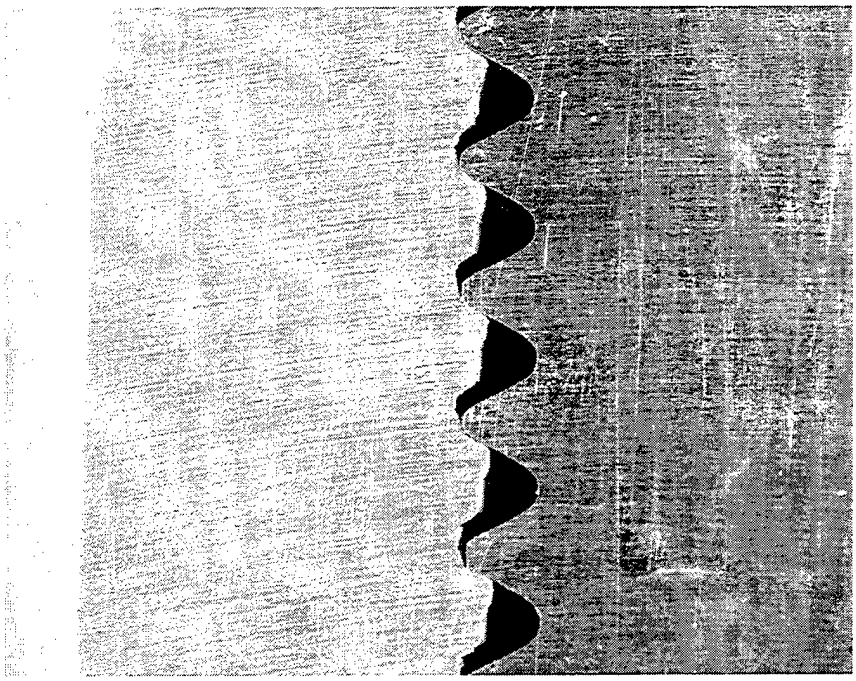

Figure 97. Enlarged view of the cross sections of the Huckbolt pin (right) and collar seen in Figure 96. Note the initial deformation of the indented interior wall of the collar. Magnification: 15×. 600-grit surface finish.

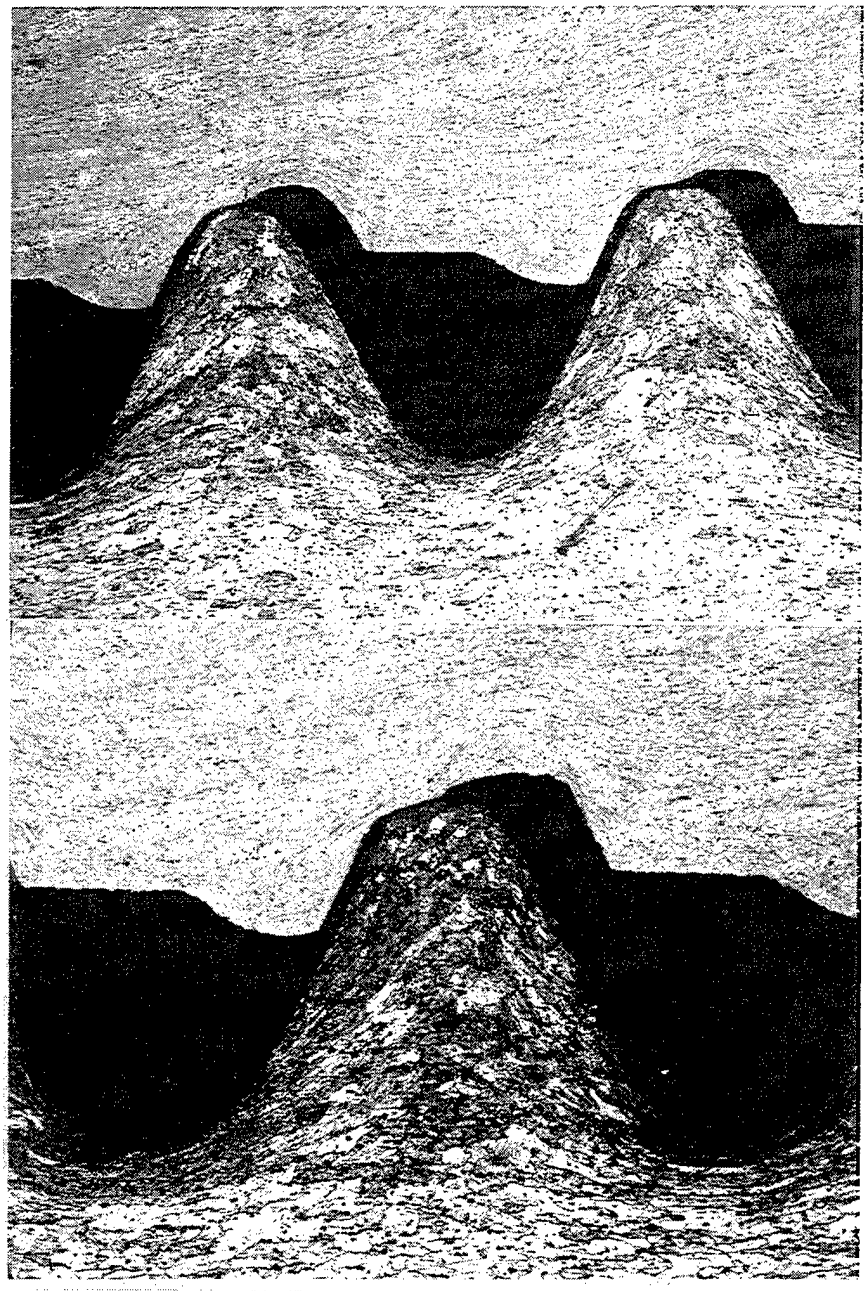

Figure 98. Two magnifications of the etched microstructure of the Huckbolt-pin-locking grooves (bottom of both photographs) and the indented interior wall of the swaged collar of Specimen F in Figures 96 and 97. Note the deformed grain structure in the locking grooves because of the cold rolling of the grooves on the pin. Also note the buildup of the metal in the interior wall of the collar by the penetrated grooves just after the maximum load was reached and before complete stripping of the indented wall had occurred. Magnification: 40× (top) and 50× (bottom). Keller's etchant.

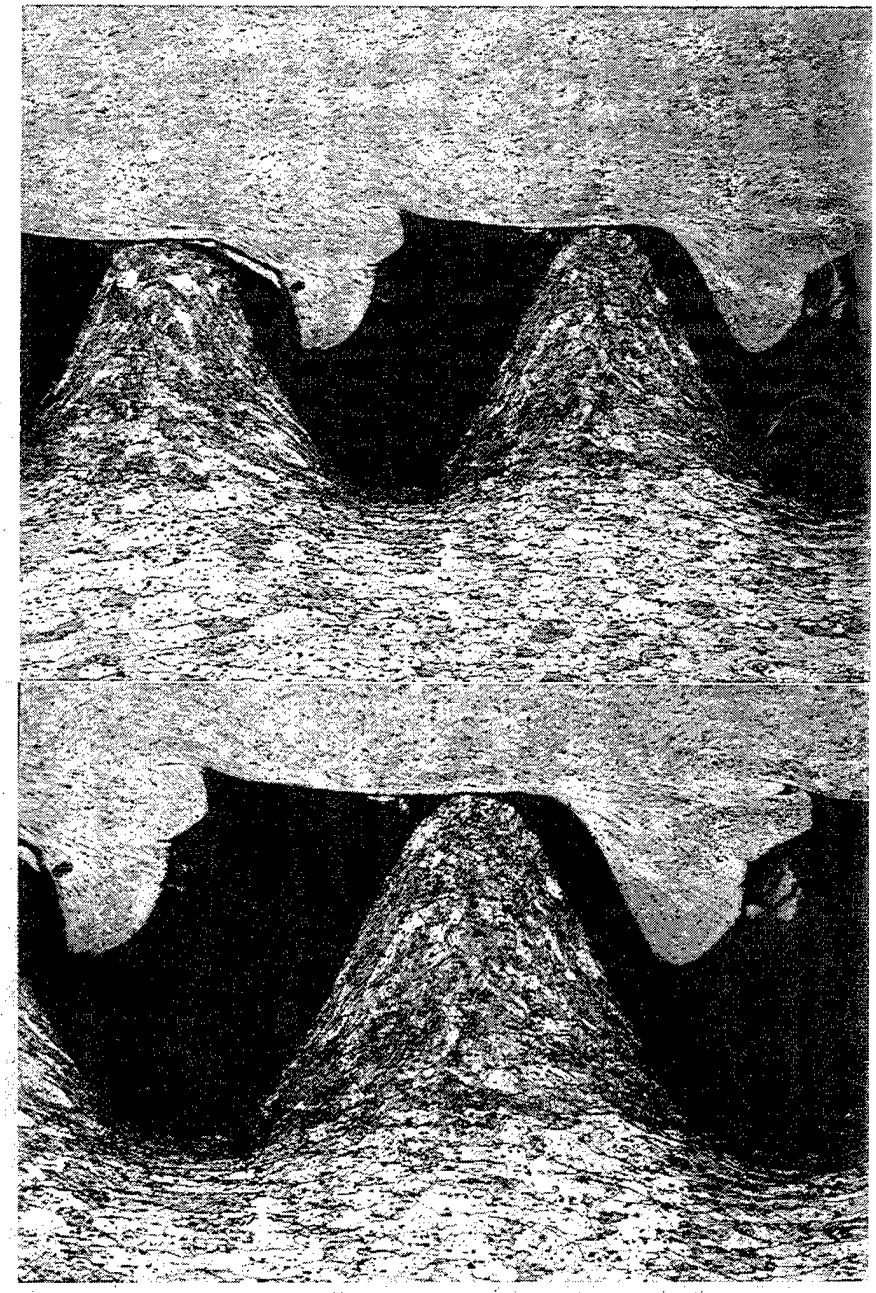

Figure 99. Two magnifications of the etched microstructure of the Huckbolt-pin-locking grooves (bottom of both photographs) and indented interior wall of the 1/4 swaged collar of shear test Specimen D. Note the buildup of the metal in the wall by the penetrated grooves after going beyond the maximum load just before complete shearing of the indented wall took place. The locking grooves of the pin were cold rolled as indicated by the deformed grain structure. Magnification: 40× (top) and 50× (bottom). Keller's etchant.

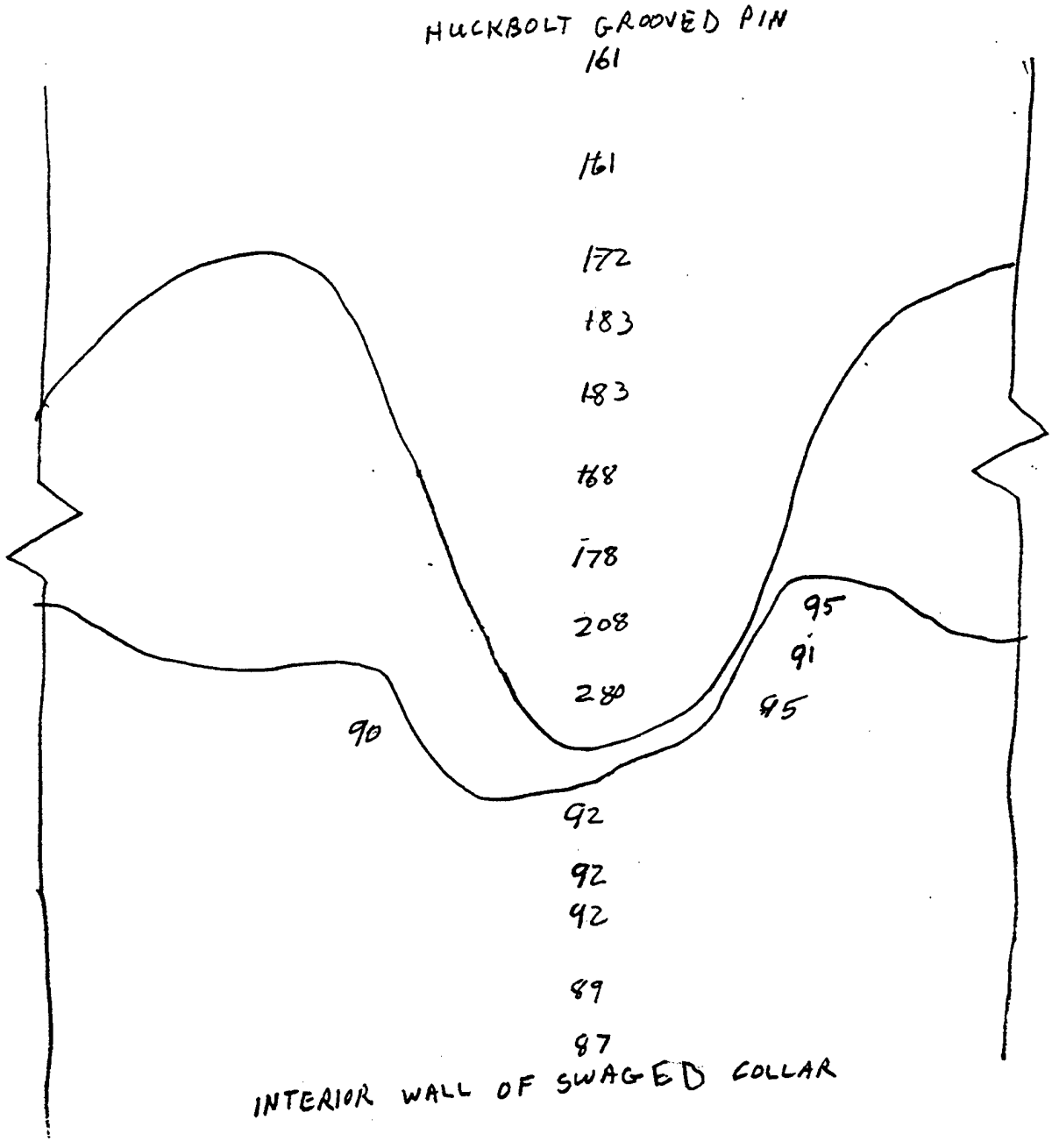

Figure 100. Sketch of the cross sections similar to the microstructure in the bottom photograph in Figure 98. This shows microhardness surveys made on the pin-locking groove (top) and indented interior wall of the swaged collar. The hardness values are Knoop (HK, 200-g load).

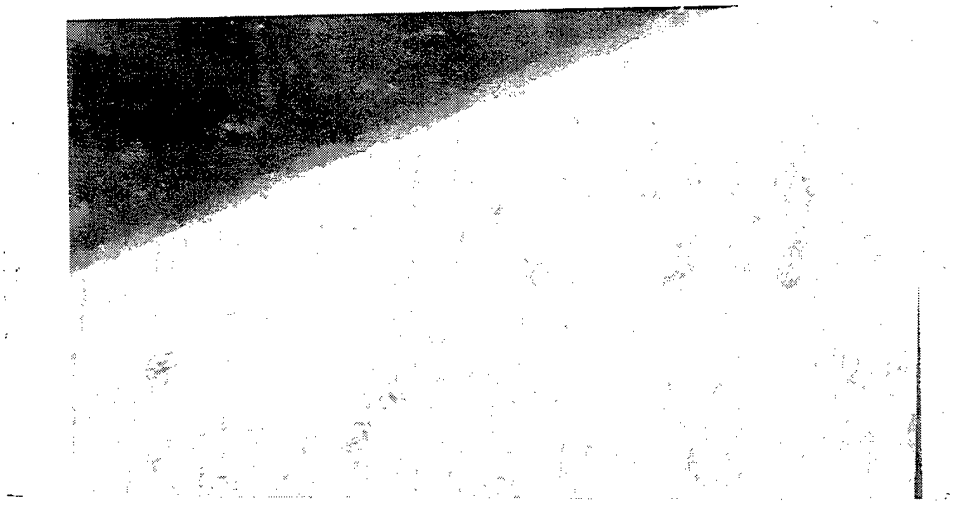

Figure 101. As-ground microstructure of the thin-anodized coatings (diagonal gray line) on the surface of a locking groove of the Huckbolt fastener pin. The thickness of the coating was 0.267 mil. The surface of the specimen was finished by fine grinding to preserve the edge of the thin coating. Magnification: 375×. 600-grit surface finish.

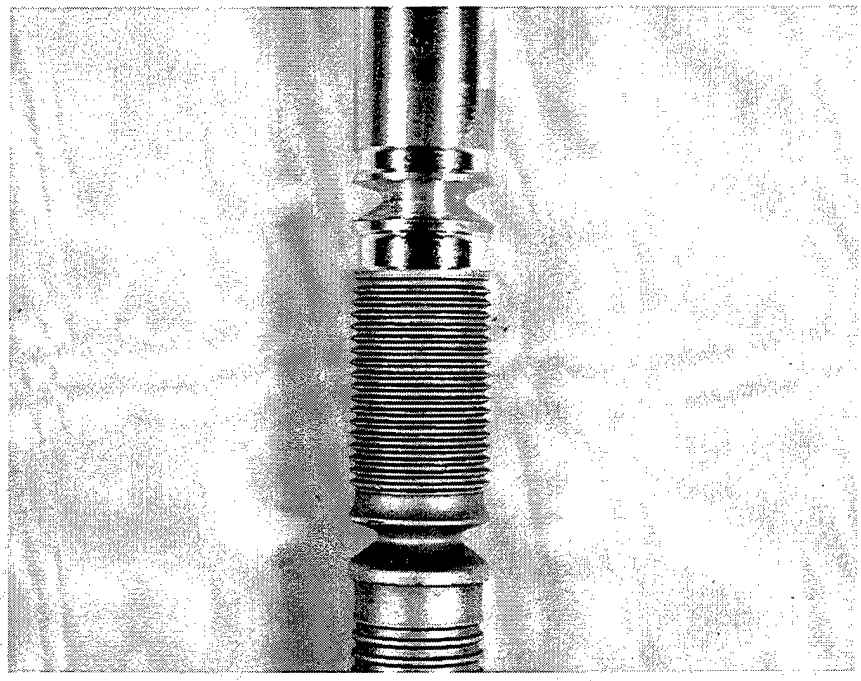

Figure 102. A view of two large breakaway notches on the same Huckbolt pin sample. The upper notch was machined to the same shape and size as the original cold-rolled notch below. The machined notch was located in the smooth shank section of the pin that was not cold rolled.

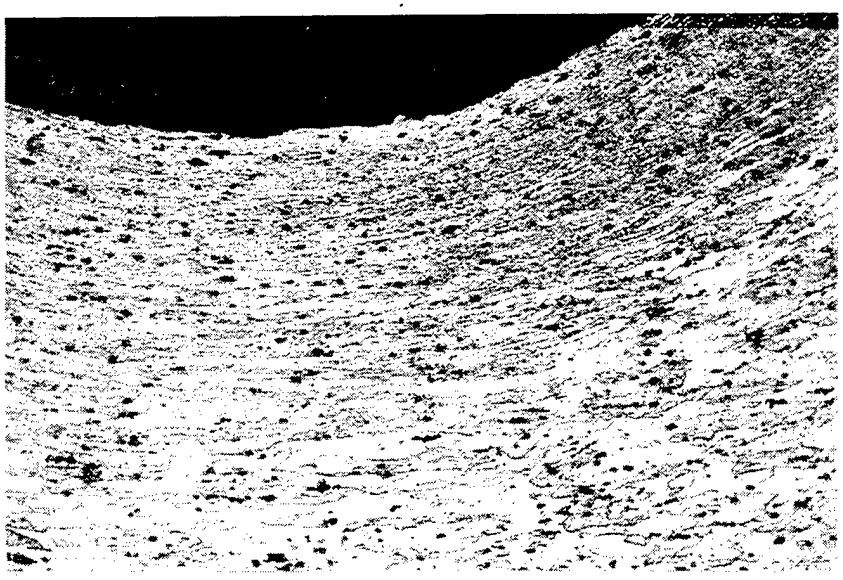

Figure 103. Etched microstructure at the root of the cold-rolled breakaway notch of a Huckbolt aluminum pin sample. Elongated grain structure is seen at the surface edge of the notch, indicative of surface cold rolling. Magnification: 100×. Keller's etchant.

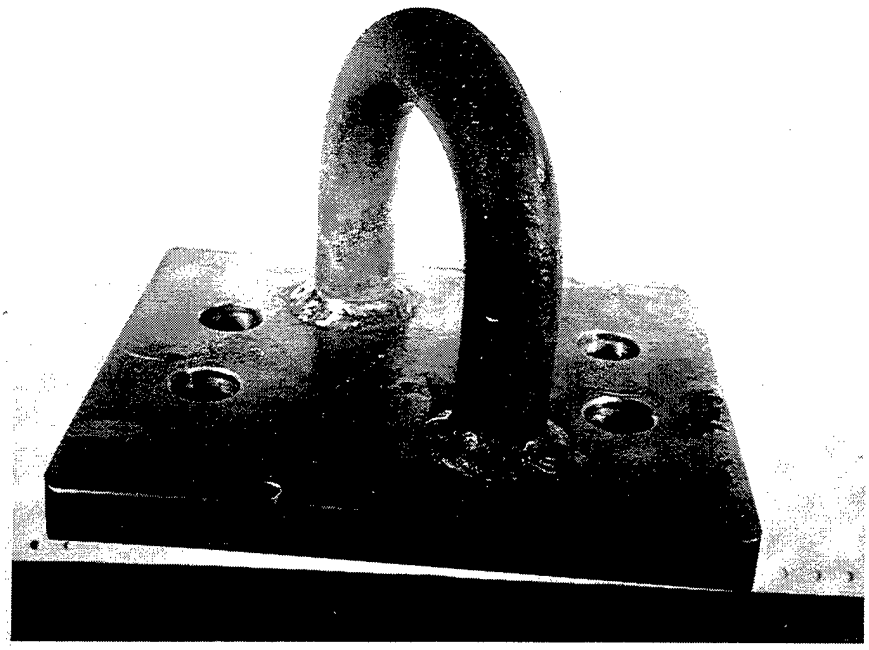

Figure 104. A view of the new lifting device fabricated for the Class 70 Modified AVLB. In addition to the fillet weld around both legs of the U-shaped bar on top of the plate, both ends of the bar also were welded on the bottom of the plate. Note the 30° orientation of the bar to the vertical axis of the device. Approximately 1/2 size.

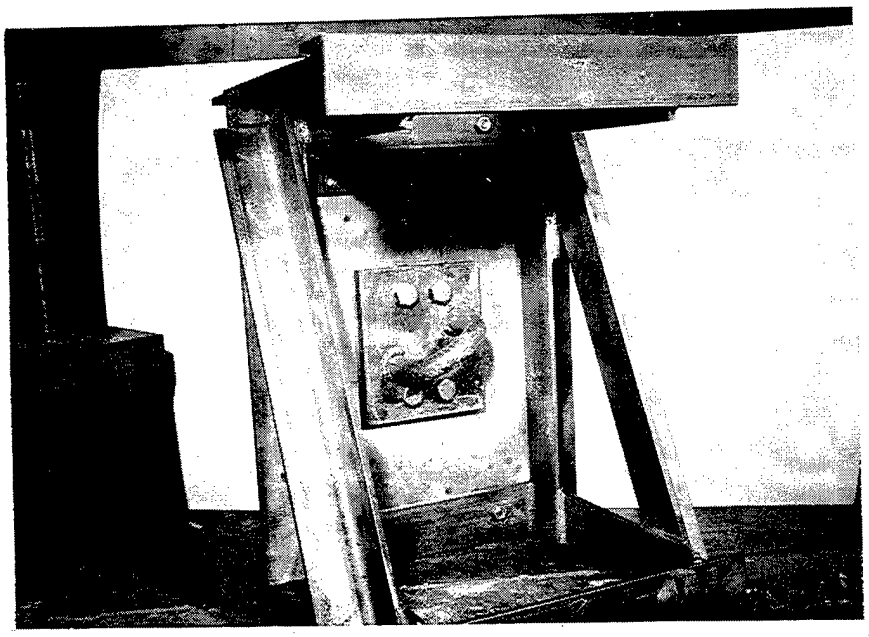

Figure 105. Front view of the test jig showing the new lifting device bolted to the front side of the aluminum girder test plate.

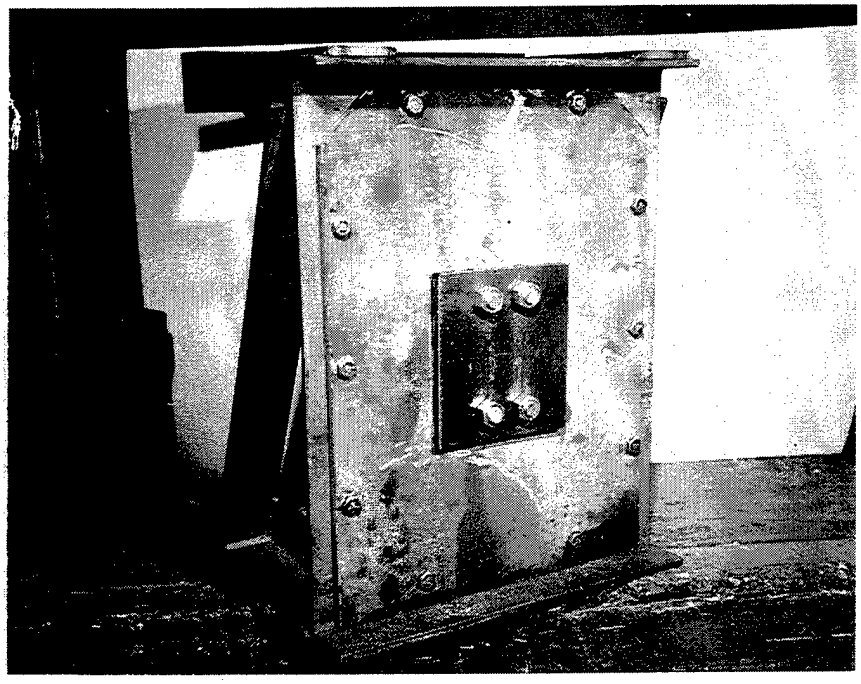

Figure 106. Back view of the test jig showing the 1/2-in-thick steel plate of the new lifting device bolted to the back side of the aluminum girder test plate, which in turn is bolted to the test jig.

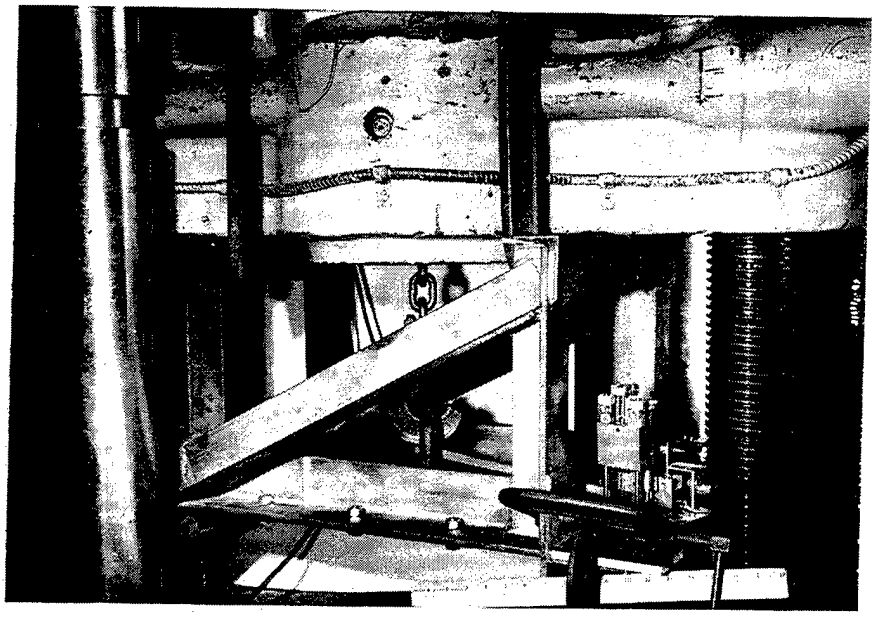

Figure 107. A view of the test jig placed in position under the lower fixed crosshead of the testing machine. It is set up for the straight-out pull test whereby the hook will pull on the U-shaped bar straight up from the test plate on the jig when the load is applied in tension during the test. Note the deflectometer in place on the test jig for the pull test.

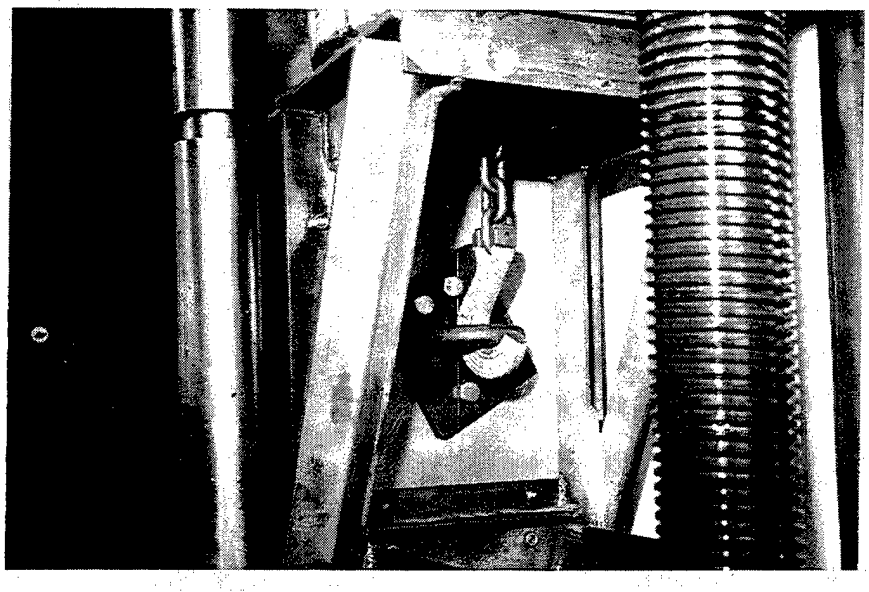

Figure 108. A view of the test jig with the U-shaped bar of the new lifting device in the horizontal position for the perpendicular pull test. This test will apply the load in tension to the apex of the bar that will bend upward.

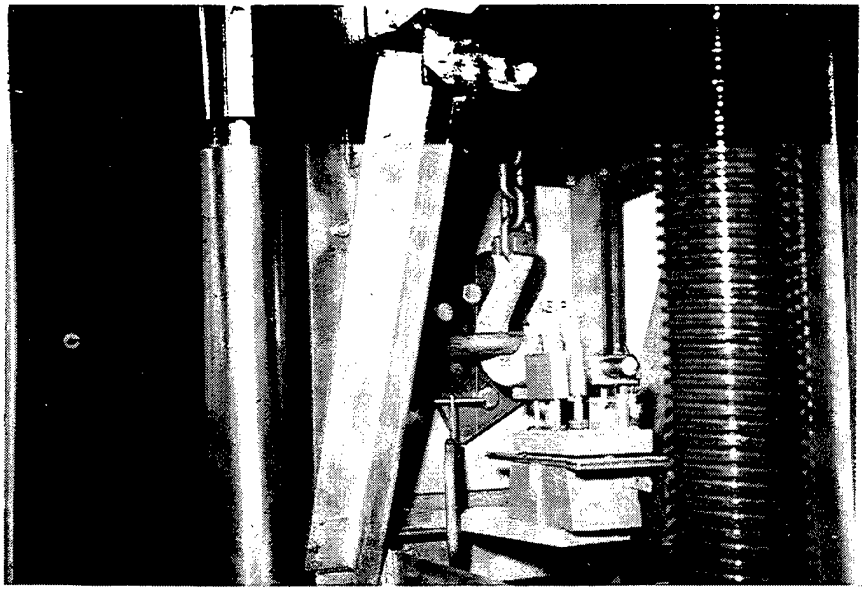

Figure 109. View of the same test jig in Figure 108 showing the deflectometer in place during the pull test to measure the movement of the bar at its apex.

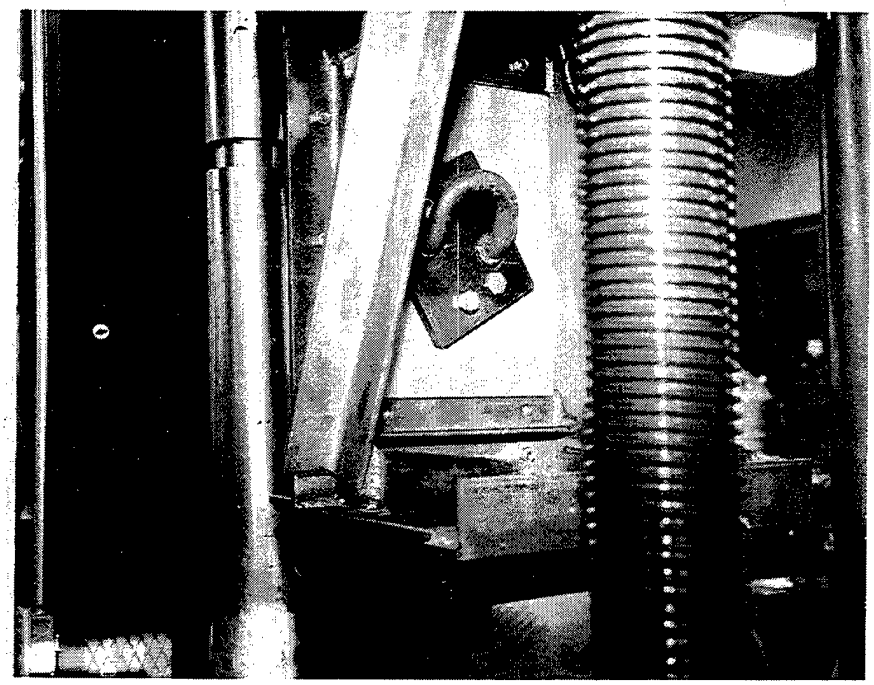

Figure 110. A view of the new lifting device after the perpendicular pull test. Note the extent of damage to the U-shaped bar on the device.

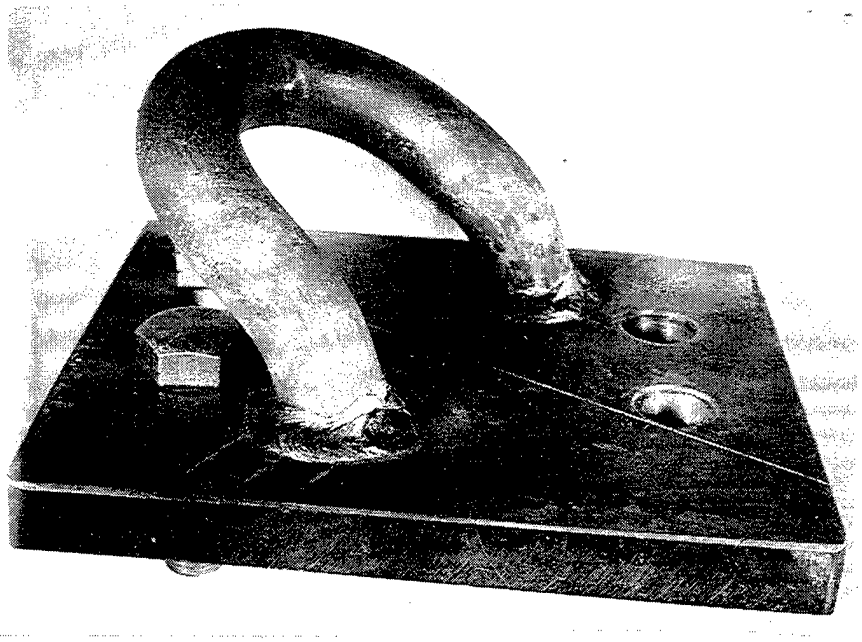

Figure 111. Close-up view of the damaged new lifting device after its removal from the test jig in Figure 110. Although not clearly seen in the photograph, cracks had occurred in the upper toe of the fillet welds on both legs of the U-shaped bar.

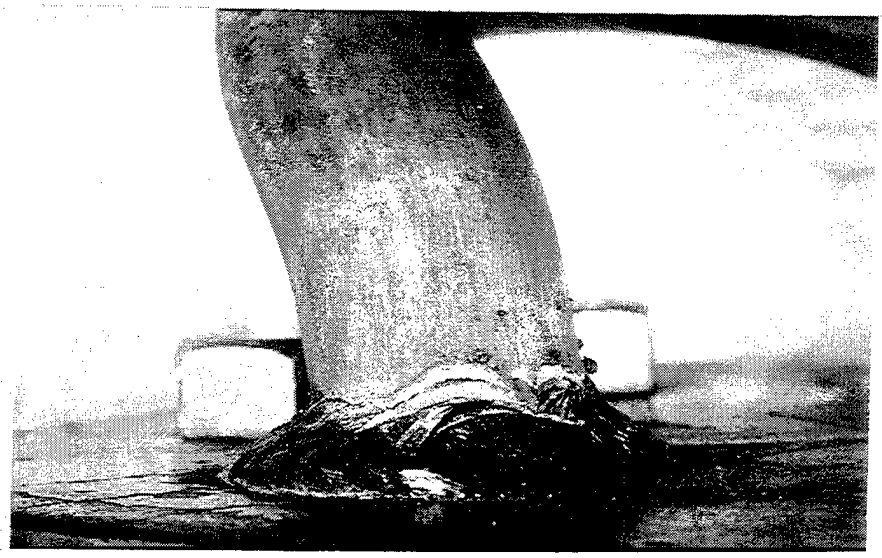

Figure 112. Closer view of the crack in the upper toe of the fillet weld in the damaged lifting device in Figure 111. Larger than actual size.

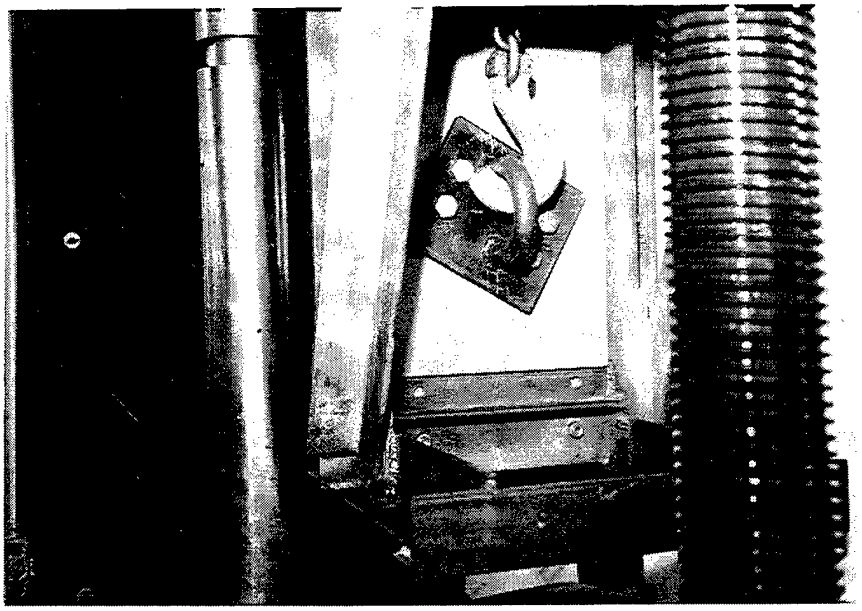

Figure 113. A view of the new lifting device mounted on the test jig with the U-shaped bar in the vertical position. The hook is under the upper leg for the parallel pull test.

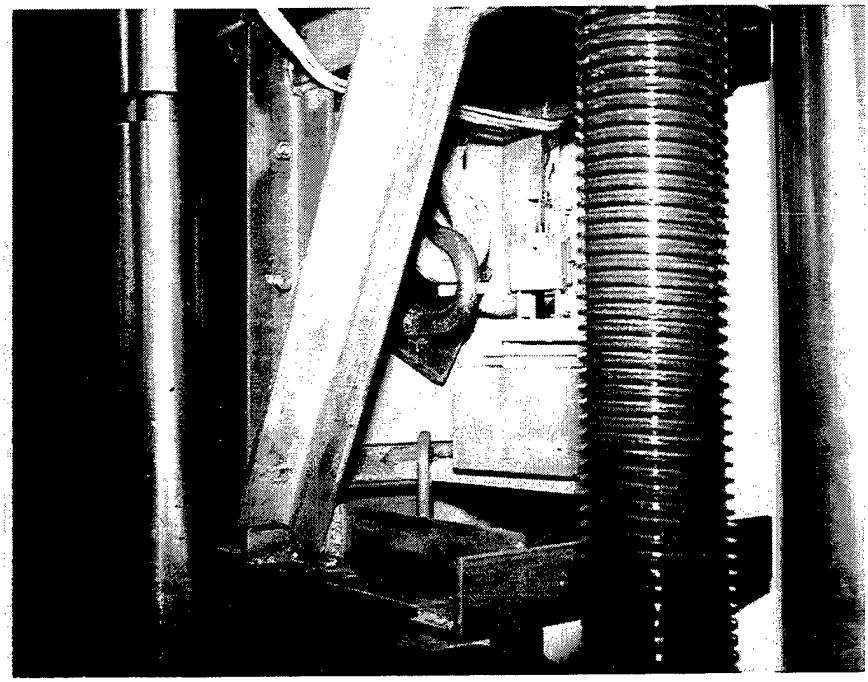

Figure 114. View of the same test jig in Figure 113 showing the deflection in place during the pull test to measure the movement of the upper bar leg on the hook.

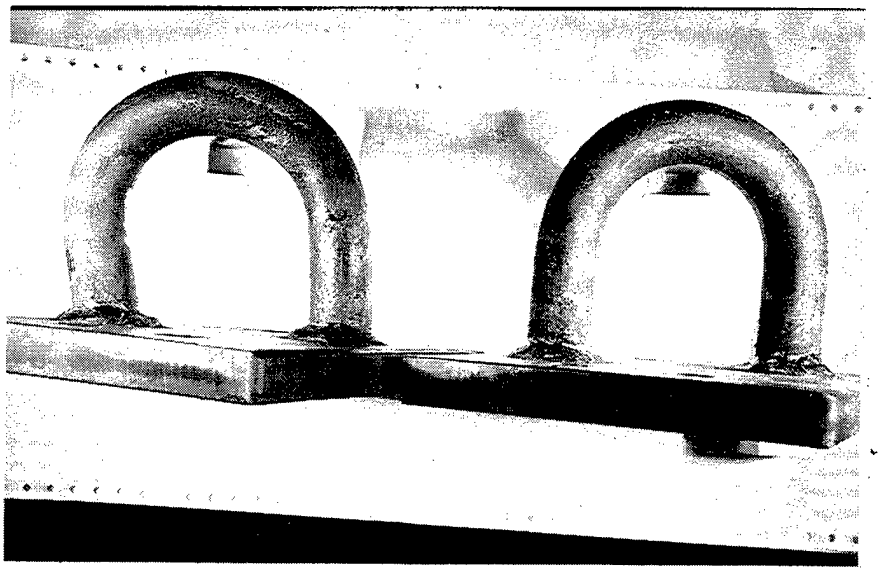

Figure 115. A view of the tested new lifting device (left) compared to the untested device after the parallel pull test. Note the extent of permanent damage to the left leg of the tested device as the result of the pull test.

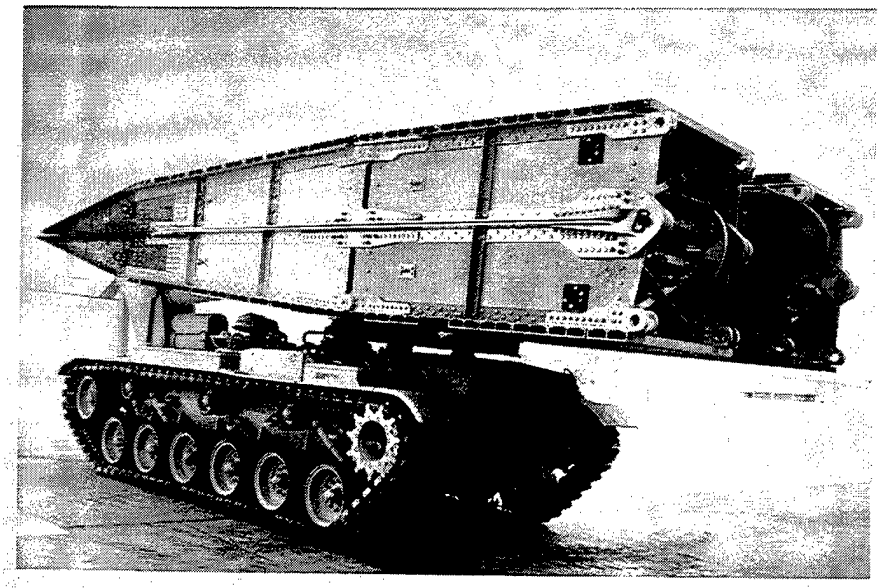

Figure 116. A Class 70 Modified AVLB in the folded position on top of the armored vehicle bridge launcher. The bridge is composed of four bridge sections (two females and two males) to form two treadways.

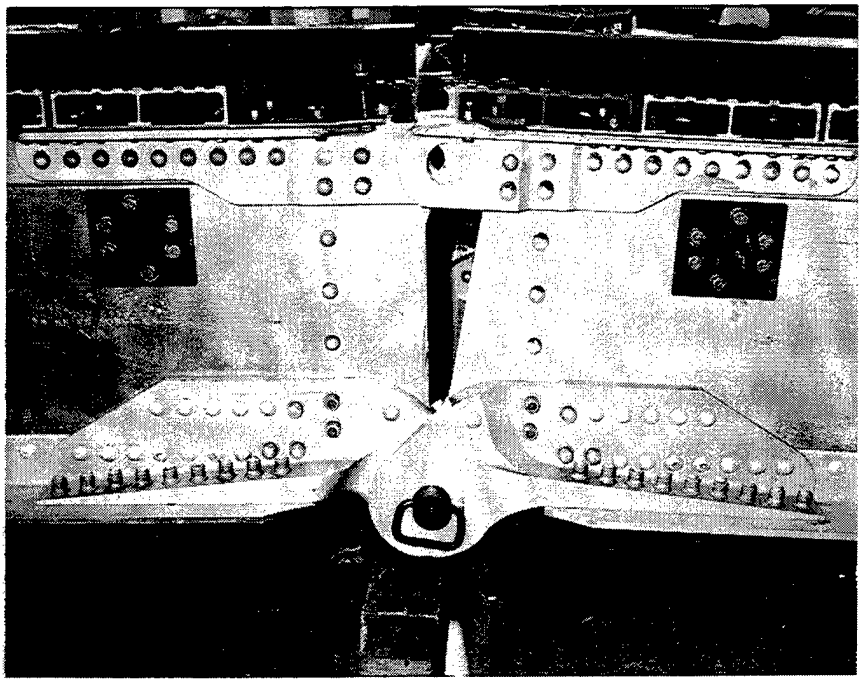

Figure 117. Close-up view of the new larger machined aluminum center hinges on the ends of the bottom chords. The hinges were made of stronger aluminum alloy 7050 and were fastened to the aluminum girder plates and larger alloy 7050 bottom chord angles with the Huckbolt fasteners. The flanged aluminum collars are seen on top of the hinge bottom flanges. Note the new steel lifting devices bolted to the girder plate of both bridge sections (the female section is on the right) after the original steel tie-down devices (see Figure 118) were removed. Also note the steel curbs bolted on top of the extruded aluminum deck panels.

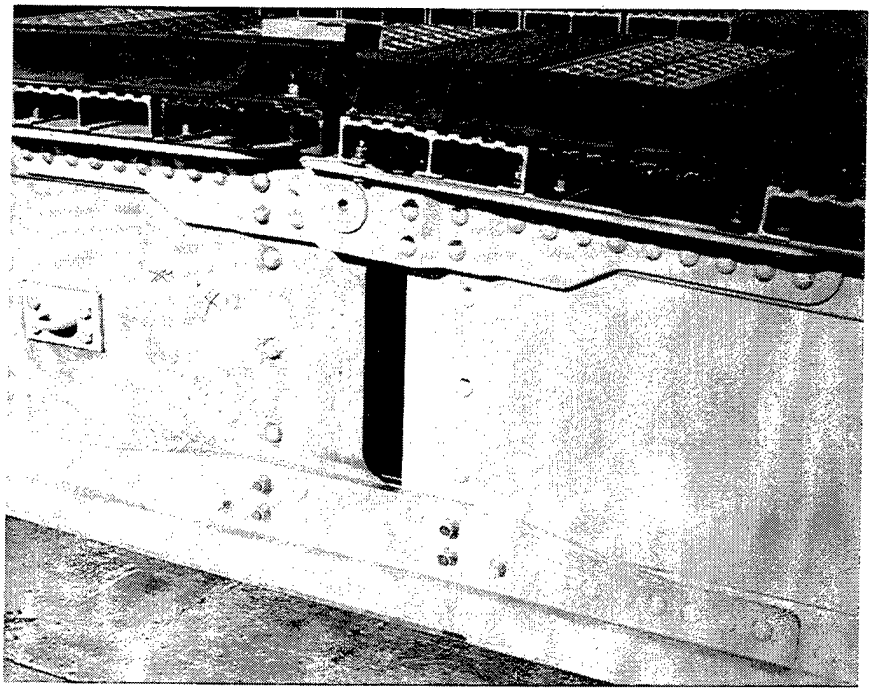

Figure 118. Close-up view of the aluminum alloy 7050 reinforcement bar fastened to the bottom chord angles and girder plates. It joined the center (left) and the end panel assemblies together permanently after the forged aluminum bottom connectors, similar to the top connectors, were eliminated as part of the Class 70 modification. The bottom chord angles were continuous across the joint. The Huckbolt fasteners were used to fasten the flat bar at the joint. The original steel tie-down device was now bolted to the girder plate of the center panel assembly.

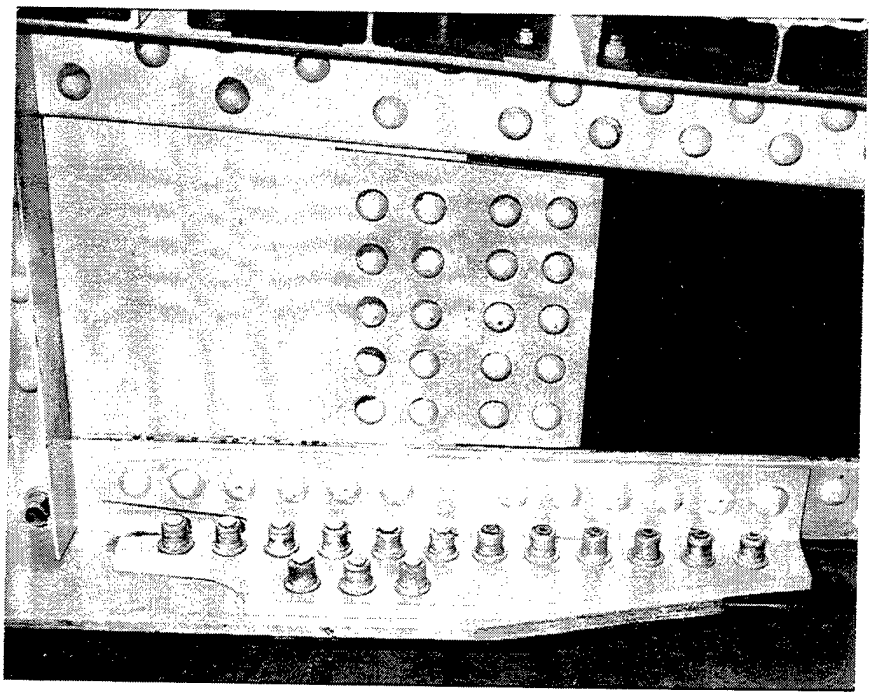

Figure 119. Close-up view of the modified larger angle splice fastened to the bottom chord angles and girder plates at the spliced joint. This is where the steel ramp end section (dark area at right) was spliced to aluminum section on left. It was made of stronger alloy 7050, and the Huckbolt fasteners were used as seen with the flanged collars. There is no sharp notch in the new angle splice as was seen in the original splices that sometimes were cracked (see Figures 2 and 120).

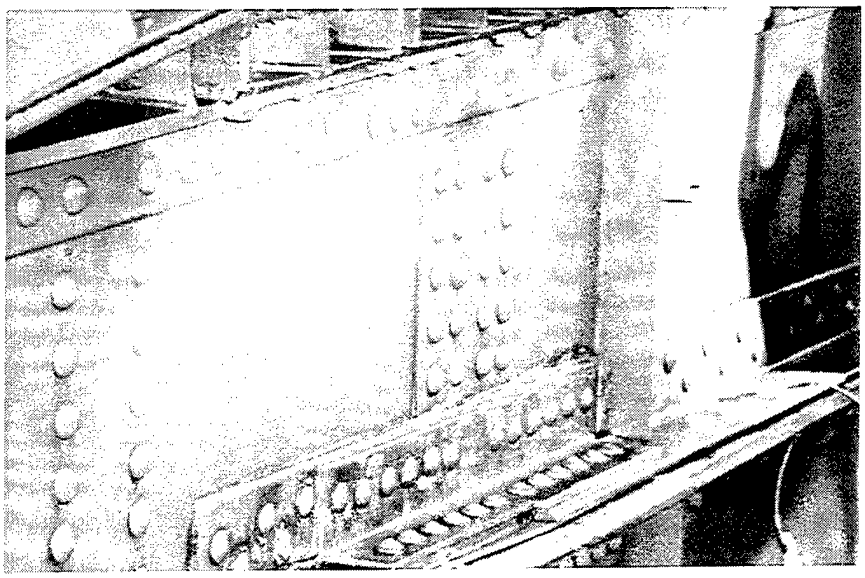

Figure 120. A view of the original angle splice on the current Class 60 AVLB for comparison to the larger modified splice in Figure 119. It contains the sharp angular notch in the cutout on the bottom angle leg. Note the use of the hot-driven aluminum rivets in the splice.

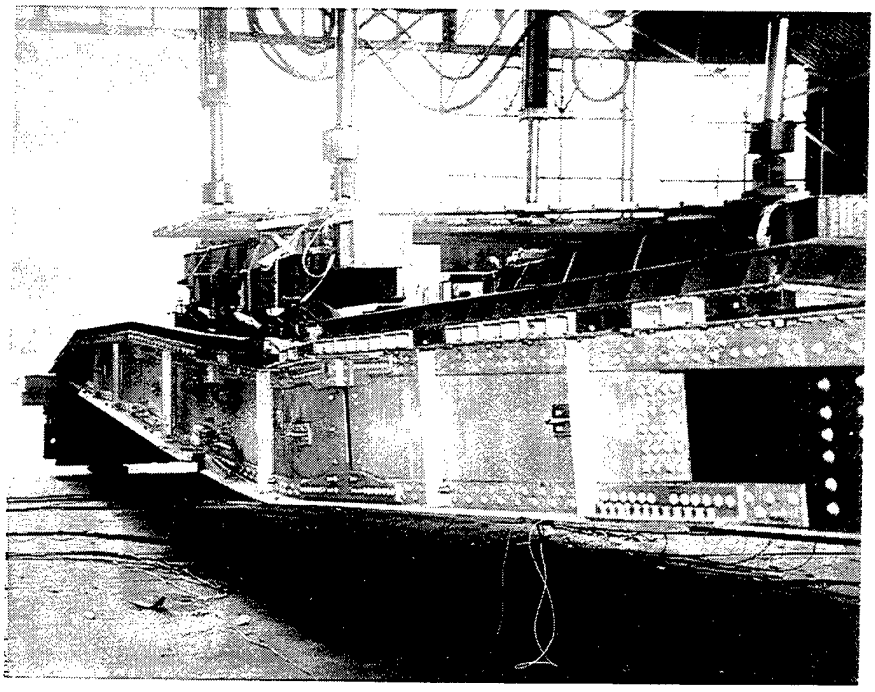

Figure 121. A side view of the collapsed No. 2 Class 70 modified AVLB after the bridge failure test. It buckled in the top chords and girder plates in the center panel assembly of the female bridge section.

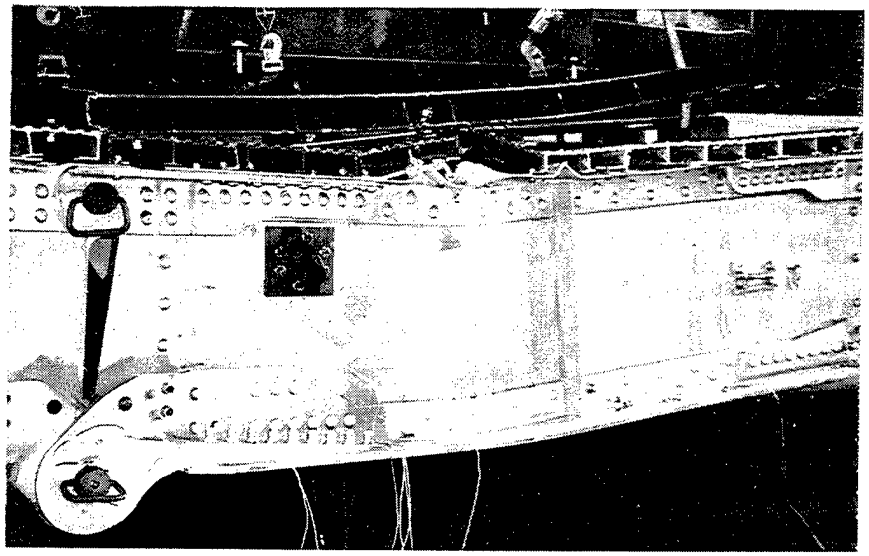

Figure 122. Close-up view of the buckled area in the No. 2 bridge in Figure 121. Note the extensive damages to the top chord, girder plate, extruded aluminum deck panels, and steel curb. The modified bottom chord angles did not crack, but bent at the buckled area. The buckling occurred closer to the center hinges of the female bridge section than in the other female section in Figure 124.

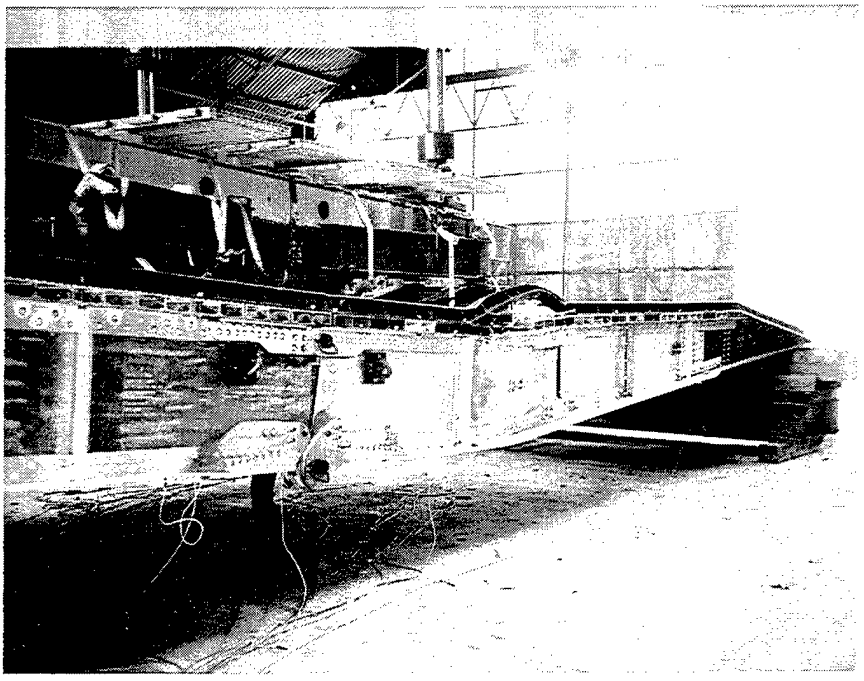

Figure 123. A view of the other side of the collapsed No. 2 bridge in Figure 121. It buckled in the top chords and girder plates in the center panel assembly of the other female bridge section.

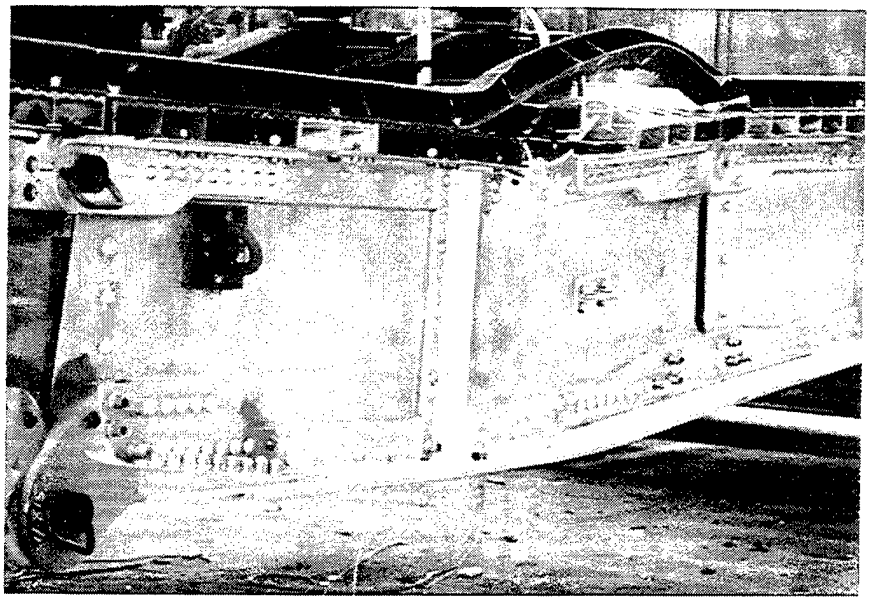

Figure 124. Close-up view of the buckled area in the No. 2 bridge in Figure 123. Note the extensive damages to the top chord, girder plate, extruded aluminum deck panels, and steel curb. The modified bottom chord angles did not crack, but bent at the buckled area.

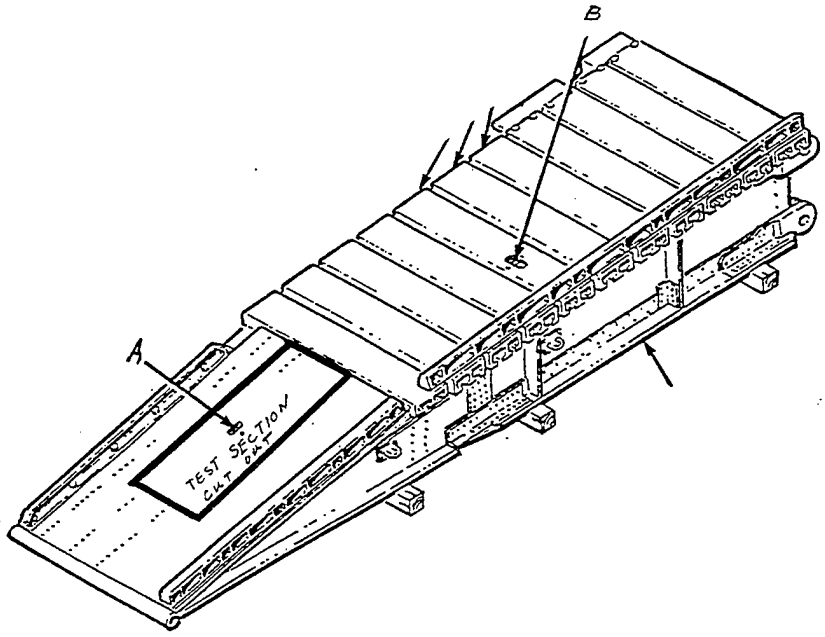

Figure 125. Sketch of the AVLB end panel assembly showing the location of the large test section cut from the lower ramp end with respect to the location of the lifting bar at point A.

Table 1. Tensile Properties of Aluminum Alloy 7050 and 2014 Extruded Structural Angle Samples From AVLB Bottom Chords

	Tensile Strength psi	0.2% Offset Yield Strength psi	Elongation % (in 2 in)
A. Alloy 7050			
A	83,320	75,257	14.7
B	80,694	72,390	13.6
AMS 4340 (Alloy 7050-T76511)	77,000 min.	68,000 min.	7.0 min.
B. Alloy 2014			
A	66,096	63,211	12.9
B	66,973	63,635	13.1
ASTM B221 (Alloy 2014-T6)	60,000 min.	53,000 min.	7.0 min.

NOTE: The rectangular tension test specimens were 1/2-in-wide reduced sections with 2-in gauge lengths.

Table 2. Compositions of the Inner (Cracked) and Outer (Not Cracked) Spliced Angle Samples and the Bottom Reinforcement Plate

Element	Inner Angle	Outer Angle	Bottom Plate	ASTM B221 (Alloy 2014)
Silicon	0.76	0.73	0.65	0.50–1.20
Iron	0.27	0.29	0.29	0.7 max.
Copper	4.35	4.23	4.58	3.9–5.00
Manganese	0.73	0.72	0.69	0.40–1.20
Magnesium	ND	ND	ND	0.20–0.80
Chromium	0.02	0.02	0.03	0.10
Titanium	0.02	0.02	0.03	0.15
Aluminum	Rem.	Rem.	Rem.	Rem.

NOTES: ND = Not determined. Magnesium contents in the samples were not determined because of the difficulty in detecting small quantities of magnesium by an x-ray wavelength dispersed spectrometer.

Table 3. Tensile Properties of Inner and Outer Aluminum Spliced Angle Samples

	Tensile Strength ksi	0.2% Offset Yield	Elongation % (in 2 in)
Inner Angle	67.3	62.8	9.5
Outer Angle	64.9	60.4	10.3
ASTM B221 Alloy 2014-T6)	60.0 min.	53.0 min.	7.0 min.

NOTE: The rectangular tension test specimens were 1/2-in-wide reduced sections with 2-in gauge lengths.

Table 4. Tensile and Shear Data of the AVLB Extruded Aluminum Deck Panel

	Specimen	0.2 Offset Yield Strength psi	Ultimate Tensile Strength psi	Elongation %
A.	Tensile properties.			
	Standard 1/2-in-wide rectangular tension test specimens cut from the deck panel sidewall (2-in gauge length).			
	1 2	63,230 65,470	67,630 69,690	9.7 10.7
	Subsize 1/4-in-wide rectangular tension test specimens cut from the deck-treated surface (1-in gauge length).			
	3 4	66,900 66,640	71,000 70,410	11.2 11.0
	Minimum tensile values.			
	ASTM B 211 Alloy 2014-T6	53,000	60,000	7 (in 2 in)
B.	Shear properties (shearing die apparatus with 1-in-diameter opening).			
	Shear test specimens cut from the deck panel sidewall).			
		Shear Strength		
	1 1	46,580 47,080		
	Typical shear strength for 2014-T6 is 42,000 psi.			

Table 5. Composition and Hardness of Steel Material of Two Lifting Bar Samples

	First Bar	Second Bar	ASTM A 36
A. Composition			
Carbon	0.22	0.23	0.25 max
Manganese	0.93	1.11	0.80–1.20
Nickel	0.01	0.01	—
Chromium	0.01	0.01	—
Copper	0.02	0.04	—
Molybdenum	—	—	—
B. Hardness, HRB (Rockwell B hardness)			
	76.5	74	
C. Approximate tensile strength, based on hardness (ksi)			
	67	65	58–80

Table 6. Composition and Hardness of the Huckbolt Aluminum Collar

	Collar Sample	Alloy 6061
A. Composition, %		
Silicon	0.52	0.40–0.80
Iron	0.37	0.70 max.
Copper	0.27	0.15–0.40
Manganese	0.06	0.15 max.
Magnesium	Not determined	0.80–1.20
Chromium	0.13	0.04–0.35
Zinc	0.12	0.25 max.
B. Hardness	62 HB	65 HB typical for T4 temper condition

Table 7. Data From Shear and Push Tests of the Huckbolt Aluminum Fasteners

Specimen A	First shear test specimen with fully swaged collar.	
	Shear test	38,100 lb (43,701-psi shear strength)
	Push test	18,000 lb (after the shear test)
Specimen B	Second shear test specimen with fully swaged collar.	
	Shear test	38,250 (43,873-psi shear strength)
Specimen C	Shear test specimen with 1/2 swaged cinch-on collar.	
	Shear test	37,000 lb (42,439-psi shear strength)
Specimen D	Shear test specimen with 1/4 swaged cinch-on collar.	
	Shear test	37,300 lb (42,784-psi shear strength)
Specimen E	Two angles fastened back to back in contact with each other (no gap).	
	Push test	17,850 lb
Specimen F	Two angles fastened together with two large flat washers in between them as a spacer.	
	Push test[a]	21,350 lb
Specimen G	Two angles fastened back to back with 1/4-in-square steel bars in between them to form a 1/4-in gap.	
	Push test[b]	18,350 lb

[a] Test was stopped just after the maximum load was reached and before complete shearing of the collar interior wall for radiographic inspection.

[b] Aluminum shims were placed in the gaps to minimize further compressing of the angle legs during the test.

Table 8. Results of Tensile Tests on Huckbolt Fastener Aluminum Pin Samples

	Sample	Breaking Load (lb)	Notch Tensile Strength (psi)	
A.	Breaking load at the original cold-rolled breakaway notch of two pin samples.			
	1	15,740	113,070	
	2	15,940	114,510	
B.	Breaking load at the machined breakaway notch of the pin sample.			
	3	13,340	90,180	
C.	Pin sample with reduced section of the same diameter (0.419 in) at the root of the original breakaway notch located at the center of the reduced section.[a]			
	Sample	Breaking Load (lb)	Tensile Strength (psi)	0.2% Offset Yield Strength (psi)
	4	9,700	70,350	43,150
D.	Subsize 1/4-in-diameter tension test specimen machined from the broken pin sample in the perpendicular pull test.			
	Sample	Tensile Strength (psi)	0.2% Offset Yield Strength (psi)	Elongation % (in 1 in)
	3a	70,810	46,750	23.0
	ASTM B 316			
	Alloy 2024-T4	62,000 min.	40,000 min.	10.0 (in 2 in)

[a] Necking occurred on both sides of the notch root in the center of the reduced section. Failure of the pin sample occurred in one of the necked regions.

NO. OF COPIES	ORGANIZATION
2	DEFENSE TECHNICAL INFO CTR ATTN DTIC DDA 8725 JOHN J KINGMAN RD STE 0944 FT BELVOIR VA 22060-6218
1	HQDA DAMO FDQ ATTN DENNIS SCHMIDT 400 ARMY PENTAGON WASHINGTON DC 20310-0460
1	US MILITARY ACADEMY MATH SCI CTR OF EXCELLENCE DEPT OF MATHEMATICAL SCI ATTN MDN A MAJ DON ENGEN THAYER HALL WEST POINT NY 10996-1786
1	DIRECTOR US ARMY RESEARCH LAB ATTN AMSRL CS AL TP 2800 POWDER MILL RD ADELPHI MD 20783-1145
1	DIRECTOR US ARMY RESEARCH LAB ATTN AMSRL CS AL TA 2800 POWDER MILL RD ADELPHI MD 20783-1145
3	DIRECTOR US ARMY RESEARCH LAB ATTN AMSRL CI LL 2800 POWDER MILL RD ADELPHI MD 20783-1145
	ABERDEEN PROVING GROUND
2	DIR USARL ATTN AMSRL CI LP (305)

NO. OF COPIES	ORGANIZATION
1	OSD OUSD AT STRT TAC SYS ATTN DR SCHNEITER 3090 DEFNS PENTAGON RM 3E130 WASHINGTON DC 20301-3090
1	ASST SECY ARMY RESEARCH DEVELOPMENT ACQUISITION ATTN SARD ZD RM 2E673 103 ARMY PENTAGON WASHINGTON DC 20310-0103
1	ASST SECY ARMY RESEARCH DEVELOPMENT ACQUISITION ATTN SARD ZP RM 2E661 103 ARMY PENTAGON WASHINGTON DC 20310-0103
1	ASST SECY ARMY RESEARCH DEVELOPMENT ACQUISITION ATTN SARD ZS RM 3E448 103 ARMY PENTAGON WASHINGTON DC 20310-0103
1	ASST SECY ARMY RESEARCH DEVELOPMENT ACQUISITION ATTN SARD ZT RM 3E374 103 ARMY PENTAGON WASHINGTON DC 20310-0103
1	UNDER SEC OF THE ARMY ATTN DUSA OR RM 2E660 102 ARMY PENTAGON WASHINGTON DC 20310-0102
1	ASST DEP CHIEF OF STAFF OPERATIONS AND PLANS ATTN DAMO FDZ RM 3A522 460 ARMY PENTAGON WASHINGTON DC 20310-0460
1	DEPUTY CHIEF OF STAFF OPERATIONS AND PLANS ATTN DAMO SW RM 3C630 400 ARMY PENTAGON WASHINGTON DC 20310-0400

NO. OF COPIES	ORGANIZATION
1	ARMY RESEARCH LABORATORY ATTN AMSRL SL PROGRAMS AND PLANS MGR WSMR NM 88002-5513
1	ARMY RESEARCH LABORATORY ATTN AMSRL SL E MR MARES WSMR NM 88002-5513
1	ARMY TRADOC ANL CTR ATTN ATRC W MR KEINTZ WSMR NM 88002-5502
1	ARMY TRNG & DOCTRINE CMND ATTN ATCD B FT MONROE VA 23651
	ABERDEEN PROVING GROUND
1	CDR USATECOM ATTN: AMSTE-TA
2	DIR USAMSAA ATTN: AMXSY-ST AMXSY-D
4	DIR USARL ATTN: AMSRL-SL, J WADE (433) M STARKS (433) AMSRL-SL-C, J BEILFUSS (E3331) AMSRL-SL-B, P DEITZ (328)
1	CDR CBDCOM ATTN: TECHNICAL LIBRARY BLDG E3330
1	DIR CBIAC BLDG E3330, RM 150

REPORT DOCUMENTATION PAGE

Form Approved
OMB No. 0704-0188

1. AGENCY USE ONLY *(Leave blank)*	2. REPORT DATE	3. REPORT TYPE AND DATES COVERED
	December 1996	Final, Feb 93-Jun 96

4. TITLE AND SUBTITLE
Mechanical Tests and Failure Analysis on Selected Components of the Class 60 Armored Vehicle Launched Bridge (AVLB) During the Class 70 Modification Modification Program

5. FUNDING NUMBERS
PR: 1L162618AH80

6. AUTHOR(S)
Howard E. Horner

7. PERFORMING ORGANIZATION NAME(S) AND ADDRESS(ES)
U.S. Army Research Laboratory
ATTN: AMSRL-WM-MA
Fort Belvoir, VA 22060-5812

8. PERFORMING ORGANIZATION REPORT NUMBER
ARL-TR-1269

9. SPONSORING/MONITORING AGENCY NAMES(S) AND ADDRESS(ES)

10.SPONSORING/MONITORING AGENCY REPORT NUMBER

11. SUPPLEMENTARY NOTES

12a. DISTRIBUTION/AVAILABILITY STATEMENT
Approved for public release; distribution is unlimited.

12b. DISTRIBUTION CODE

13. ABSTRACT *(Maximum 200 words)*

The current Class 60 armored vehicle launched bridge (AVLB), with an overall length of 63 ft, is capable of carrying Class 60 (military load classification [MLC] - 60 tons) tracked and wheeled loads over a 60-ft-wide gap. The heavier, wider M1A1 main battle tank (Class 70 load) can cross the AVLB over a 50-ft-wide gap with precautions. Several modifications were proposed to upgrade a number of AVLBs from Class 60 to Class 70 for the 60-ft clear span crossings. The objective of the work was to conduct necessary mechanical tests on selected AVLB components to obtain pertinent data to verify their load carrying capability and the proposed modifications.

Various AVLB components were cut or removed from several AVLBs as samples for a variety of mechanical and special tests. Special test jigs were designed and built to test the samples of the components on the testing machine. Failure analyses were performed on the components that failed during the special tests or the fatigue tests of the modified AVLBs undergoing the simulated crossings. Two Class 60 AVLBs were converted to Class 70, with extensive modifications to the bottom chords, and then were tested. One of them was deliberately tested to failure by static overloading to observe the mode of failure. The bridge buckled in the top chords at about 190 tons. The modified bottom chords did not fail by cracking, indicating the success of the Class 70 modification program to upgrade the AVLB.

14. SUBJECT TERMS
aluminum alloy 7050, aluminum alloy 2014, failure analysis, bridges, mechanical tests, Huckbolt fasteners, bottom chords

15. NUMBER OF PAGES
134

16. PRICE CODE

17. SECURITY CLASSIFICATION OF REPORT	18. SECURITY CLASSIFICATION OF THIS PAGE	19. SECURITY CLASSIFICATION OF ABSTRACT	20. LIMITATION OF ABSTRACT
UNCLASSIFIED	UNCLASSIFIED	UNCLASSIFIED	SAR

NSN 7540-01-280-5500
Standard Form 298 (Rev. 2-89)
Prescribed by ANSI Std. 239-18 298-102

INTENTIONALLY LEFT BLANK.

USER EVALUATION SHEET/CHANGE OF ADDRESS

This Laboratory undertakes a continuing effort to improve the quality of the reports it publishes. Your comments/answers to the items/questions below will aid us in our efforts.

1. ARL Report Number/Author ARL-TR-1269 (Horner) Date of Report December 1996

2. Date Report Received _____

3. Does this report satisfy a need? (Comment on purpose, related project, or other area of interest for which the report will be used.) _____

4. Specifically, how is the report being used? (Information source, design data, procedure, source of ideas, etc.) _____

5. Has the information in this report led to any quantitative savings as far as man-hours or dollars saved, operating costs avoided, or efficiencies achieved, etc? If so, please elaborate. _____

6. General Comments. What do you think should be changed to improve future reports? (Indicate changes to organization, technical content, format, etc.) _____

CURRENT ADDRESS

_____
Organization

_____
Name E-mail Name

_____
Street or P.O. Box No.

_____
City, State, Zip Code

7. If indicating a Change of Address or Address Correction, please provide the Current or Correct address above and the Old or Incorrect address below.

OLD ADDRESS

_____
Organization

_____
Name

_____
Street or P.O. Box No.

_____
City, State, Zip Code

(Remove this sheet, fold as indicated, tape closed, and mail.)
(DO NOT STAPLE)

DEPARTMENT OF THE ARMY

OFFICIAL BUSINESS

NO POSTAGE
NECESSARY
IF MAILED
IN THE
UNITED STATES

BUSINESS REPLY MAIL
FIRST CLASS PERMIT NO 0001,APG,MD

POSTAGE WILL BE PAID BY ADDRESSEE

DIRECTOR
US ARMY RESEARCH LABORATORY
ATTN AMSRL WM MA
FT BELVOIR VA 22060-5812